Synergy of a STING agonist and an IL-2 superkine in cancer immunotherapy against MHC I-deficient and MHC I+ tumors

By

Natalie K. Wolf

A thesis submitted in partial satisfaction of the

requirements for the degree of

Doctor of Philosophy

in

Molecular and Cell Biology

in the

Graduate Division

of the

University of California, Berkeley

Committee in charge:
Professor David H. Raulet, Chair
Professor Russell E. Vance
Professor Michel DuPage
Professor David V. Schaffer

Spring 2022

Abstract

Synergy of a STING agonist and an IL-2 superkine in cancer immunotherapy against MHC I-deficient and MHC I+ tumors

by

Natalie K. Wolf

Doctor of Philosophy in Molecular and Cell Biology

University of California, Berkeley

Professor David H. Raulet, Chair

Over the past decade, there have been many advances made in the field of cancer immunotherapy, one of the major therapies discovered is that of checkpoint blockades. While these therapies have vastly improved patient outcomes, many cancers do not respond to checkpoint blockade highlighting the need for further development of new therapeutics. Most current cancer immunotherapies are based on mobilizing CD8 T cell responses. However, many types of tumors evade CD8 T cell recognition by displaying few or no antigens, or losing expression of MHC I. These considerations underlie the need for complementary therapies that mobilize other antitumor effector cells. NK cells are cytotoxic innate-like lymphocytes that are hardwired to recognize stressed cells, such as tumor cells and certain infected cells, and mediate spontaneous killing of MHC I-deficient tumor cells. CD4 T cells recognize tumor cells through epitopes displayed on MHC II and have been shown to be capable of eliciting antitumor responses against tumor cells. Identifying new immunotherapies, aimed at targeting NK and CD4 cells for antitumor responses, could potentially activate responses against CD8 T cell-resistant tumors.

Cyclic dinucleotides (CDNs) activate the cGAS-STING pathway of the innate immune system and are candidates as immunotherapy agents. Intratumoral CDN injections induce type I IFNs and inflammatory cytokines that amplify the CD8 T cell response and induce tumor regression. Recently, CDN therapy was shown to induce long-term tumor regressions in some MHC I-deficient tumor models, mediated primarily by NK cells and in some cases, CD4 T cells. However, in harder-to-treat tumor models, CDN therapy shows few to no long-term remissions and early phase clinical trials of STING agonists in patients have not yielded sustained clinical remissions indicating a need for improvements in this immunotherapy approach.

My thesis work aims to examine the potential to extend the efficacy of CDN therapy, by combining CDN with the IL-2 superkine, H9-MSA, to target and activate NK cells and CD4 T cells in the tumor microenvironment against MHC I-deficient tumors and CD8 T cells against MHC I WT tumors. Chapter 3 addresses the synergy observed with CDN and H9-MSA therapy in mobilizing powerful NK cell antitumor responses against MHC I-deficient tumors. CDN/H9-

MSA therapy markedly enhanced tumor rejection of two hard-to-treat MHC I-deficient tumor models. These responses were mediated by NK cells and in some cases CD4 T cells and were accompanied by increased recruitment to and sustained activation of NK cells in the tumor. This combination therapy regimen activated NK cells systemically, as shown by antitumor effects distant from the site of CDN injection and enhanced cytolytic activity of splenic NK cells against tumor cell targets ex vivo. H9-MSA also showed strong synergy with another innate activator, CpG. The CDN/H9-MSA therapy showed promising effects in treating tumors in mice with a complex microbiota, a known factor to negatively influence immunotherapies.

CD4 T cell antitumor responses were also induced by CDN or the CDN/H9-MSA combination therapy against two different MHC I-deficient tumor models. Chapter 4 explores the role of tumor specific CD4 T cells induced by CDN therapy alone or CDN/H9-MSA combination therapy, independently of NK cells. CDN treatment increased systemic levels of tumor specific CD4 T cells, with a Th1-like phenotype. Mice treated with CDN/H9-MSA induced potent CD4 T cell and CD4/CD8 T cell responses against an MHC I-deficient tumor model in the absence of NK cells. The antitumor CD4 T cell response did not rely on MHC II expression on the tumor cells to elicit tumor rejection. Tumor-specific priming of these CD4 T cells showed enhanced cytokine production in combination therapy treated mice. Finally, this chapter explores the CDN/H9-MSA combination therapy regimen synergistically mobilizing powerful CD8 T cell responses in the case of MHC I+ tumors, both syngeneic and carcinogen (methylcholanthrene, MCA)-induced models, suggesting the generality of the approach.

The final chapter of my thesis focuses on attempts to improve CDN/H9-MSA therapy in both syngeneic and MCA-induced sarcoma models. With many factors in the tumor microenvironment influencing the immune responses, we endeavored to amplify the impact of tumor infiltrating NK cells and T cells through various forms of activation or through the inhibition of suppressive factors found in the TME. Blockade of immunosuppressive metabolites and checkpoint receptors did not enhance CDN/H9-MSA therapy against MHC I-deficient tumors. However, addition of checkpoint blockade to the CDN/H9-MSA therapy regimen greatly increased the survival of mice in the spontaneous MCA-induced sarcoma model.

Overall, the work in this thesis demonstrates the impact of a novel combination therapy in mobilizing powerful NK and T cell-mediated antitumor activity, providing important justification for evaluating approach of combining a STING agonist with the IL-2 superkine, for treating human cancers that are refractory to available treatment options.

Table of Contents

List of Figures

Acknowledgements

To the many, many people in my life who have helped be become the person I am today, thank you. Graduate school has been full of many highs and many lows and without all your support, guidance, and love, I would not be where I am today.

2010 was the hardest year of my life. When I first came to your office for a routine procedure, never did I expect to receive such a phone call from you, Dr. Ecker. I will never forget those words when you told me I had cancer. While that was the hardest phone call I've heard had to take, it saved my life and for that I will forever be grateful. Dr. Weigel, you took the time to answer many questions throughout my year of treatment and always did so with a smile on your face. You helped me to think more about research and it is part of the reason I am graduating today. Thank you both.

To my research mentors at the University of Minnesota: Eric Rahrmann, you took a chance on me, bringing me in as a new freshman to work with you in the lab. Your welcoming presence made being in lab such a joy; I will never forget ABBA playing in the background with you singing along as I extracted RNA from countless samples. You provided endless guidance and helped to encourage me to continue pushing forward in science. I will always remember the beer lunches, Stub's trips, and enjoying a pint with you and Katie at The Eagle Inn in Cambridge. Thank you for starting my path towards this Ph.D. Branden Moriarity, thank you for keeping me on as an undergrad when it was time for Eric to move on. You continued to train me and helped me to understand how to scientifically approach new projects, making me a better scientist each and every day. You helped me to believe I could get a Ph.D. and are one of the reasons I am here today. I hope you still have the beer fridge stocked for all of your meetings and continue the many, many happy hour trips to Stub and Herb's. David Largaespada, as my time in the lab continued, you allowed me to take on my own projects and pursue questions with more independence. You helped me to see I truly loved exploring new questions in the lab and provided me with many opportunities to present my work to numerous audiences. You and Sue have always been so supportive and I'm glad we were able to enjoy a nice glass of wine together in Paris! Thank you, Eric, Branden and David.

To my Minnesota friends: I would have never survived undergrad, tech work or grad school without you all. Felicia, while we may have started on an awkward note, I wouldn't want anyone else in my life to provide me with the endless laughs and shenanigans that you do. Thank you for supporting me from afar and making it like feel like no time has passed when we finally get to see each other. To members of the Larg/Moriarity labs, Nick, Emily, Rory, Robin, Kyle, Smeester, and Alex, lab would have been so boring without you all there along my side. The many happy hour trips, beer Olympics, Fischer Bowling, Paris, and pandemic board game nights; so many memories that I will forever cherish.

To my Ph.D. advisor, David Raulet, thank you for the best Ph.D. experience I could have asked for here at UC Berkeley. You were excited to welcome me into the lab and were so supportive of my desire to pursue a more translational research project at a very basic science university. You taught me how to truly become a great scientist and are someone I will always admire deeply. Your many, many stories during my time in lab are memories I will always

cherish. Thank you for your unending support during quals, a global pandemic, finishing my paper and this thesis. You truly care about your lab members both on professional and personal levels and have showed me compassion in my times of need. You have provided me with endless opportunities, and I truly could not have asked for a better mentor. I am sad to be leaving the lab, but know this is not a goodbye, but a see you later. Thank you.

To the Raulettes, I don't know if I would have made it through grad school without you all. Lily, my lab mom, always there for moral support and able to fix any problem in the lab. You made my life so much easier and were always willing to look at the hundreds of dog and niece/nephew pictures I have to show off. Djem, The best baymate and friend. I can't imagine a better friend to have along my side as I ventured through grad school. You are always willing to listen to any problem and provide the best reaction, whether good or bad, to any news. I have enjoyed our many conversations, about life and lab, while getting coffee at Yalis' and over many good beers at Jupiter. Chris, how could I have ever done my project without you?! You taught me everything I know about mouse work and were always willing to listen and give new experiment ideas. I enjoyed all our times together in lab as well as at Hotsy Totsy after a great kickball win on a Friday night. Boom! Cristina, my other CDN/H9-MSA buddy in the lab. You were a grounding presence for me and helped me to look at the bigger picture in life. Thank you for your being a shoulder I could lean on and commiserate with over a nice glass of wine. Joanna, my mimosa buddy, your guidance helped me navigate my last years of grad school and survive a global pandemic. Thank you for endless trips to Jupiter and mimosas at BSC. Rutger, you were the party of the lab, but were also so hard working. Thank you for helping to instill these values into myself and making grad school a fun experience. Alan, it took me a while to open up to you, but once I did, we spent many hours having coffee together discussion any possible topic. I miss those chats as well as all of your ridiculous jokes and laughter that you brought to the lab each and every day. Yeara, starting in the lab during a pandemic I sure was very hard, but you radiate such positivity all of the time, it helped us all get through. I thank you for all of your advice and guidance and for always being willing to get a beer with me at Jupiter, even in between your incubations. Chenyu, thank you for letting me mentor you with the therapy projects and for carrying on the tumor legacy of the lab! And to Albert and Milind, thank you for all of your advice in my next career steps. My labmates, my friends, my adopted family, thank you for everything.

To my Berkeley community: to you all, thank you for helping to make Berkeley my home away from home. To the classmates, you were the first people I met and became friends with when I moved to Berkeley and helped me to establish a stable community here with people I could always turn to in times of need. A special thanks to the immunology crew who helped ease the pain of studying for quals and who are always willing to commiserate about grad school and life. Victoria, thank you for constant support as a dear friend in many times of need throughout these stressful six years, always giving the biggest and best hugs. Andrea, thank you being such a positive friend and for helping me take much needed breaks from lab with our tea chats. Nora, thank you for the much needed laughter throughout grad school and for keeping me sane during the pandemic with zoom game nights and outdoor hangs. To my first roommates and friends, Emily and Ashley, thank you for making me feel comfortable in a place where I knew no one and providing me with so much advice throughout the years. Emily, the house mom, thank you for all of the MCB advice and Ashley, thank you for all of the long immunology chats, even

if they were at 1am immunology in our the kitchen. To my kickball team, Kick In A Box, something I looked forward to every Friday night, kickball and Hotsy Totsy (and the occasional trip to Mel-o-dee's!). We never won the championship but came so close! Thomas and Nina, we met at kickball, but our friendship became so much more than that. Thank you for the unending support and always bringing so much positive energy into my life. Kathleen, my other kickball buddy, who was always willing to dance it up with me at Mel-o-dee's. Thank you for the life advice and the many delicious drinks at Tupper and Reed. To my thesis committee, Russell Vance, Michel DuPage and David Schaffer, your guidance and thoughtful discussions were instrumental in formulating my thesis. To the 4th floor immunology community, thank you for your constant feedback and support and for building a community that I will forever be grateful to have been a part of.

To my family, I cannot say thank you enough for love and support. When I made the decision to move to Berkeley for grad school, I was sad to be moving away from you all and missing out on various family gatherings. I always felt included, even from afar, and I thank you for that. Shelley and Sheryl, thank you for coming to visit with mom this last year. It was so fun having you here and being able to show you around Berkeley. Thank you both for the cards, congratulatory texts and never-ending support throughout my time in grad school. Jill and Steve, my second Mom and Dad. Thank you for taking me in one summer while I was completing an internship at the Mayo and spoiling me rotten. Thank you for always taking the time to chat with me on the phone and for always checking in.

To my brother, Kendall, I cannot thank you enough for all of the love and support you have shown me throughout grad school and beyond. Growing up, we were always friends, but you truly became someone I could rely on after I got sick. I know that was a hard time for you as well, but you always made a point of being there. I truly appreciate how much you call to check in and I couldn't ask for a better friend or brother. And to Kirsten, you came into the family right as I was getting ready to leave for Berkeley but have constantly made the effort to get to know me from afar. It has been amazing to have gained a sister and someone who has helped to make our family more complete. Thank you both for your constant love and support and for an amazing time when you came out to Berkeley for a visit. Thank you for always making it a priority to see me when I am home. And to you both, thank you for giving me my two best buds, Maeve and Fritz.

To my Mom and Dad (Pa), I owe everything to you both. Throughout my entire life you have supported whatever I have wanted to pursue. When I became sick, you both were my rocks, always by my side, someone I could lean on. That was the hardest time of my life, and I would not have made it through without you both. As I started down the path of research, you both were very encouraging, even when I had to go in on weekends to 'split atoms'. And when I decided to move to Berkeley for grad school, you were both so excited and supportive, even though it meant I would be far away. You are both always there when I need a shoulder to cry on and to celebrate all the highs of grad school with me. Pa, thank you for always providing the best entertainment and making me laugh when I need it the most. Mom, you are my best friend and don't know where I would be without you. Thank you both for your never-ending love and support. I love you both. This Ph.D. is for you.

Chapter 1
Introduction

Portions of this chapter were adapted and/or reprinted with permission from "Wolf NK*, Kissiov DU*, Raulet DH. Roles of natural killer cells in immunity to cancer, and applications to immunotherapy. Nature Reviews Immunology, *In press* 2022."

Introduction to the immune system

Every day our bodies encounter numerous microorganisms, including bacteria, viruses, fungi and parasites, that have evolved to invade our bodies and use us as hosts to live and replicate. Many of these microorganisms can lead to serious diseases, yet our bodies have developed a way to prevent illness from occurring, our immune systems. The immune system is a collection of many cells and processes which function together to act as a host defense system against unwarranted microorganisms. Our immune systems include two subsystems: the innate and the adaptive immune systems.

The innate immune system acts as the body's first line of defense, responding within minutes or hours to protect the host. The innate immune system in composed of anatomical barriers and numerous cells, such as phagocytic cells (dendritic cells, macrophages and neutrophils) and cytotoxic cells (natural killer cells). Innate immunity relies on pattern-recognition receptors (PRRs) to detect a wide variety of pathogens that share common features not normally found in mammalian cells, known as pathogen-associated molecular patterns (PAMPs). Examples of these include lipopolysaccharides (LPS), present in bacterial outer membranes, and foreign viral or bacterial nucleic acids. Additionally, the innate immune response can recognize tissue damage or cell stress through damage-associated molecular patterns (DAMPs), including extracellular ATP and cytosolic DNA. Some innate recognition, for example by NK cells, involves recognition of proteins that are induced by cell stress pathways as well. In addition, the loss of expression of key molecules, such as MHC molecules, can also be recognized by NK cells. Engagement of PRRs and other innate receptors triggers signals that activate a pro-inflammatory response through cell activation and cytokine production, or direct killing of infected cells, that can contain and eliminate infections. These many types of innate signals also help to activate and shape the adaptive immune response.

The adaptive immune system, led by T and B lymphocytes, uses incredible antigenic specificity to foreign microbes and is often indispensable in clearing an infection. Unlike the innate immune response, the adaptive immune response takes a few days to a week to develop after infection. T cells and B cells express rearranged antigen-specific receptors creating a large repertoire of cells capable of recognizing a near infinite number of antigens. Upon binding their cognate antigen, T cells and B cells undergo clonal expansion, giving rise to a large number of lymphocytes, each bearing a distinct antigen-specific receptor. After the infection is cleared, adaptive immunity retains immunological memory, to mount a response very quickly to subsequent infections. The coordination of the innate and adaptive immune systems helps to keep each of us alive and well.

Immune system and cancer

It has long been suggested that the immune system is important for recognizing and controlling cancer, but this belief was not widely accepted until the last decade or so. The idea

that the immune system could control cancer was first introduced by Paul Ehrlich in 1909 and again by Burnet and Thomas in the 1950's, the "cancer immunosurveillance" hypothesis (Kim et al., 2007). This hypothesis is based on the concept that tumors cells are recognized as 'non-self' and therefore can be targeted specifically. Cancer cells share 'hallmarks' which are acquired during their development. These include sustained proliferative signaling and replicative immortality, resistance to growth suppressors and apoptosis, induction of angiogenesis, and tissue invasion and metastasis (Hanahan and Weinberg, 2000) and more recently reprogramming of energy metabolism and evading immune destruction (Hanahan and Weinberg, 2011). These hallmarks are acquired through genomic instability generating mutations which in turn allow for adaptive immune cell recognition (Schumacher and Schreiber, 2015). Tumors can also trigger the innate immune response through DAMPs. In addition, natural killer cells, the cell type most studied in this thesis, have been implicated in immunosurveillance and tumor rejection.

Natural Killer cells

Natural killer (NK) cells are cytotoxic innate-like lymphocytes that are hardwired to recognize stressed cells, such as tumor cells and certain infected cells, and to mediate the killing of tumor cells. Unlike the specific recognition T cells and B cells display, NK cells recognize their target cells via a system of germline-encoded activating and inhibitory receptors that recognize membrane-bound ligands on potential target cells (Lanier, 2005; Vivier et al., 2011; Wolf et al., 2022b). As well as directly killing transformed cells, NK cells can produce pro-inflammatory cytokines, such as IFNγ and TNF, which can augment cell responses in the tumor microenvironment (Barry et al., 2018; Bottcher et al., 2018; Kearney et al., 2018). NK cell cytotoxicity involves the secretion of cytotoxic granules containing the pore-forming protein perforin and procaspase-cleaving granzyme B (GZMB), which triggers apoptosis in target cells (Voskoboinik et al., 2015). NK cells may also induce target cell apoptosis via the death receptors TRAIL and FASL (Zamai et al., 1998).

NK cell activating and inhibitory receptors

The NK activating and inhibitory receptors are summarized in Figure 1.1.. Inhibition and activation are integrated, or balanced against each other, such that inhibition may be overcome by strong activation and vice versa.

Among the activating receptors expressed by NK cells are the high-affinity Fc receptors CD16 and CD32, which efficiently trigger cytotoxicity and cytokine release and enable NK cells to kill antibody-coated cells via antibody-dependent cellular cytotoxicity (ADCC) (Bhatnagar et al., 2014). ADCC is a key activity of NK cells that is relevant for antibody-mediated cancer therapeutics.

Other activating receptors expressed by NK cells belong to various broad families, including C-type lectins (such as NKG2D and NK1.1), natural cytotoxicity receptors (NCRs, such as NKp46 in mouse and human, and NKp44 and NKp30 in human) and a few of the killer immunoglobulin-like receptors (KIRs) and Ly49 receptors (though most of those receptors are inhibitory). Activating NK receptors generally signal through associated signaling adapter proteins: for instance, NKG2D uses the DAP10 adaptor in humans and both DAP10 and DAP12

in mice; stimulatory KIRs signal with DAP12; NCRs with CD3ζ or FcRγ; CD16 with CD3ζ or FcRγ; and Ly49D and Ly49H with DAP12 (Barrow et al., 2019). Most of the adapters contain immunoreceptor tyrosine-based activation motifs (ITAMs) in their cytoplasmic domain, whereas DAP10 contains a distinct motif that recruits PI3 kinase.

With respect to tumor cell recognition, most of the relevant activating NK cell receptors recognize host gene-encoded ligands that are induced by cell stress pathways. Thus, NK cells are dedicated, in part, to eliminating stressed cells, such as cancer cells. Recognition of this type has been called 'induced-self recognition' and is best studied in the case of the NKG2D receptor. NKG2D recognizes numerous ligands, all of which are distant relatives of MHC I proteins. The human NKG2D ligands include MICA and MICB, and ULBP1-ULBP6. In mice the ligands include the RAE-1 family members (RAE-1α-RAE-1ε), MULT1, and three H60 isoforms (Raulet et al., 2013). NKG2D ligands are upregulated in response to heat shock-induced stress (Bauer et al., 1999; Nice et al., 2009), the DNA damage response pathway (Gasser et al., 2005), the integrated stress response (Gowen et al., 2015; Hosomi et al., 2017), cellular hyperproliferation (Jung et al., 2012), and activated p53 (Textor et al., 2011). With respect to the other NK cell activating receptors, NKp30 binds to B7-H6, which is also induced by the integrated stress response (Obiedat et al., 2020). The definition of ligands for the other activating NCRs on tumor cells has remained mostly elusive, although various immune molecules and glycans that bind these receptors have been reported (Barrow et al., 2017; Barrow et al., 2019; Narni-Mancinelli et al., 2017; Niehrs et al., 2019).

Most inhibitory receptors expressed by NK cells recognize MHC I molecules on target cells. Hence, target cells that express high levels of MHC I are better protected from NK cell killing, and MHC I loss results in increased NK cell-mediated killing. NK cell-mediated killing resulting from the loss of MHC I by a target cell is called 'missing-self recognition' (Liao et al., 1991; Ljunggren and Karre, 1990). Due to this property, NK cells are especially promising candidates for mediating therapy against MHC I-deficient tumors, which are resistant to recognition by $CD8^+$ T cells. Inhibitory receptors specific for MHC I signal through immunoreceptor tyrosine-based inhibitory motifs (ITIMs) in their cytoplasmic domains. In humans, the KIR family encodes approximately seven (depending on the genotype) inhibitory receptors, which discriminate different groups of HLA class I molecules (Pende et al., 2019). Mice lack KIR genes, but instead harbor a family of lectin-like Ly49 receptors, approximately seven of which are inhibitory and discriminate different H-2 class I molecules (Carlyle et al., 2008; Yokoyama and Seaman, 1993). In addition to these receptors, both humans and mice express a CD94–NKG2A heterodimeric receptor, which recognizes peptides derived from classical MHC I molecules, presented by the nonclassical HLA-E molecule (in humans) or Qa-1 molecule (in mice) (Lanier, 2005; Raulet et al., 2001). All of these receptors dampen or prevent killing of cells, including tumor cells, that express high levels of MHC I molecules. Furthermore, the different inhibitory receptors discriminate MHC I allelic products, and are distributed to different subsets of NK cells in an overlapping fashion. A consequence of this is that some NK cells in an individual may be uninhibited if they engage a tumor cell that selectively loses even one of its normal complement of MHC I molecules (Johansson et al., 2005; Ohlen et al., 1989), resulting in tumor cell killing. Greater killing is observed in the case of tumor cells that lose most or all MHC I expression, for example because of loss of expression of the MHC I light chain β2 microglobulin (Liao et al., 1991). Although MHC I-deficient cells are most efficiently killed by

NK cells, some tumor cells with normal expression of MHC I are sensitive to NK cell killing, presumably because they express sufficiently high levels of activating ligands to overcome inhibitory signaling (Cerwenka et al., 2001; Diefenbach et al., 2001). Therefore, the potential of NK cells in cancer therapy is not restricted to tumors with low MHC I expression.

NK cell cytotoxicity and activation

NK cell cytotoxicity involves the secretion of cytotoxic granules containing the pore-forming protein perforin and procaspase-cleaving granzyme B (GZMB), which triggers apoptosis in target cells (Voskoboinik et al., 2015). NK cells may also induce target cell apoptosis via the death receptors TRAIL and FASL (Zamai et al., 1998).

Although apoptosis has been considered the canonical mechanism of NK cell-mediated killing, recent work demonstrates that NK cells can also induce pyroptotic death in target cells, by multiple mechanisms. Once granzyme B from NK cells (or T cells) is delivered into target cells via cytotoxic granules it can cleave not only caspase 3 to induce apoptosis, but gasdermin E, if the cells express it. Cleaved gasdermin E can insert into membranes, resulting in pyroptosis (Zhang et al., 2020). Caspase 3 can also cleave and activate gasdermin E. In addition to granzyme B, cytotoxic granules in both NK cells and T cells contain granzyme A, which can induce pyroptotic death in cells expressing gasdermin B (Zhou et al., 2020b). Gasdermin B is highly expressed in the epithelia of the digestive tract and tumors derived therefrom. If the activation of pyroptosis results in the release of inflammatory cytokines or other pro-inflammatory mediators, it can drive a feed-forward process that amplifies both natural and therapy-induced antitumor immune responses (Nicolai and Raulet, 2020).

NK cells also exert antitumor effects through secretion of chemokines and cytokines, which can directly and indirectly recruit other immune cells and induce cytotoxic and cytostatic effects on target cells, in addition to further stimulating broader cellular immune responses. Interferon-γ (IFNγ) and tumor necrosis factor α (TNFα) produced by stimulated NK cells can mediate tumor cell death (Wang et al., 2012). In addition, IFNγ stimulates upregulation of MHC II molecules on antigen-presenting cells (APCs), macrophage activation and augmented priming of T cell responses (Scharton and Scott, 1993). NK cells also produce chemokines that recruit and activate key APCs at the tissue site of insult (Barry et al., 2018; Bottcher et al., 2018), thereby amplifying T cell immunity. These findings provide further impetus for cancer therapies focused on amplifying NK cell responses in tumors.

The degree to which NK cells are active against tumor cells is highly dependent on the activation state of the NK cells, which is regulated in large part by cytokines derived from other innate immune cells, including dendritic cells (DCs) and monocytes (Raulet, 2004; Wagner et al., 2017). Several cytokines serve overlapping and distinct roles in NK cell activation, including cytokines that signal through the common γ chain (chiefly IL-2 and IL-15), IL-12 and IL-18, and type I interferons (Wiedemann et al., 2021). In addition to supporting NK cell proliferation and survival, IL-15 and IL-2 promote stronger cytotoxic activity by NK cells (Wagner et al., 2017) (including ADCC (Zhang et al., 2018a)), induce human NK cell expression of the activating receptors NKp44 and NKp30 (Paust et al., 2017), and augment NK cell expression of the NKG2D activating receptor (Wagner et al., 2017). IL-12 and IL-18 synergistically stimulate the

production of IFNγ by NK cells (Robinson et al., 1997; Tomura et al., 1998). Type I IFN also plays a critical role in activating NK cells, acting directly on NK cells to induce effector molecules such as granzyme B (Martinez et al., 2008; Nicolai et al., 2020) and protecting the cells from fratricide by other NK cells (Madera et al., 2016). Type I IFN also acts indirectly by inducing production of IL-15 by DCs and other cell types (Mattei et al., 2001), which then may act on NK cells (Nicolai et al., 2020).

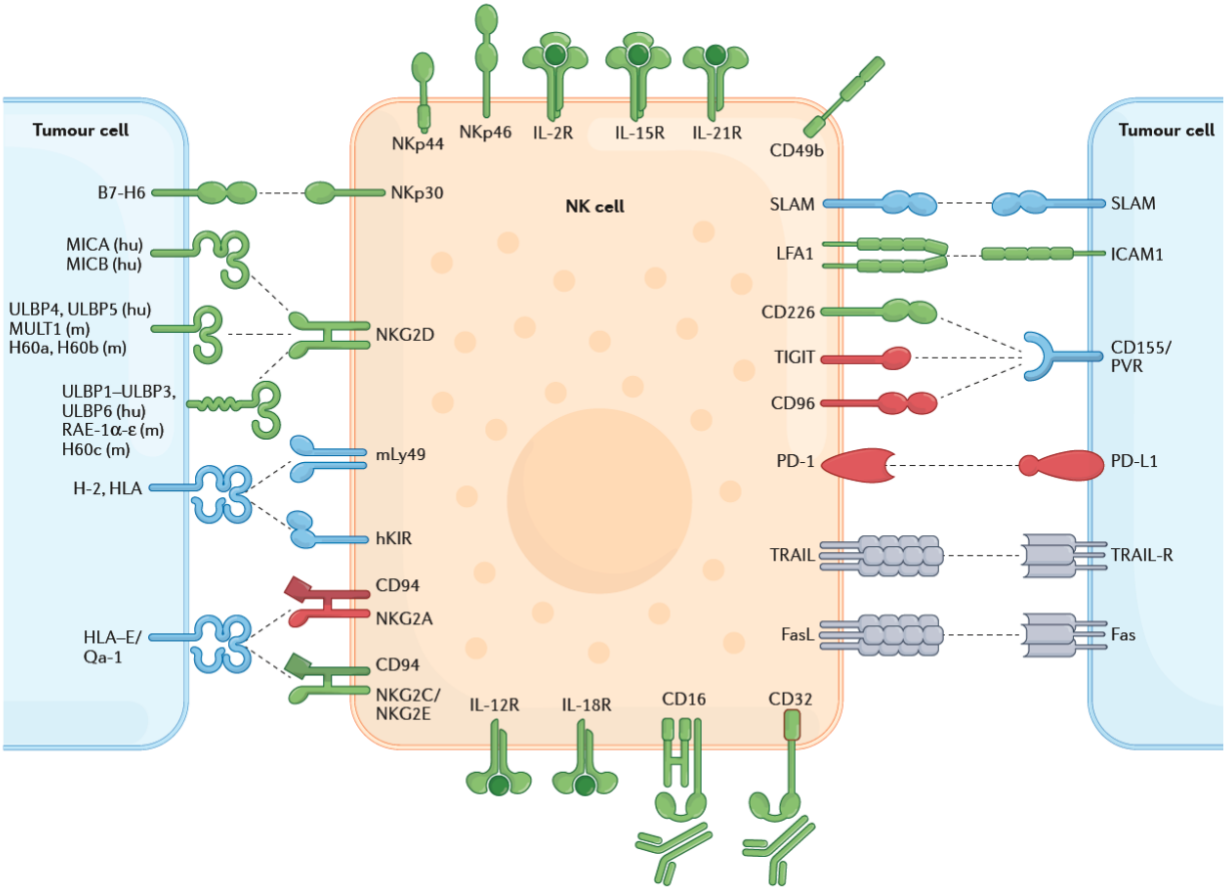

Figure 1.1. NK cell function is regulated by cell surface receptors and cytokines. The figure depicts receptor–ligand interactions that activate (depicted in green) or inhibit (depicted in red) NK cell responses against tumor cells and other cells, or that can either activate or inhibit NK cells depending on the specific family member or the context (blue receptors). Some ligands bind to both inhibitory and activating receptors on NK cells, as indicated. SLAM receptors can impart activating or inhibitory signals depending on expression of adapter proteins by NK cells. Key cytokine receptors are also depicted. The receptors for different IL-2 family cytokines consist of multiple chains, of which one (gamma) is a shared signaling component.

Spontaneous NK cell responses to cancer

Numerous studies suggest a role for NK cells in tumor immunosurveillance. It is well established that NK cells potently eliminate various tumor cell lines injected at low doses into

syngeneic mice (Cerwenka et al., 2001; Diefenbach et al., 2001; Karre et al., 1986; Seaman et al., 1987), but the more revealing studies employed spontaneous models of cancer. Long-term depletion of NK cells resulted in higher incidence or severity of cancer in a carcinogen-induced (methylcholanthrene) model of sarcoma and in a spontaneous B lymphoma model in mice (Smyth et al., 2001; Street et al., 2004), suggesting that NK cells normally suppress the development of such tumors. Additional evidence supporting a role for NK cells comes from studies showing a higher incidence of spontaneous tumors, or of aggressive tumors, in mouse models of cancer where the mice lack the key activating receptor NKG2D, though those receptors are expressed by some non-NK cells as well (Guerra et al., 2008). Furthermore, aggressive tumors arising in one such model of cancer were devoid of NKG2D ligands when the host mice were wild-type for *Nkg2d*, but expressed NKG2D ligands when the host lacked the NKG2D receptor. These data suggested that tumor cells that grew out in the wild-type mice had been selected for loss of NKG2D ligands (Guerra et al., 2008). Another line of evidence indicated that early infiltration of tumors with IFNγ producing NK cells was associated with remodeling of the tumor microenvironment and unleashed cytotoxic T lymphocyte (CTL)-mediated tumor eradication in mouse cancer models (Bonavita et al., 2020).

Consistent with the evidence that NK cells have a role in suppressing malignancies in mice, numerous studies from the cancer genome atlas (TCGA) have associated NK cell infiltration with overall survival outcomes in several types of cancer, including melanoma, breast cancer, glioma, lung adenocarcinoma and others (Bonavita et al., 2020; Bottcher et al., 2018; Cozar et al., 2021; Cursons et al., 2019; Marcus et al., 2018; Varn et al., 2017). A caveat to these association studies is that infiltration of tumors by T cell and NK cells is generally correlated. This correlation is consistent with evidence that NK cells play a role in promoting the antitumor T cell responses but can make it difficult to disaggregate the contributions of each cell type in different types of cancer.

Tumor elimination by NK cells in spontaneous or tumor-transfer models of cancer is often dependent on perforin expression, suggesting a key role for direct tumor killing. However, recent studies indicate an important role for NK cells as sentinels that detect nascent tumors and mobilize more potent immune responses by recruiting DCs to the tumor microenvironment (TME). NK cell-derived CC-chemokine ligand 5 (CCL5) and XC chemokine ligand 1 (XCL1) were shown to play critical roles in recruiting cDC1s to tumors under experimental conditions (Bottcher et al., 2018). Furthermore, intratumoral NK cells are a major source of FLT3 ligand within tumors, which stimulates cDC1 differentiation and expansion (Barry et al., 2018). Activated cDC1s activate anti-tumor responses, including T cell responses. Therefore, tumor infiltration by NK cells that mobilize intratumoral cDC1 populations is likely to be a key step in anti-tumor immunity, at least in some contexts. Furthermore, features of the TME, such as production of prostaglandins, were shown to impair NK cell-mediated recruitment cDC1s (Bottcher et al., 2018; Zelenay et al., 2015). These findings provide further impetus for the use of cancer therapies that stimulate the recruitment of NK cells to tumors.

Tumor evasion of NK cell surveillance

Evasion of immunity is a hallmark of established tumors. Escape mechanisms include adaptations that prevent NK cell activation or recruitment to tumors or that suppress tumor cell killing by NK cells. Some of these adaptations similarly impact T cell responses.

Numerous molecules produced in the TME are broadly immunosuppressive (Melaiu et al., 2019). Extracellular adenosine and prostaglandins are small molecules that are commonly produced in the TME and clearly suppress NK cell activity (Young et al., 2018; Zelenay et al., 2015). Suppressive cytokines, such as TGFβ, also impact NK cells, in part by suppressing expression of the NKG2D and NKp30 activating receptors (Castriconi et al., 2003) and in part by converting NK cells into intermediate type 1 innate lymphoid cells (intILC1) and ILC1 populations in the TME (Gao et al., 2017). TGFβ may also act indirectly by supporting the differentiation of regulatory T (Treg) cells, which can suppress NK cell as well as T cell responses (Ghiringhelli et al., 2006; Kerdiles et al., 2013). Myeloid-derived suppressor cells and tumor-associated macrophage populations also suppress responses of both NK cells and T cells (Bruno et al., 2019).

The antitumor activity of NK cells, like that of T cells, is generally dampened in obesity (Michelet et al., 2018), and this is associated with metabolic reprogramming of NK cells in the TME (Poznanski et al., 2021). Metabolic states impact spontaneous and therapy-induced NK cell responses to cancer (O'Shea and Hogan, 2019; Terren et al., 2020; Terren et al., 2019).

Additional mechanisms of tumor cell escape from NK cell surveillance involve inhibitory receptor engagement. NK cells express inhibitory receptors that engage MHC I molecules, but also can display other inhibitory receptors, including the immune checkpoint receptors T cell immunoreceptor with Ig and ITIM domains (TIGIT), CD96, PD-1 and SIRPα (Chan et al., 2014; Concha-Benavente et al., 2018; Deuse et al., 2021; Hsu et al., 2018; Stanietsky et al., 2009). Tumor cells may upregulate ligands for these receptors and thus inhibit NK cell-mediated antitumor effects. Certain inhibitory receptors, such as PD-1 and SIRPα, are upregulated on NK cells after activation or specifically in tumors. Some of the inhibitory ligands, such as the PD-L1 ligand for PD-1, are upregulated due to the action of immuno-stimulatory molecules such as type I IFN or IFNγ, whereas others may be adaptations arising from genetic or epigenetic changes in tumors followed by selection of tumors resistant to immunosurveillance.

Another mechanism of escape is that NK cells within tumors often acquire a desensitized hyporesponsive state, similar to the hyporesponsive state of NK cells in mice that fail to express MHC I-specific inhibitory receptors (Ardolino et al., 2014; Bi and Tian, 2017). A comparison of infiltrating immune cells in wild-type mice harboring implanted MHC I-sufficient or MHC I-deficient tumors showed that NK cells within progressing MHC I-deficient tumors acquired a dysfunctional state, whereas those within MHC I-expressing tumors were more functional (Ardolino et al., 2014).

NK cell desensitization also occurs when NK cells are persistently exposed to NK-activating ligands in vivo. This occurs in many or most tumors (Coudert et al., 2008), but also in disease-free states, as endothelial cells and other cells in healthy mice express activating NKG2D ligands (Thompson et al., 2017). Expression of such ligands was strongly increased on endothelial cells in the tumor vasculature, raising the possibility that desensitization could

significantly impair antitumor responses mediated by NK cells (Thompson et al., 2017). In mouse models, macrophages in tumors also upregulate NKG2D ligands in response to colony-stimulating factor 1 (CSF1, also known as M-CSF) produced by tumor cells (Thompson et al., 2018). However, definitive evidence is lacking that interactions of NK cells with NKG2D ligands expressed by macrophages causes desensitization of NK cells within tumors.

The cGAS-STING pathway and agents that stimulate innate immunity

The innate immune pathway, the cyclic guanosine monophosphate-adenosine monophosphate synthase–stimulator of interferon genes (cGAS-STING) pathway, has shown to be promising as a therapeutic target. The cytosolic sensor, cGAS, generates the second messenger 2',3' cyclic guanosine monophosphate–adenosine monophosphate (cGAMP) in response to binding double-stranded DNA (Diner et al., 2013; Wu et al., 2013). cGAMP binds and activates the ER membrane stimulator of interferon genes, STING, leading to activation of both IRF3 and NF-kB pathways, and the abundant production of type I interferons and other inflammatory cytokines (Ishikawa and Barber, 2008).

In DNA virus infections, accumulation of viral DNA in the cytosol is thought to trigger cGAS to initiate antiviral immune responses. In the case of cancer cells, chromosomal instability — a hallmark of cancer and/or mitochondrial dysfunction — can lead to accumulation of DNA in the cytosol (Harding et al., 2017; Ho et al., 2016; Lam et al., 2014). This in turn can activate the cGAS-STING pathway through the production and transfer of cGAMP to other cells that can activate STING promoting activation of both CD8 T cells and NK cells (Marcus et al., 2018; Woo et al., 2014). In some tumor cells, STING activation likely occurs in the same cancer cells in which cGAS activation and cGAMP production occurs, and this may be adequate to drive sufficient production of cytokines by the tumor cells to activate NK cell and T cell responses. In other tumors, however, repression of transcription of STING, TBK1 and/or other genes in tumor cells can thwart the production of immune-stimulating cytokines and other mediators by cancer cells themselves(Xia et al., 2016a; Xia et al., 2016b; Yang et al., 2013a). Accumulating evidence indicates that these defects can be overcome by mechanisms that transport 2'3' cGAMP produced in cancer cells to nearby cells such as myeloid cells (Marcus et al., 2018). STING activation in those cells supports an antitumor immune response(Carozza et al., 2020; Marcus et al., 2018; Schadt et al., 2019). Recently identified membrane transporters of 2'3' cGAMP, including SLC19A1 LRCC8 and SLC46 proteins (Cordova et al., 2021; Lahey et al., 2020; Luteijn et al., 2019; Ritchie et al., 2019; Zhou et al., 2020a), may mediate the transport of 2'3' cGAMP from tumor cells to myeloid cells and other cells in the TME, enabling local immune activation and an antitumor cellular immune response.

With respect to initiating NK cell (and T cell responses), several mechanisms impair activation of the cGAS-STING pathway in the context of cancer. cGAS expression is repressed in some tumours, preventing production of cGAMP that serves to initiate the immune response (Konno et al., 2018). Perhaps more commonly, the capacity of cancer cells to produce immunoactivating cytokines following cGAS activation is stymied due to downregulation of STING, TBK1 and other intermediates in the pathway (Konno et al., 2018; Xia et al., 2016a; Xia et al., 2016b; Yang et al., 2013a). In this case, however, transfer of cGAMP from tumor cells to neighbouring cells can bypass STING deficiency (Marcus et al., 2018). Cancer cells can counter

this bypass mechanism by producing excess ENPP1, an extracellular enzyme that degrades cGAMP, and has the additional effect of generating AMP in the process, which is converted into immunosuppressive adenosine (Carozza et al., 2020; Li et al., 2021). Hence, ENPP1 expression in cancer correlates with reduced infiltration of immune cells and increased metastasis, and agents that inhibit ENPP1 are being tested for their capacity to promote antitumor immune responses.

NK cell activity can be strongly amplified by activators of innate immunity, such as pathogen associated molecular patterns (PAMPs). More recently, evidence has accumulated that STING agonists, such as cyclic dinucleotides, are potent NK cell activators (Marcus et al., 2018; McWhirter et al., 2009). In work which I contributed to, injection of STING agonists into tumors mobilized powerful NK cell-mediated antitumor responses in six different MHC I-deficient tumor transplant models in mice (Nicolai et al., 2020). One to three injections of the synthetic STING agonist 2'3' RR-c-di-AMP into established subcutaneous tumors resulted in NK cell-dependent tumor rejection and long-term survival of 50% or more of the mice in four of the six models tested, most of which were solid tumor models. $CD8^+$ T cells played no role in these antitumor responses. This study is one of several showing the potential for NK cells in the therapeutic rejection of solid tumors (Ni et al., 2012; Nicolai et al., 2020; Wolf et al., 2022a). Furthermore, the STING agonist induced potent systemic antitumor effects that impacted the growth of tumors distant from the injection site. These findings suggest that activation of STING locally is sufficient to engender powerful NK cell-dependent tumor rejection responses. The results further suggest that the spontaneous activation of the STING pathway by tumor-derived cGAMP (Marcus et al., 2018), mentioned previously in this review, provides relatively weak activating signals that are insufficient for clearance of established tumors, perhaps because the amount of cGAMP produced by tumors is limiting. Analysis of tumor rejection induced by a STING agonist in one MHC I-deficient model demonstrated that the response was dependent on type I interferon, which acted directly on NK cells but also indirectly on DCs, where it induced IL-15–IL-15Rα complexes on the cell membrane (Nicolai et al., 2020).

As an alternative approach to circumvent the need for intratumoral injections and to mimic aspects of clinical practice, hydrogels containing 2'3' RR-c-di-AMP were implanted at the site of primary tumor resections in MHC I^+ mouse models (Park et al., 2018). In a breast and a lung adenocarcinoma model, this led to improved tumor-free survival compared to intratumoral injections, via the action of both $CD8^+$ T cells and NK cells. This approach prevented local tumor reoccurrences and induced systemic antitumor immunity.

Clinical trials with locally applied STING agonists showed that patients tolerated the treatments, but little efficacy has been reported so far (Harrington et al., 2018; Meric-Bernstam et al., 2019). Improvements are likely to be in store, as groups have developed orally available STING agonists/mimetics that are effective in animal models (Chin et al., 2020; Pan et al., 2020), and various combination therapies are being tested in conjunction with these and other STING agonists.

IL-2 cytokine and superkines

IL-2, originally described as a T cell growth factor, also stimulates NK cell activation and proliferation. Culturing of peripheral blood lymphocytes (PBLs) with high dose IL-2 leads to the outgrowth of lymphocyte activated killer (LAK) cells that lyse freshly isolated tumor cells, and many of these LAK cells are NK cells (Rosenberg et al., 1985). Adoptive transfer of LAK cells in combination with low-dose IL-2 injections has been shown to inhibit metastases formation in vivo in a melanoma model in mice. High dose IL-2 immunotherapy resulted in long-term survival of a small percentage of patients with metastatic renal carcinoma and metastatic melanoma (Waldmann, 2006), which led to FDA approval of IL-2 for these indications. The degree to which NK cells, as opposed to T cells, mediated these effects is not known. Moreover, the low rate of efficacy and the high toxicity of high dose IL-2 therapy — with adverse events including vascular leak syndrome, heart failure and liver damage (Rosenberg et al., 1987) — has limited the utility of this approach in the clinic. Another problematic aspect of this approach is that IL-2 administration selectively expands Treg cell populations, which may counteract the beneficial effects of the therapy.

To optimize the efficacy of IL-2 as an immunotherapeutic agent, groups have modified or engineered IL-2. One approach has been to extend the in vivo half-life of the molecule, which can be accomplished by fusing cytokines to albumin (Zhu et al., 2015) or Fc domains of antibodies, or by conjugation of polyethylene glycol (PEG) to the molecule (Charych et al., 2016). A variant of IL-2, known as bempegaldesleukin (formerly NKTR-214), is a PEGylated version of the molecule. In addition to extending the in vivo half-life of the protein, PEGylation selectively masks the region of IL-2 that binds to IL-2Rα, making it an IL-2Rβγ-biased cytokine (Charych et al., 2016). Compared to IL-2 administration, bempegaldesleukin administration resulted in the selective expansion of $CD8^+$ T cells and NK cells and a higher $CD8^+$ T cell:Treg cell ratio. Bempegaldesleukin therapy showed better single agent efficacy than IL-2 against transplanted melanoma tumors in mice. It provided synergistic antitumour activity in combination with anti-CTLA4 in mouse tumour models, and was well-tolerated in non-human primates, with no evidence of vascular leak syndrome, a common side effect of IL-2 therapy. Bempegaldesleukin is well tolerated in patients (Bentebibel et al., 2019) and is currently being tested in combination with nivolumab (a PD-1 inhibitor) in numerous Phase II and III clinical trials. However, recent results from Nektar's Phase III clinical trial were disappointing (BMS and Nektar).

Another powerful approach has been to engineer the molecule to alter its binding to IL-2 receptor components. Native IL-2 binds with high affinity to IL-2Rα (highly expressed by Treg cells) and with low affinity to IL-2Rβ, meaning that very high concentrations of IL-2 are required to stimulate cells that lack IL-2Rα, which is the case for most NK cells and resting T cells. A mutant form of IL-2 called super-2, or H9, was selected with five amino acid substitutions that together increase the binding affinity to IL-2Rβ by 200-fold (Levin et al., 2012). Super-2 showed very potent activity in stimulating NK cells. Furthermore, compared to IL-2, super-2 administration resulted in accumulation of fewer Treg cells, and lower toxicity, despite the fact that super-2 retains its capacity to bind IL-2Rα. Importantly, in syngeneic mouse tumor models, super-2 showed better single agent efficacy against melanoma, colon carcinoma and lung adenocarcinoma tumors than IL-2 (Levin et al., 2012).

An important feature of super-2 is its potential ability to reverse or delay the previously discussed desensitization of NK cells that occurs in tumors (Ardolino et al., 2014). Administration of super-2 in mice with established MHC I-deficient tumors sustained tumor control in an NK-dependent fashion. Future clinical studies will address whether super-2, or similar superkines that do not bind at all to IL-2Rα (Mullard, 2021; Silva et al., 2019; Wolf et al., 2022a), provide benefit to cancer patients.

Dissertation question and overview

Great advances have been made in the immunotherapy field over the past decade, vastly improving patient outcomes over that of traditional therapies (Kalbasi and Ribas, 2020; Sharma et al., 2021). Many current cancer immunotherapies are targeted at mobilizing CD8 T cells, but numerous tumors have few or no antigens for CD8 T cells, or have lost MHC I thereby evading CD8 T cell responses. There is therefore a need to improve on these therapies by mobilizing other immune cells to the tumor microenvironment, such as NK cells. A recent therapy candidate, cyclic dinucleotide (CDN), has been used to activate the cGAS-STING pathway of the innate immune system. Recently, it has been shown that intratumoral CDN injection can induce primary tumor regression and that type I IFNs produced downstream of STING amplify the CD8 T cell response. MHC I-deficient tumors are not susceptible to CD8 T cell-mediated rejection, but data from our lab has shown STING activation resulted in remissions of >50% of tumors in four of the six MHC I-deficient models studied. In two models, the rate of permanent remissions was much lower: ~20% in the MC38-*B2m-/-* model and 0% in the B16-F10-*B2m-/-* model (Nicolai et al., 2020). At the same time, early phase clinical trials of STING agonists in patients have not yielded sustained clinical remissions (Harrington et al., 2018; Meric-Bernstam et al., 2019), indicating a need for improvements in this immunotherapy approach.

My thesis focuses on boosting CDN therapy in MHC I-deficient and MHC I+ tumor models through the addition of an engineered IL-2 superkine, H9-MSA, to enhance the antitumor response of NK cells and T cells. In chapter 3 of this dissertation, I detail results showing that engineered IL-2 family cytokines synergize with CDN therapy to mobilize anti-tumor responses by NK cells and in some cases CD4 T cells in the rejection of MHC I-deficient tumor models. I show in our *B2m*-/- tumor models that the anti-tumor responses are due, in part at least, to sustained activation and cytotoxicity of NK cells. In chapter 4, I examine the role of T cells in mediating tumor rejection after CDN/H9-MSA therapy in both MHC I-deficient and MHC I+ tumor models. And finally, in chapter 5, I examine the addition of numerous therapies to the CDN/H9-MSA combination treatment to try to enhance NK cell and T cell antitumor responses. Overall, this work is significant in exploring the role of combination therapy to enhance the responsiveness of NK cells and T cells to exert stronger antitumor activity.

Chapter 2
Methodology

Study Design

For most experiments in this study, tumors were established s.c. in mice, PBS or CDN was injected i.t. once, and PBS or H9-MSA was injected i.p. multiple times. Tumor growth, toxicity, overall survival, and NK cell activation status were recorded. Male and female mice were used equally within an experiment, and treatments were randomized among mice in the same cage. Experimental groups consisted of 5 to 10 mice. Mice were terminated in the studies when tumors reached an average diameter of 1.5 cm or mice showed a body condition score of less than 2. We did not use a power analysis to calculate sample size. All experiments were performed at least twice and, in some cases, experiments were pooled. The investigators were not blinded.

Mouse strains

Mice were maintained at the University of California, Berkeley. C57BL/6J and *Rag2-/-* mice were purchased from the Jackson Laboratory. NK-DTA mice were generated in our laboratory by breeding $Ncr1^{iCre}$ to $Rosa26^{LSL\text{-}DTA}$ (Jackson Labratories). All mice used were between 8 and 20 weeks of age. All experiments were approved by the University of California (UC) Berkeley Animal Care and Use Committee and were performed in adherence to the NIH Guide for the Care and Use of Laboratory Animals (National Research Council Committee for the Update of the Guide for the and Use of Laboratory, 2011).

Cell lines and culture conditions

B16-F10 cells (obtained from the UC Berkeley Cell Culture Facility) and MC38 cells, obtained from JP Allison (M.D. Anderson Cancer Center, Houston TX, USA) were cultured in Dulbecco's modified Eagle's medium (ThermoFisher Scientific). RMA cells (obtained from Michael Bevan, who received it from Dr. K. Karre, Karolinska Institute, Stockholm, Sweden) were cultured in RPMI 1640 medium (ThermoFisher Scientific). *B2m-/-* versions of B16-F10, MC38 and RMA were previously generated in the lab using CRISPR-Cas9 (Nicolai et al., 2020). In all cases, medium contained 5% fetal bovine serum (FBS) (Omega Scientific), 0.2 mg/mL glutamine (Sigma-Aldrich), 100 U/mL penicillin (ThermoFisher Scientific), 100 mg/mL streptomycin (ThermoFisher Scientific), 10 μg/mL gentamycin sulfate (ThermoFisher Scientific), 50 μM β-mercaptoethanol (EMD Biosciences), and 20 mM Hepes (ThermoFisher Scientific). Cells were cultured in 5% CO_2. All cell lines tested negative for mycoplasma contamination.

Protein Design and Purification

H9, H9-MSA and IL-2-MSA were purified by Dr Lora Picton in the laboratory of our collaborator KC Garcia (Stanford University). DNA encoding wild-type human IL-2 or human IL-2 with H9 mutations (L80F, R81D, L85V, I86V, I92F) (*35*) was cloned into the insect expression vector pAcGP67-A, which includes a C-terminal 8xHIS tag for affinity purification. DNA encoding mouse serum albumin (MSA) was purchased from Integrated DNA Technologies (IDT) and cloned into pAcGP67-A as an N-terminal fusion between the N-terminus of hIL-2 and C-terminus of MSA (indicated as IL-2-MSA or H9-MSA).

Insect expression DNA constructs were transfected into Trichoplusia ni (High Five) cells (Invitrogen) using the BaculoGold baculovirus expression system (BD Biosciences) for secretion and purified from the clarified supernatant via Ni-NTA followed by size exclusion chromatography with a Superdex-200 column and formulated in sterile Phosphate Buffer Saline (PBS) (Gibco). Endotoxin was removed using the Proteus NoEndo HC Spin column kit following the manufacturer's recommendations (VivaProducts) and removal (to a final amount of between 0.01-1.1 EU/mg of protein) was confirmed using the Pierce LAL Chromogenic Endoxotin Quantification Kit (ThermoFisher). IL-2 proteins were concentrated and stored at -80 °C until use.

In vivo tumor transplant experiments

Cells were washed and resuspended in PBS (ThermoFisher Scientific). 100 μl containing 4×10^6 cells were injected s.c.. Tumor volume was estimated using the ellipsoid formula: $V = (4/3)\pi abc$ where a, b and c correspond to height, width and length of the tumors measured with digital calipers. Five days after tumor cell inoculation, when tumors reached a volume of 50 mm^3, they were injected i.t. with PBS or 50 μg of the STING agonist mixed-linkage [2′3′] dithio-(Rp, Rp) cyclic diadenosine monophosphate (ADU-S100, abbreviated as CDN in this paper, a gift of Aduro Biotech) in a total volume of 100 μl PBS. Mice were also injected i.p. with PBS, 20 μg of H9, 10 μg of IL-2-MSA or 10 μg H9-MSA in a total volume of 100 μl PBS, which was repeated every three days (except for Fig. S1, where it was repeated every two days) until the mice were euthanized or one week after a mouse had no palpable tumor. In some experiments, after tumor cell inoculation, tumors were grown to either 150 mm^3, 300 mm^3 or 450 mm^3 before being treated with CDN/H9-MSA.

Bilateral tumor experiments

All mice were depleted of CD4 and CD8 T cells. Tumor cells were washed and resuspended in PBS. 100 μl containing 4×10^6 cells were injected subcutaneously on the right flank of the mice and 100 μl containing 2×10^6 were injected subcutaneously on the left flank of the mice. Tumor growth was measured using digital calipers and tumor volume was estimated using the ellipsoid formula: $V = (4/3)\pi abc$. Five days after tumor inoculation, when the right flank tumors were ~50 to 100 mm^3, the right flank tumors were injected intratumorally with PBS or CDN and the mice were treated i.p. with H9-MSA or PBS as described above for single tumor experiments.

Co-housing pet-store mice experiments

Female mice were purchased from a local pet store and tested in the facility for pathogens. 7-week-old female C57BL/6J mice were purchased from Jackson Laboratory. Eight C57BL/6J mice were combined with one pet store mouse in each rat cage and co-housed together for 60 days. C57BL/6J mice were weighed every day for the first 10 days and then once every week thereafter. Mice that exhibited >15% weight loss during the co-housing period or displayed a body score less than 2 were terminated in the study. In our study, 14/40 mice survived the co-housing period. After the 60-day co-housing period, the pet-store mice were

euthanized and the C57BL/6J mice were injected with 4×10^6 cells MC38 *B2m*-/- cells s.c. as described in the in vivo transplant experiment section.

Methylcholanthrene (MCA)-induced sarcoma experiments

Mice were injected subcutaneously on the right flank with 100 mg of 3-methylcholanthrene (MCA) (Crescent Chemical) in peanut oil, after which they were monitored weekly. When palpable tumors (~50 mm^3) were detected, usually 8-10 weeks after MCA injection, the mice were randomized and entered into the study. Tumors were injected i.t. with PBS or 50 μg of CDN in a total volume of 100 μl PBS on days 0, 3, and 6, which was repeated every 6 six days. Mice were also injected intraperitoneally with PBS or 10 μg H9-MSA in a total volume of 100 μl PBS starting on day 0, which was repeated every three days

In vivo cellular depletions and cytokine blockade

For cellular depletion experiments, mice were depleted of NK cells, CD8 cells and/or CD4 cells by i.p. injections of 200 μg of anti-NK1.1 (clone PK136, purified in our laboratory), anti-CD8b.2 (clone 53-5.8, Leinco) or anti-CD4 (clone GK1.5, Leinco), respectively, 2 days and 1 day before initiation of therapy, and again every six days thereafter until mice were euthanized or no palpable tumor was detected for one week. Whole rat immunoglobulin G (IgG; Jackson ImmunoResearch) was used as a control for depletions. Depletions were confirmed by flow cytometry.

In some experiments, mice received 500 μg of anti-IFNAR-1 (clone MAR1-5A3, Leinco), 200 μg anti-TNF-α (clone TN3-19.12, Leinco), 100 μg anti-GR-1 (clone RB6-8C5, Leinco), 200 μg anti-Ly6G (clone 1A8, Leinco), 200 μg anti-IL-5 (clone TRFK5, Leinco), 200 μl Clodronate Liposomes (Liposoma) or control rat IgG i.p. in a volume of 100 μL PBS i.p. on days -1 and 0 before the initiation of therapy, and again every three days throughout the experiment.

Additional therapies (Innate stimulants, cytokine therapy, and checkpoint blockade therapy

For the comparison of innate stimulants, mice were injected i.t. with PBS or 50 μg of either CDN, CpG ODN DS-L03 (Invivogen), HMW PolyI:C (Invivogen) or R848 (Invivogen) in a total volume of 100 μl PBS.

For additional cytokine therapy, mice received of 100 ng recombinant IL-12 (p70) (Biolegend) and 100 ng recombinant IL-18 (Biolegend) each in a total volume of 100 uL PBS i.p. starting on day 0 and repeated every 3 days.

For RAE-1ε blockade, mice received 200 μg anti-RAE-1ε (Innate Pharma) in a volume of 100 μL PBS i.p., starting on day 0 and repeated every three days.

For checkpoint blockade, in addition to CDN and/or H9-MSA treatment, mice received either 200 μg anti-CD137 (41BB, clone 3H3, Leinco), 200 μg anti-PD-1 (clone RMP1-14, Leinco), 200 μg anti-CTLA4 (clone 9H10, Leinco), or 200 μg anti-TIGIT (either clone

MUR10A from Arcus Biosciences or 1G9 from BioXCell) each in a volume of 100 μl PBS i.p., every three days. In the MCA experiments, some of the mice received a combination of anti-TIGIT and anti-PD-1; in most of these mice, the anti-TIGIT treatment was staggered 1 day after anti-PD-1 treatment, but in some cases the two antibodies were injected on the same day.

Oral drug delivery

In some experiments, tumor bearing mice received experimental drugs, AB928 and TPST-1495, by oral administration. AB928 was formulated in a PEG:Solutol solution (provided by Arcus Biosciences), which was kept in solution throughout dosing by stirring it at 420 RPM on a heated stir plate at 40C. Mice were treated with 100 mg/kg of AB928 or PEG:Solutol solution twice daily by oral gavage.

TPST-1495 (provided by Tempest Therapeutics) was resuspended to a final concentration of 110 mg/mL in 0.5% 400cps methylcellulose by sonication and gentle heating. The solution was stable at 4C for 15 days. Mice were treated with 100 mg/kg of TPST-1495 or 0.5% 400cps methylcellulose twice daily by oral gavage.

Toxicity

To assess toxicity of therapies, tumors were established, and the baseline weights were recorded just before therapies were initiated as described. Mouse weights were recorded daily. Mice appearing to experience toxicity through a loss in body weight were assessed for a known IL-2 toxicity, pulmonary edema. Pulmonary edema was determined by measuring lung wet weight/body weight ratios six days after initiating treatment.

Flow cytometry

Single-cell suspensions of tumors were generated by dicing tumors with a razor blade followed by enzymatic digestion for 30 minutes at 37C in medium containing 1 mg/mL Collagenase D (Roche Diagnostics) and 1mg/mL DNase I (ThermoFisher Scientific). The samples were further dissociated in a gentleMACS Dissociator (Miltenyi) before passage through a 70-μm filter. Cells were stained directly for determining NK cell numbers and Ki67 staining or incubated for 4 hours in medium containing Brefeldin A (Biolegend) and Monensin (Biolegend) for granzyme B staining before surface staining and intracellular staining. LIVE/DEAD stain (ThermoFisher Scientific) was used to exclude dead cells. Before staining with antibodies, FcgRII/III receptors were blocked by resuspending the cells in 50 μl undiluted culture supernatant of the 2.4G2 hybridoma cell line (prepared in the lab) and incubating for 20 minutes at 4C. Cells were washed in PBS containing 2.5% FCS and stained with antibodies directly conjugated to fluorochromes for 30 minutes at 4C in the same buffer. For intracellular staining of granzyme B and Ki67, cells were fixed and permeabilized using Cytofix/Cytoperm buffer (BD Biosciences) and stained with antibodies directly conjugated to fluorochromes for 1hr at RT in 1X Perm/Wash buffer (BD Biosciences). NK cells were gated as viable, $CD45^+$, $CD3^-$, $CD19^-$, $F4/80^-$, $Ter119^-$, $NK1.1^+$, $NKp46^+$ cells. Flow cytometry was performed using an LSRFortessa or an LSRFortessa X-20 (BD Biosciences). Data were analyzed using FlowJo software.

Antibodies for flow cytometry

The following antibodies were used: From BioLegend we purchased anti-CD45 (30-F11, Alexa Fluor 700) , anti-CD3ε (145-2C11, APC-Cy7, PE-Cy5), anti-CD4 (GK1.5, BV421), anti-CD8α (53-6.7, BV650, BV605), anti-CD19 (6D5, PE-Cy5, BV605), anti-Ter119 (TER-119, PE-Cy5), anti-F4/80 (BM8, PE-Cy5), anti-NKp46 (29A1.4, PerCP-Cy5.5), anti-NK1.1 (PK136, BV711, FITC), anti-CD69 (H1.2F3, BV605), anti-Sca-1 (D7, BV510), anti-Ki67 (SolA15, eFluor 450), anti-CD107a (1D4B, Alexa Fluor 647), anti-Tbet (4B10, BV421), anti-FoxP3 (MF-14, AF488), anti-IFN-γ (XMG1.2, PE), anti-TNFα (MP6-XT22, APC), anti-IL-2 (JES6-5H4, BV605), anti-TIGIT (1G9, PE-Cy7), anti-PD-1 (29F.1A12, BV711), anti-CD137 (17B5, APC). From BD Biosciences we purchased anti-granzyme B (GB11, PE-CF594), anti-Bcl-6 (K112 91, BV711), anti-RORγt (Q31-378, AF647) and anti-GATA3 (L50-823, PE-Cy7).

Ex vivo cytotoxicity assay

Cytotoxicity by splenocytes was assessed with a standard 5-hour ^{51}Cr-release assay. 24 and 72 hours after treating mice with PBS, CDN (i.t.), H9-MSA (i.p.) or CDN/H9-MSA, spleens were harvested and single cell suspensions were treated with ACK lysis buffer. The ^{51}Cr-release assay was performed as described (Nicolai et al, 2019) using B16-F10 *B2m*-/- cells as target cells. For NK cell-depleted samples, mice were injected twice (2 days and 1 day before the initiation of treatment) intraperitoneally with 200 μg of anti-NK1.1 (PK136) and spleens were collected and treated as described above. Efficacies of cellular depletions were confirmed by flow cytometry.

Generation of B16-F10 MHC II knockout cell line

Plasmids containing Cas9 and the *Ab1*-targeting guide (sgRNA sequence: TCGTATGCGCTGCGTCCCGT) were previously cloned in to PX458 following the 'Zhang lab general cloning protocol' provided by the Zhang Laboratory at Massachusetts Institute of Technology. To generate the *Ab1* knockout cell line, the plasmids were transiently transfected using Lipofectamine 2000 (ThermoFisher Scientific) into B16-F10 *B2m*-/- cells. After one week, cells were transiently transfected with a plasmid containing CIITA-GFP (obtained from Dr. Cheong-Hee Chang) to induce MHC II in order to enable MHC II+ and MHC II- cells to be distinguished by flow cytometry. Cells were staining for MHC II and sorted using a FACSAria sorter for negative cells based on staining and GFP expression.

Tetramer staining of tumor specific CD4 T cells

Spleens of Naïve or *B2m-/-* tumor-bearing mice were harvested six days after CDN, H9-MSA, CDN/H9-MSA or PBS treatment. Single cell suspensions of spleens were made by passage through a 40-μm filter and were then and treated with ACK to lyse red blood cells. Splenocytes were then stained in triplicate with a PE-conjugated MHC II I-A^b tetramer containing the MuLV 123-141 epitope EPLTSLTPRCNTAWNRLKL for RMA *B2m-/-* tumor-bearing mice or Trp1 113-126 epitope CRPGWRGAACNQKI for B16-F10 *B2m-/-* tumor-bearing mice. The tetramers were kindly provided by the Tetramer Core Facility at the National

Institutes of Health. Tetramer staining was carried out in 100 μl RPMI medium for 3 hours at 37 degrees C in a round-bottom 96 well plate at a dilution of 1:400 for the MuLV tetramer or 1:200 for the Trp1 tetramer. Tetramer-stained splenocytes were then stained with Live/Dead, 2.4G2, and antibodies or reagents for surface markers and intracellular markers as described above. Triplicate samples were pooled prior to running flow cytometry.

Peptide stimulation assay

Spleens of naïve or tumor-bearing mice were harvested six days after CDN, H9-MSA, CDN/H9-MSA or PBS treatment. Single cell suspensions of spleens were made by passage through a 40-μm filter and were then and treated with ACK to lyse red blood cells. Splenocytes were then added in triplicate to a round-bottom 96 well plate in 100 μl RPMI media gp70 peptide (DEPLTSLTPRCNTAWNRLKL, from Peptide 2.0) for RMA-*B2m-/-* tumor-bearing mice or Trp1 peptide (CRPGWRGAACNQKI, from Peptide 2.0) for B16-F10-*B2m-/-* tumor-bearing mice at a concentration of 5 μg/ml. One hour later, Brefeldin A (Biolegend) and Monensin (Biolegend) were added to the stimulation mix. 4 hours later, cells were stained with Live/Dead, 2.4G2, and surface markers as described above. Triplicate samples were pooled prior to running flow cytometry.

Statistics

Statistics were performed using Prism (GraphPad). For tumor growth and survival data, two-way analysis of variance (ANOVA) and log-rank (Mantel-Cox) tests were used. Two-way ANOVA was used for cytotoxicity. For flow cytometry data in Chapter 3, single therapies were compared to either control PBS or CDN/H9-MSA using one-way ANOVA followed by Dunnett's multiple comparisons. For the bar graphs in Chapter 4, the data was analyzed by 2-tailed unpaired Student's t-test. For flow cytometry data in Chapter 5, all therapies were compared to control PBS using one-way ANOVA followed by Dunnett's multiple comparisons. Significance was indicated as follows: *$P < 0.05$; **$P < 0.01$; ***$P < 0.001$; ****$P < 0.0001$.

Chapter 3
CDN and H9-MSA combination therapy enhance NK cell antitumor responses from against MHC I-deficient tumors

Portions of this chapter were adapted and/or reprinted with permission from "Wolf, N.K., Blaj, C., Picton, L, Snyder, G., Zhang, L. Nicolai, C.J., Ndubaku, C.O., McWhirter, S.M. Garcia, K.C. and Raulet, D.H. Synergistic effects of a STING agonist and an IL-2 superkine in cancer immunotherapy against MHC I-deficient and MHC I+ tumors. *Proc Natl Acad Sci U S A*, In press (2022)."

Abstract

Cyclic dinucleotides (CDNs) and TLR ligands mobilize antitumor responses by NK cells and T cells, potentially serving as complementary therapies to immune checkpoint therapy. In the clinic thus far, however, CDN therapy has yielded mixed results, perhaps because it initiates responses potently, but does not provide signals to sustain activation and proliferation of activated cytotoxic lymphocytes. To improve efficacy, we combined CDNs with a half-life extended IL-2 superkine, H9-MSA. CDN/H9-MSA therapy induced dramatic long-term remissions of the most difficult-to-treat MHC I-deficient and MHC I^+ tumor transplant models. H9-MSA combined with CpG oligonucleotide also induced potent responses. Mechanistically, tumor elimination required CD8 T cells and not NK cells in the case of MHC I+ tumors, and NK cells but not CD8 T cells in the case of MHC-deficient tumors. Furthermore, combination therapy resulted in more prolonged and more intense NK cell activation, cytotoxicity and expression of cytotoxic effector molecules in comparison to monotherapy. Remarkably, in a primary autochthonous sarcoma model that is refractory to PD-1 checkpoint therapy, the combination of CDN/H9-MSA combined with checkpoint therapy yielded long-term remissions in the majority of the animals, mediated by T cells and NK cells. This novel combination therapy has potential to activate responses in tumors resistant to current therapies and prevent MHC I-loss accompanying acquired resistance of tumors to checkpoint therapy.

Significance statement

Immunotherapy provides long-term remissions in numerous types of cancer but is ineffective in most tumors with poor immune cell infiltrates or lacking T cell epitopes or MHC I molecules. Agents that activate the STING protein showed promise in several MHC I+ and MHC-deficient mouse tumor models in mice, where they induced powerful antitumor CD8+ T cell and NK cell responses, respectively. They were less effective in numerous other tumor models and yielded mixed results in the clinic in human patients. This report demonstrates strong synergy between a STING agonist and an IL-2 superkine in effectively curing difficult-to-treat MHC-deficient and MHC-positive tumor models in mice by mobilizing T cells and NK cells. This combination therapy shows considerable promise for clinical application.

Introduction

Recent advances in immunotherapy have vastly improved patient outcomes (Kalbasi and Ribas, 2020; Sharma et al., 2021). However, for most cancers the majority of patients do not show clinical benefit. Most of the approved therapies are "checkpoint" therapies predicated on amplifying $CD8^+$ T cell responses (Leach et al., 1996; Sharma et al., 2021). However, some tumors lack many neoantigens for T cell recognition (Alexandrov et al., 2013; Yarchoan et al., 2017), or acquire defects in antigen presentation or MHC I expression before or during therapy

that confer resistance (Garrido and Algarra, 2001; Maleno et al., 2011; McGranahan et al., 2017; Roemer et al., 2016; Sade-Feldman et al., 2017).

Natural Killer (NK) cells kill cancer cells (Bauer et al., 1999; Marcus et al., 2014; Raulet and Guerra, 2009; Vivier et al., 2011) and amplify adaptive immune responses (Barry et al., 2018; Bottcher et al., 2018; Kearney et al., 2018) by recognizing stressed-induced ligands (Jamieson et al., 2002; Raulet et al., 2013) and/or the absence of MHC class I on tumor cells (Karlhofer et al., 1992; Moretta and Moretta, 1997; Shifrin et al., 2014). Their capacity to kill MHC I-deficient tumor cells, including those lacking neoantigens, suggests that mobilizing antitumor NK cells is an attractive approach to counteract evasion of T cell responses.

The cyclic guanosine monophosphate-adenosine monophosphate synthase–stimulator of interferon genes (cGAS-STING) innate immune sensing pathway has shown promise in preclinical studies as a therapeutic target. The pathway is triggered by cytosolic DNA in mammalian cells (Sun et al., 2013), but can also be potently activated by exposure of cells to cyclic dinucleotides (CDNs) such as 2',3' cyclic guanosine monophosphate–adenosine monophosphate (cGAMP), an intermediate in the pathway that enters the cytosol of cells, and binds and activates the stimulator of interferon genes (STING) protein (Diner et al., 2013; Gao et al., 2013; Wu et al., 2013). Activated STING in turn activates both IRF3 and NF-kB pathways, leading to production of type I interferons and other inflammatory cytokines and chemokines (Ishikawa and Barber, 2008). The same pathway is activated naturally, but probably quite weakly, in many tumors due to the escape of nuclear or mitochondrial DNA to the cytosol in cancer cells (Marcus et al., 2018; Woo et al., 2014).

Synthetic cyclic di-nucleotides (CDNs) serve as potent STING agonists that, when injected intratumorally or systemically, superactivate antitumor T cell responses (Corrales et al., 2015; Sivick et al., 2018). Similarly, we recently demonstrated that intratumoral injections of CDNs induce robust NK cell-mediated rejection of six different established MHC I-deficient murine tumors, generated by CRISPR/Cas9 disruption of the *B2m* gene in each line (Nicolai et al., 2020). The CDN injections induced high levels of type I IFN, which was essential for NK cell activation, and acted directly on NK cells as well as indirectly by inducing trans-presentation of IL-15 by DCs. We observed permanent remissions of >50% of tumors in four of the six MHC I-deficient models studied. In two models, the rate of permanent remissions was much lower: ~20% in the MC38-*B2m-/-* model and 0% in the B16-F10-*B2m-/-* model (Nicolai et al., 2020). At the same time, early phase clinical trials of STING agonists in patients have not yielded sustained clinical remissions (Harrington et al., 2018; Meric-Bernstam et al., 2019), indicating a need for improvements in this immunotherapy approach.

Superkines are an emerging category of immunotherapy agents that powerfully activate immune cells. The superkine H9, also known as super-2, is a variant of IL-2 that was selected to bind with high affinity to the IL-2Rβ/γ complexes that NK cells express (Levin et al., 2012). H9 activates NK cells at much lower concentrations than IL-2, and was shown to stimulate antitumor responses in mouse tumor models with lower toxicity than IL-2 (Levin et al., 2012). Furthermore, H9 administration reversed or delayed the onset of NK cell desensitization and prolonged the survival of mice with MHC I-deficient tumors, in an NK cell-dependent fashion (Ardolino and Raulet, 2016). Because STING agonists provide a potent initial stimulus for NK

cell responses but may not provide continual cytokine production to sustain the responses, we evaluated the combination of a STING agonist with repeated administrations of the H9 superkine to sustain effective NK cell responses against cancer. The results demonstrate remarkable efficacy of this combination therapy in MHC I-deficient tumor models.

Results

Half-life extended IL-2 superkine, H9, synergized with CDNs to induce rejection of MHC class I-deficient tumors

Injections of the STING agonist ADU-S100 (mixed-linkage [2′3′] dithio-(Rp, Rp) cyclic diadenosine monophosphate, hereafter referred to as CDN) intratumorally resulted in long-term tumor regressions in the majority of animals in four of six MHC I-deficient (*B2m-/-*) tumor models previously tested. Poor efficacy was observed in two models, the B16-F10-*B2m-/-* melanoma model (no long-term survivors) and the MC38-*B2m-/-* colorectal cancer model (~20% long-term survivors). In order to sustain the initial response in difficult to treat models, we combined CDN therapy with administration of the H9 superkine. Like IL-2, H9 has a short half-life in vivo. To extend the half-life and reduce toxicity due to high dose administration, H9 was fused to mouse serum albumin (Zhu et al., 2015) to create H9-MSA. Monotherapy with repeated doses of 5 μg or 20 μg H9-MSA slowed tumor growth and extended survival of the tumor bearing mice to a similar extent, resulting in long term survival of ~20% of the animals. In contrast, H9 by itself had no significant antitumor activity (Figure 3.1A).

In the same tumor model, a single i.t. injection of CDN also slowed tumor growth, but combining CDN with 10 μg or 20 μg doses of H9-MSA provided dramatically improved outcomes, resulting in long-term (>100 d) tumor-free survival in 75-85% of the mice (Figure 3.1A, Figure 3.2A, Figure 3.2B, Figure 3.3A). CDN combined with H9 (lacking MSA) was less efficacious, and CDN combined with IL-2 was little better than CDN alone (Figure 3.1C).

The CDN/H9-MSA combination was even more effective in the MC38-*B2m-/-* model, resulting in long-term tumor-free remissions in 100% of the animals (Figure 3.2C, Figure 3.3B). Treatments with CDN or H9-MSA alone were much less effective (Figure 3.2C, Figure 3.3B). Thus, the combination of STING agonist and half-life extended H9 superkine was extremely effective in eliminating tumors in two very difficult-to-treat MHC I-deficient murine cancer models.

The combination of CDNs (one treatment) and 10 μg H9-MSA (every two days) resulted in modest weight loss and a minor increase in the lung/body weight ratio, a metric for pulmonary edema, a known side effect of IL-2 therapy (Conant et al., 1989) (Figure 3.4A-C). Greater weight loss and pulmonary edema were associated with the 20 μg dose of H9-MSA by itself. CDNs alone had the least toxicity in all tests performed, corresponding to transient weight loss that in a separate experiment was maximal on day 1. Administering 10 μg H9-MSA every three days further minimized toxicity while maintaining efficacy, and we employed that dose and schedule for most of the experiments in this study.

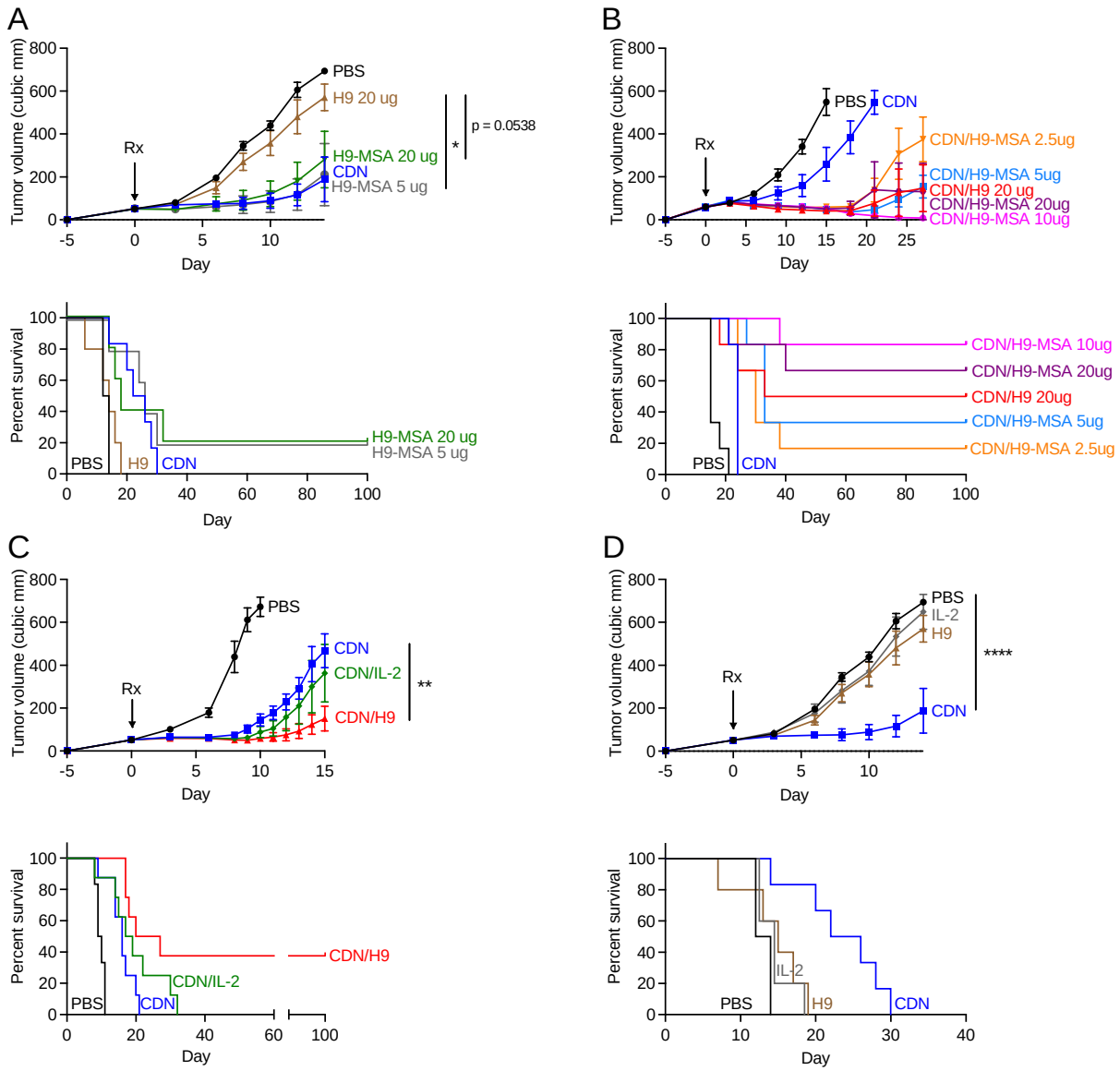

Figure 3.1 Synergistic impact of H9 or H9-MSA administration and CDN therapy on tumor rejection. B16-F10-*B2m*-/- tumor cells were implanted s.c.in C57BL/6J mice on day -5 and grown to approximately 50 mm^3. On d0, tumors were injected once intratumorally with 50 μg CDN or PBS, and/or i.p. with the indicated cytokines or PBS. The cytokine or PBS injections were repeated every two days until mice were euthanized or until 1 week after a mouse completely cleared a tumor. Tumor growth curves and survival data are shown. **(A)** Half-life extended H9 (H9-MSA) showed significant antitumor effects as a monotherapy, even with a lower administered dose (5 μg). **(B)** Dose titration of H9-MSA in combination with CDN therapy, showing that doses >5 μg were necessary for optimal combination therapy effects. **(C)** When combined with CDN therapy, H9 administration, but not IL-2 administration, resulted in improved antitumor effects including long term survival of a significant percentage of the animals. **(D)** CDN monotherapy, but not monotherapy with IL-2 or H9, delayed tumor growth. The data in panels A-C were from one large experiment. Tumor growth data were analyzed by 2-way ANOVA. Survival data were analyzed using

log-rank (Mantel-Cox) tests. The data in all panels are representative of two independent experiments. N=6-7 mice per group. Error bars represent standard error of the mean (SEM). *P< 0.05, **P < 0.01, ***P < 0.001, ****P < 0.0001.

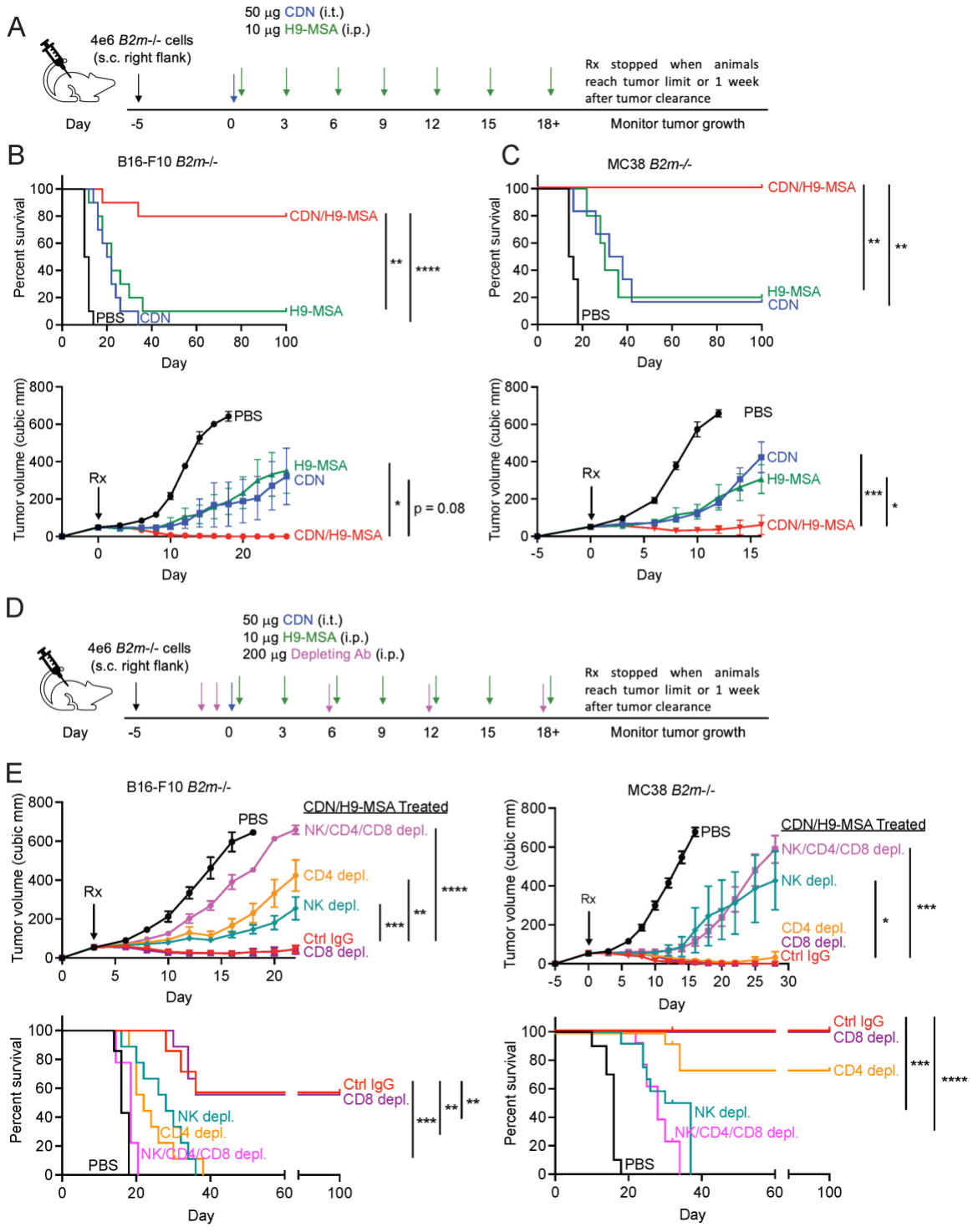

Figure 3.2. Cell types mediating rejection of MHC I-deficient tumors induced by CDN combined with IL-2 superkine, H9-MSA. (A) Timeline. Tumor cells were implanted s.c. in C57BL/6J mice and grown to approximately 50 mm^3 (day 0). Tumors were injected once i.t. with 50 μg of CDN or PBS. Mice were also injected i.p. with 10 μg H9-MSA or PBS on day 0. The cytokine or PBS injections were repeated every three days until euthanization or 1

week after tumor clearance. **(B, C)** Tumor growth curves and survival of mice with B16-F10-*B2m*-/- (B) and MC38-*B2m*-/- (C) tumors. **(D)** Timeline for cellular depletions. Tumors were established and treated as in (A), except groups of mice were depleted of NK cells, CD8 T cells and/or CD4 T cells, or injected with control IgG. **(E)** Tumor growth curves and survival of mice with B16-F10-*B2m*-/- (left) and MC38-*B2m*-/- (right) tumors. Tumor growth data was analyzed by 2-way ANOVA. Survival data was analyzed using log-rank (Mantel-Cox) tests. The data in all panels are representative at least two independent experiments. N=7-10 mice per group. Error bars represent standard error of the mean (SEM). *P< 0.05, **P < 0.01, ***P < 0.001, ****P < 0.0001.

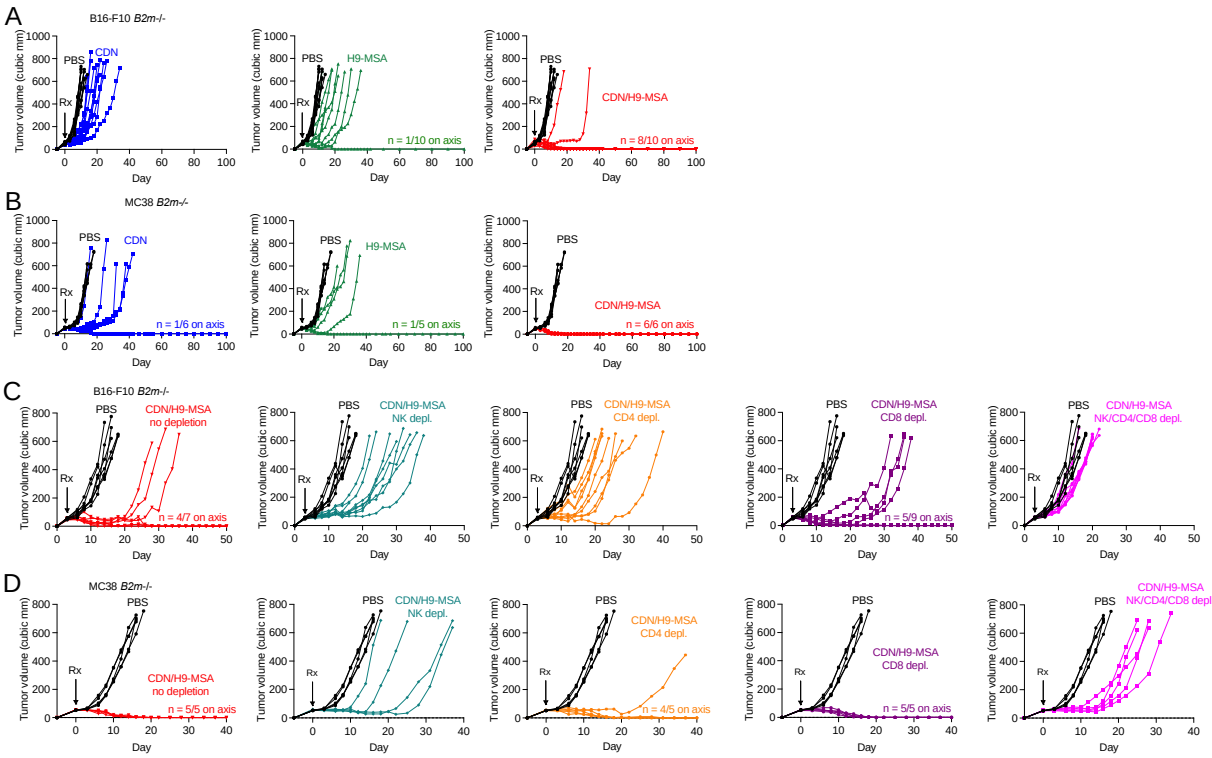

Figure 3.3. Spider plots showing growth of individual tumors from Figure 3.2. (A, C) B16-F10-*B2m*-/- tumors **(B, D)** MC38-*B2m*-/- tumors. **(A, B)** impact of combination therapy vs monotherapies. **(C, D)** Impact of cellular depletions on the efficacy of CDN/H9-MSA combination therapy.

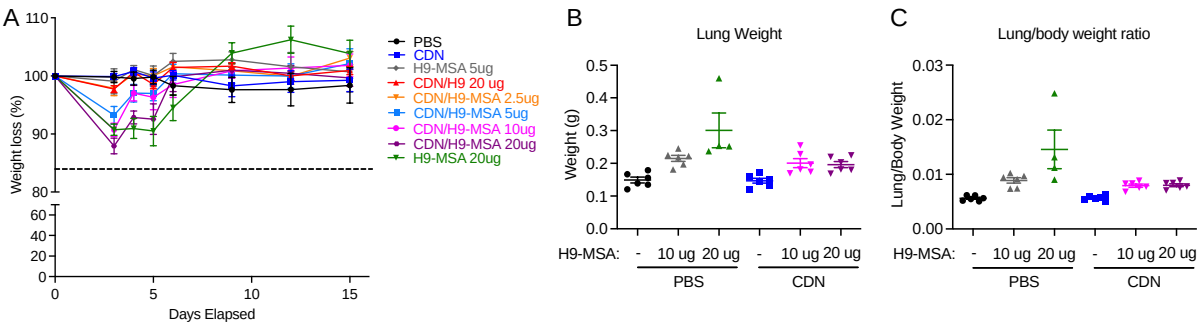

Figure 3.4. Toxicity associated with H9-MSA or combination therapy. Tumors were generated and mice received therapy as described in Figure 3.1, legend. Mice were weighed on the indicated days after initiating therapy (d0). In a separated experiment, lungs were harvested on day 6, and wet weights were determined. (A) Percentages of d0 body weights over time. (B) Lung weight (grams) on day 6. (C) The lung/body weight ratio, a measure of pulmonary edema, is shown for each mouse on day 6. Each analysis was confirmed in a repeat experiment. Error bars represent standard error of the mean (SEM).

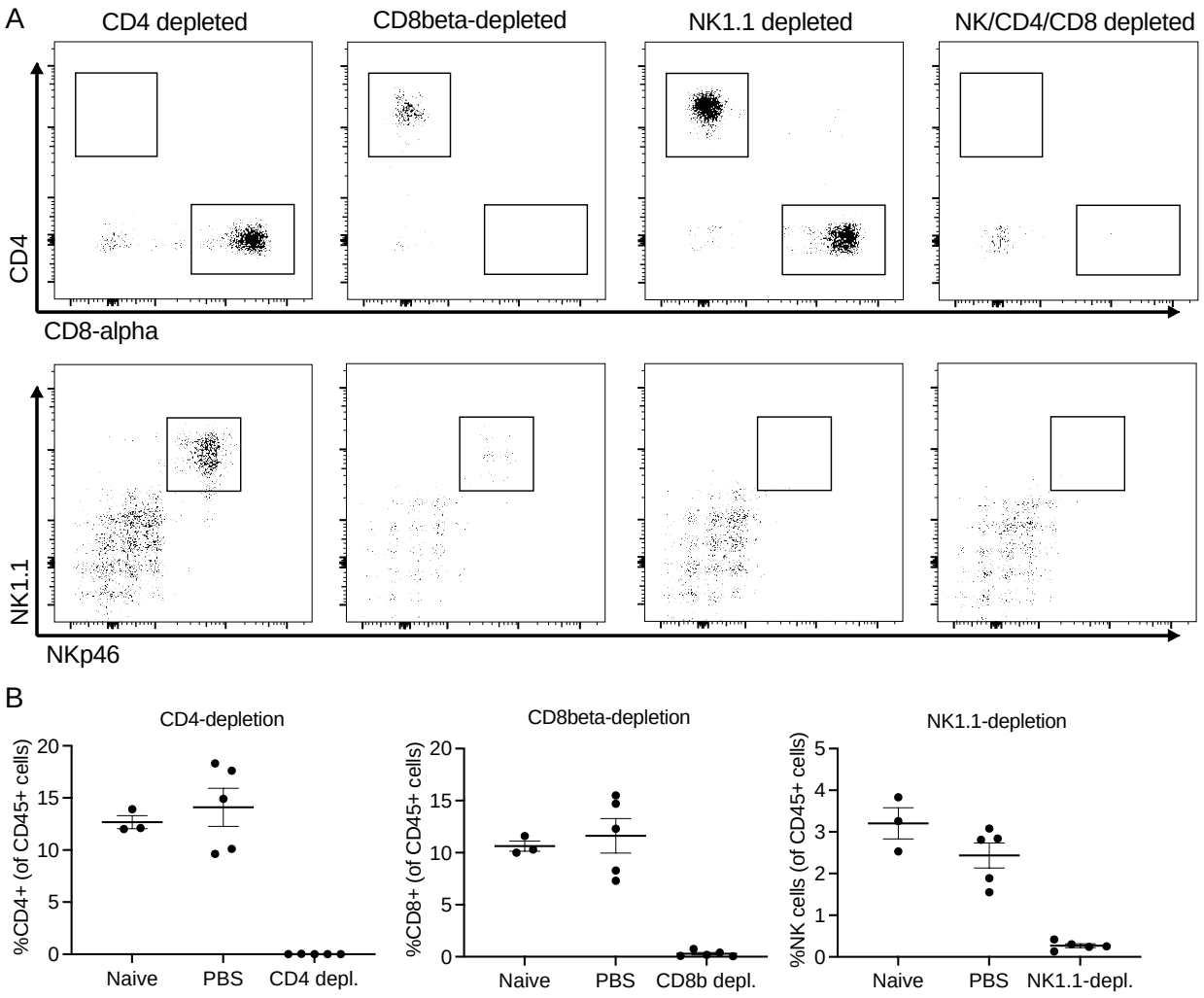

Figure 3.5. Verification of in vivo cellular depletions. (A) Successful T cell and NK cell depletion protocols. As described in Methods, mice were treated on days -2 and -1 with antibodies to deplete CD4+ cells, CD8β+ cells, NK1.1+ cells or all three. On day 0, blood cells were collected, ACK-treated. Gated viable, CD45+, CD19-, Ter119-, F4/80- cells were examined. **(B)** Representative percentages of the indicated cells after the indicated depletions compared to contemporaneous controls. Error bars represent standard error of the mean (SEM).

Rejection of MHC I-deficient tumors induced by CDN/H9-MSA therapy was NK cell-dependent and CD8 T cell-independent

In the MC38-*B2m*-/- model, depleting either CD4+ or CD8β+ cells starting after tumors were established but just before therapy was initiated (Figure 3.2D, Figure 3.5) did not significantly diminish efficacy, whereas depleting NK cells alone greatly diminished therapeutic efficacy, resulting in terminal morbidity of all the animals (Figure 3.2E, Figure 3.3D). Depleting all three types of lymphocytes had no greater effect than depleting NK cells. Therefore, NK cells, and not CD4 or CD8 T cells, mediate tumor rejection.

In the B16-F10-*B2m*-/- model, depleting CD8 T cells had no effect, but depleting either NK cells or CD4 T cells diminished therapeutic efficacy (Figure 3.2E, Figure 3.3C). Depleting all three populations had an even greater effect, suggesting that combination therapy separately mobilized both antitumor NK cells and antitumor CD4 T cells, and that each acted to some extent independently. Antitumor CD4 T cells were previously implicated as antitumor effector cells in studies of wild type B16 tumors (Quezada et al., 2010; Tay et al., 2021).

To address whether nonconventional T cells or B cells were necessary for tumor rejection, we tested the combination therapy in tumor-bearing B6-*Rag2*-/- mice, which lack all T cells (including $NK1.1^+$ T cells) and B cells but retain NK cells. In both tumor models, CDN and H9-MSA were more potent in combination than separately in the B6-*Rag2*-/- mice (Figure 3.6). In the MC38-*B2m*-/- model, the combination therapy was as effective in *Rag2*-/- mice as in WT mice, resulting in 100% survival of the mice (Figure 3.6A, C, Figure 3.7A). As before, NK-depletion greatly diminished efficacy, resulting in 100% mortality. In the B16-F10-*B2m*-/- model, combination therapy only delayed tumor growth in *Rag2*-/- mice, and 100% of the animals eventually succumbed (Figure 3.6B, D, Figure 3.7B). This finding is consistent with the data showing that CD4 cell depletion greatly diminished the rejection of these tumor cells in WT mice (Figure 3.2B). NK depletion in *Rag2*-/- mice accelerated tumor growth, as expected. Thus, combination therapy mobilized a fully effective antitumor NK response against MC38-*B2m*-/- tumors, with no discernable role for conventional or nonconventional T cells. In contrast, both antitumor NK cells and antitumor CD4 T cells participated in rejecting B16-*B2m*-/- tumors in WT mice, albeit to a significant extent independently. Separately, each effector cell type delayed tumor growth but did not eliminate the tumors, but together they eliminated the tumors in most animals. There was no indication of a role for nonconventional T cells in elimination of B16-*B2m*-/- tumor cells, since the defect in tumor rejection in *Rag2*-/- mice was similar to the defect in WT mice depleted of CD4 T cells. CD8 T cells played no discernable role in either response.

Some delay in tumor growth was still evident after depleting all three lymphocyte populations in both tumor models (Figure 3.2) and in the *Rag2*-/- tumor models following NK cell depletion (Figure 3.6). This delay was partially prevented by simultaneously blocking TNF-α and type I interferon receptors (IFNAR-1) (Figure 3.8A), suggesting that these cytokines impeded tumor growth independently of CD4, CD8 and NK cells after CDN/H9-MSA therapy, consistent with published reports (Francica et al., 2018; Nicolai et al., 2020; Sivick et al., 2018). Blocking either TNF-α and type I interferon receptors separately (Figure 3.8B) also showed a significant increase in tumor growth indicating that these cytokines each played a separate, if minor, role in impeding tumor growth. However, some slowing of tumor growth was still

apparent when blocking both cytokines in the absence of T cells and NK cells, suggesting that an unidentified mechanism also plays a role.

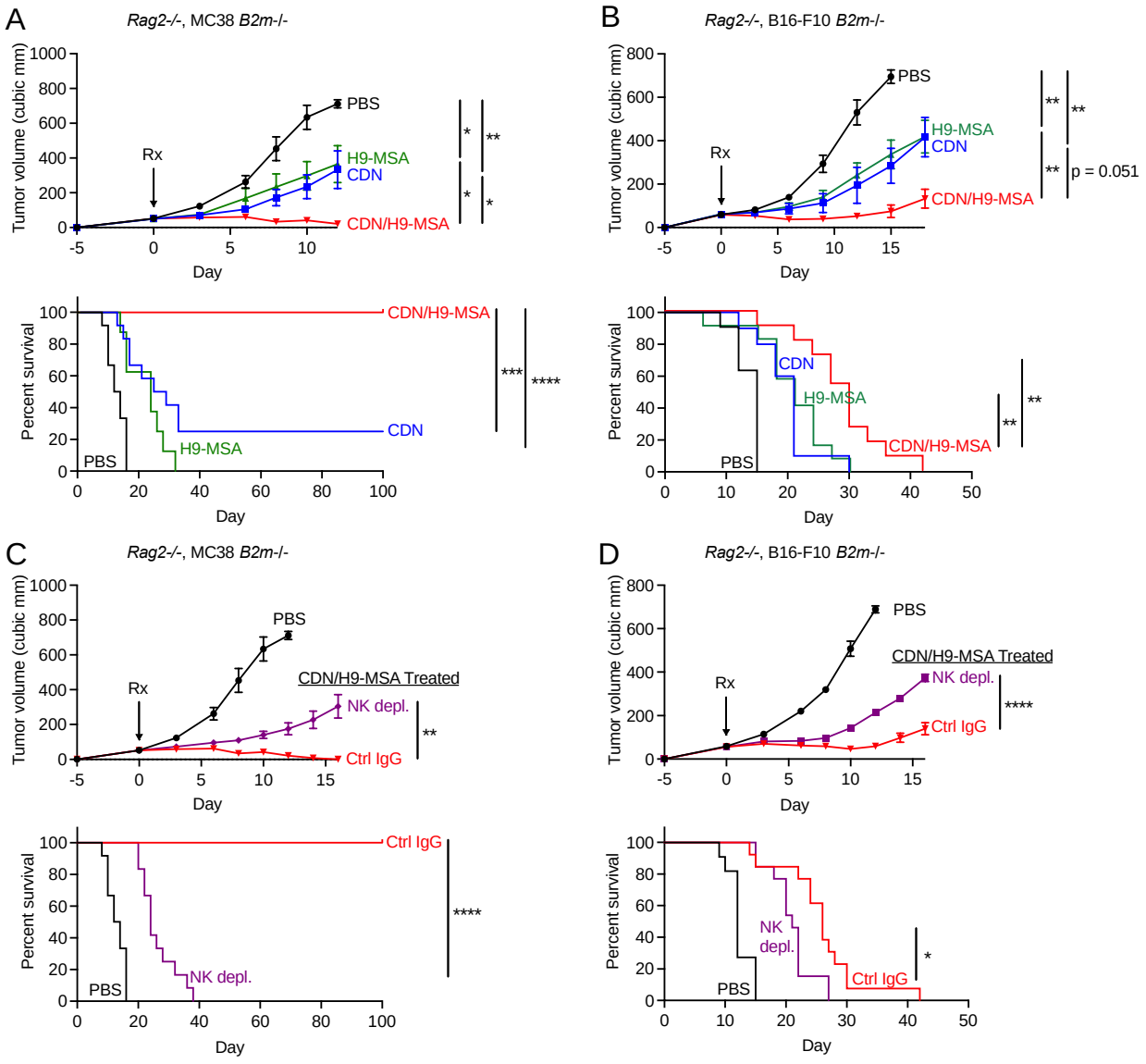

Figure 3.6. NK cell dependent rejection of MHC I-deficient tumors induced by CDN/H9-MSA treatment in *Rag2*-/- mice. MC38-*B2m*-/- **(A, C)** and B16-F10-*B2m*-/- **(B, D)** tumors were established as in Figure 3.2 legend in *Rag2*-/- mice, and subjected to therapy as indicated. **(A, B)** Combination therapy was more effective than monotherapies in both tumor models. **(C, D)** The therapeutic effects were decreased by NK-depletion in both models. Tumor growth data were analyzed by 2-way ANOVA. Survival data were analyzed using log-rank (Mantel-Cox) tests. The data in all panels were representative of at least two independent experiments. n=9-12 mice per group. Error bars represent standard error of the mean (SEM). *P< 0.05, **P < 0.01, ***P < 0.001, ****P < 0.0001.

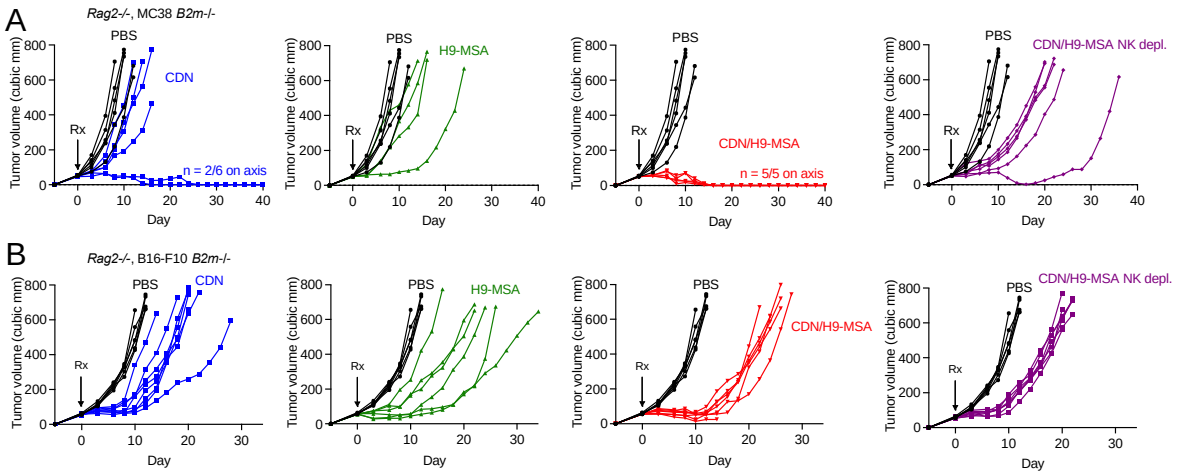

Figure 3.7. Spider plots showing growth of individual tumors from Figure 3.6. (A) *Rag2-/-* mice with MC38-*B2m-/-* tumors. **(B)** *Rag 2-/-* mice with B16-F10-*B2m-/-* tumors.

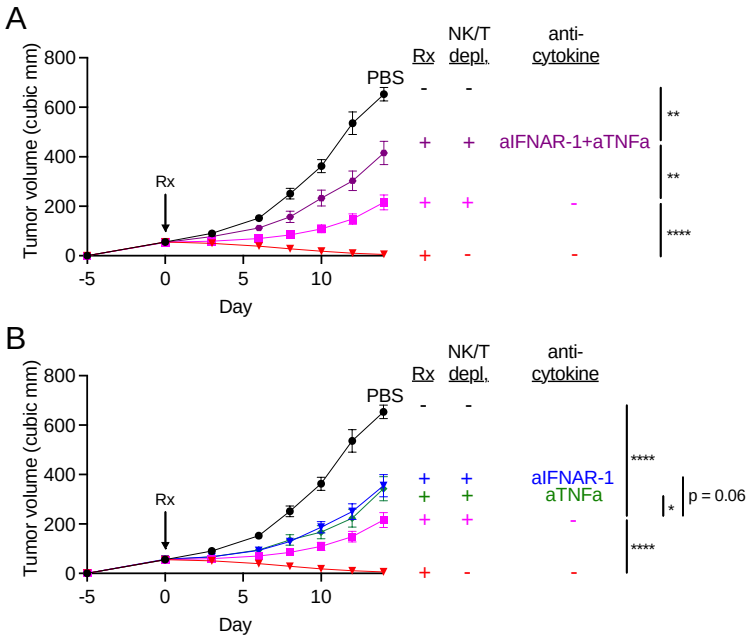

Figure 3.8. Blockade of TNF-a and IFNAR-1 partially reverses the tumor growth delay imparted by CDN/H9-MSA administration in mice depleted of T cells and NK cells. B16-F10-*B2m-/-* tumors were generated and mice received therapy as described in Figure 3.2 legend. Mice were depleted of NK cells, CD4 T cells and CD8 T cells i.p. on days -2 and -1 before the initiation of therapy and repeated every 6 days. Additionally, mice received anti-IFNAR-1 and/or anti-TNF-α i.p. on day -1 and day 0 before the initiation of therapy and again every three days. **(A)** Blockade of TNF-α and IFNAR-1 or **(B)** blockade of TNF-α or IFNAR-1 led to more rapid tumor growth in the NK/T cell depleted animals. Tumor growth data were analyzed by 2-way ANOVA. The data in all panels are a combination of 2 experiments. n=10-11 mice per group. Panel A and B are from the same experiments but separated for clarity. Error bars represent standard error of the mean (SEM). *P< 0.05, **P < 0.01, ***P < 0.001, ****P < 0.0001.

H9-MSA was more effective than WT IL-2-MSA in combination with CDNs

We next directly compared H9-MSA to WT IL-2-MSA in the context of the combination therapy in WT mice with established B16-*B2m-/-* tumors. The mice were depleted of CD4 and CD8 T cells before the initiation of therapy to narrow the analysis to the effects of NK cells. The CDN/H9-MSA combination was again more effective than CDN or H9-MSA alone (Figure 3.9A, Figure 3.10). The CDN/IL-2-MSA combination, in contrast, was only slightly more effective than CDN or IL-2-MSA alone (Figure 3.9B). In the head-to-head comparison, the CDN/H9-MSA combination was more effective than the CDN/IL-2-MSA combination, both in terms of delaying tumor growth and delaying terminal morbidity (Figure 3.9C). Therefore, H9-MSA is more effective than IL-2-MSA in activating NK cells against B16-*B2m-/-* tumors.

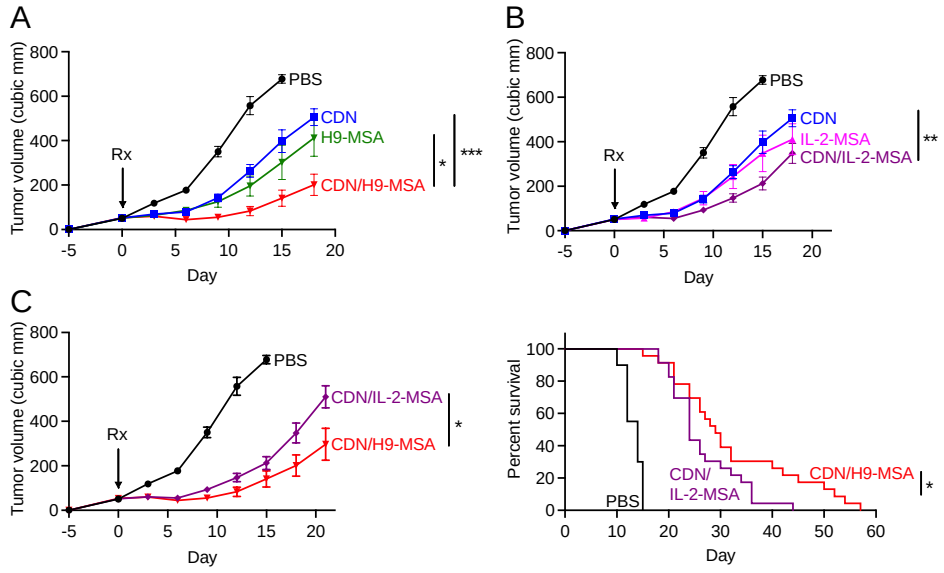

Figure 3.9. Greater efficacy of H9-MSA compared to IL-2-MSA in mice lacking CD4 and CD8 T cells. B16-F10-*B2m*-/- tumors were established as in Figure 3.2 legend in C57BL/6J mice. In all panels, the mice were depleted of both CD4 and CD8 T cells before initiating therapy. **(A-C)** Comparisons of the effects of CDN, H9-MSA and IL-2-MSA separately (A, B) or in combinations (CDN/IL-2-MSA vs CDN/H9-MSA) (A-C) using the schedule shown in Fig. 1, one dose of 50 μg of CDN and 10 μg doses of H9-MSA or IL-2-MSA. Curves in A-C were all from the same experiment. Tumor growth data were analyzed by 2-way ANOVA. Survival data were analyzed using log-rank (Mantel-Cox) test. The data in all panels are representative at least two independent experiments. n=9-20 mice per group. Error bars represent standard error of the mean (SEM). *P< 0.05, **P < 0.01, ***P < 0.001, ****P < 0.0001.

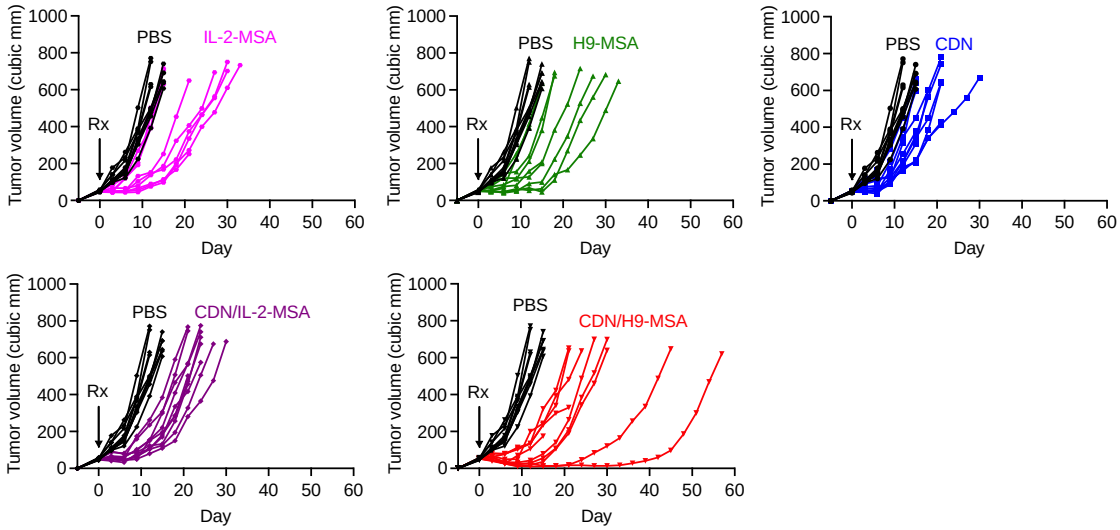

Figure 3.10. Spider plots showing growth of individual tumors from Figure 3.9. Spider plots for comparison of IL-2-MSA and H9-MSA treatments.

A distinct innate activator, CpG oligonucleotide, synergized with H9-MSA in providing antitumor efficacy

To address if H9-MSA would synergize with various innate agonists, we compared TLR agonists including CpG oligodeoxynucleotides (ODN), PolyI:C and R848, in addition to CDN, for inducing a potent antitumor response against MHC I-deficient tumors. These TLR agonists, like CDN, induce the production of interferons and other cytokines downstream of IRF3 and NK-κB. We tested the therapy combinations in mice that had been depleted of CD4 and CD8 T cells in order to evaluate their efficacy in activating antitumor NK cell responses. Similar to our findings with CDN (Figure 3.11A, Figure 3.12), combining H9-MSA (i.p.) with CpG ODN (administered once, i.t.) resulted in delayed tumor growth and extended survival (Figure 3.11B). CpG ODN DS-L03, is a TLR9 agonist optimized to stimulate high levels of type I IFN (Yang et al., 2013b). Intratumoral treatments with R848 (Figure 5.11C) and PolyI:C (Figure 5.11D) did not show synergy with H9-MSA, though it remains possible that alternative doses could have activity. These findings indicated that at least two IFN-inducing innate agonists, CDN and CpG ODN, showed synergistic effects with H9-MSA. However, CDN combined with H9-MSA was the more potent combination.

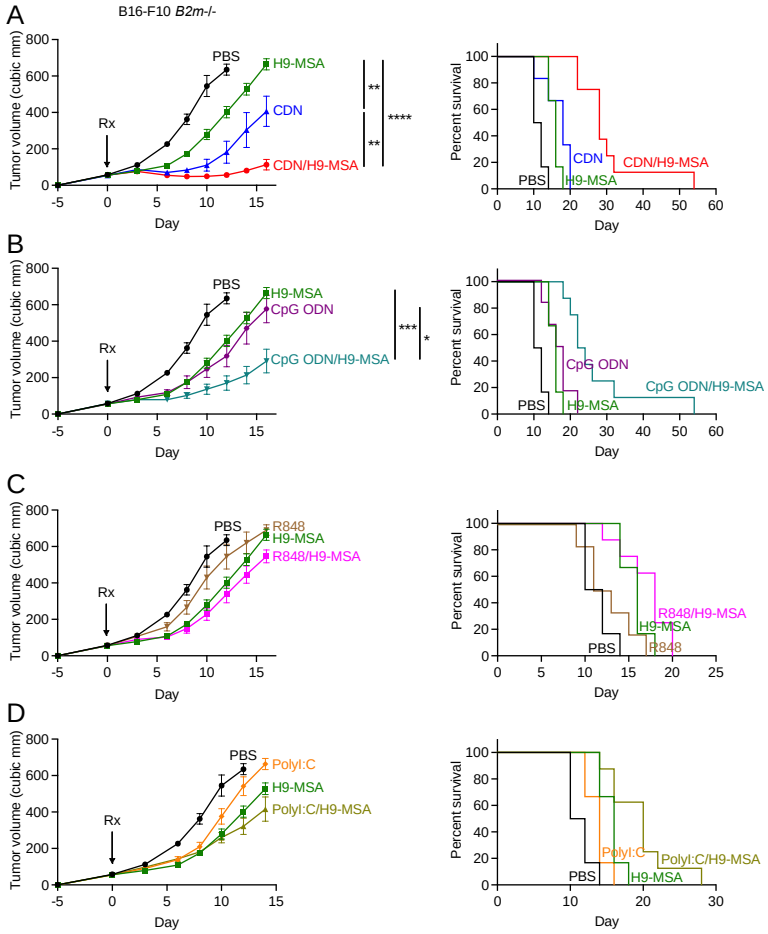

Figure 3.11. Comparison of innate agonists separately or in combination with H9-MSA. B16-F10 *B2m-/-* tumor cells were implanted s.c. in C57BL/6J mice on day -5 and grown to

approximately 50 mm^3. On d0, tumors were injected once intratumorally with 50 μg indicated innate agonist or PBS, and/or i.p. with 10 μg of H9-MSA or PBS. The cytokine or PBS injections were repeated every two days until mice were euthanized or until 1 week after a mouse completely cleared a tumor. In all panels, the mice were depleted of both CD4 and CD8 T cells before initiating therapy. **(A-D)** Comparison of the effects of (A) CDN, (B) CpG ODN, (C) R848 and (D) PolyI:C separately or in combination with H9-MSA. Graphs are all from the same experiment. Tumor growth data were analyzed by 2-way ANOVA. Survival data were analyzed using log-rank (Mantel-Cox) tests. The data in all panels are representative at least two independent experiments. n=5-7 mice per group. Error bars represent standard error of the mean (SEM). *P< 0.05, **P < 0.01, ***P < 0.001, ****P < 0.0001.

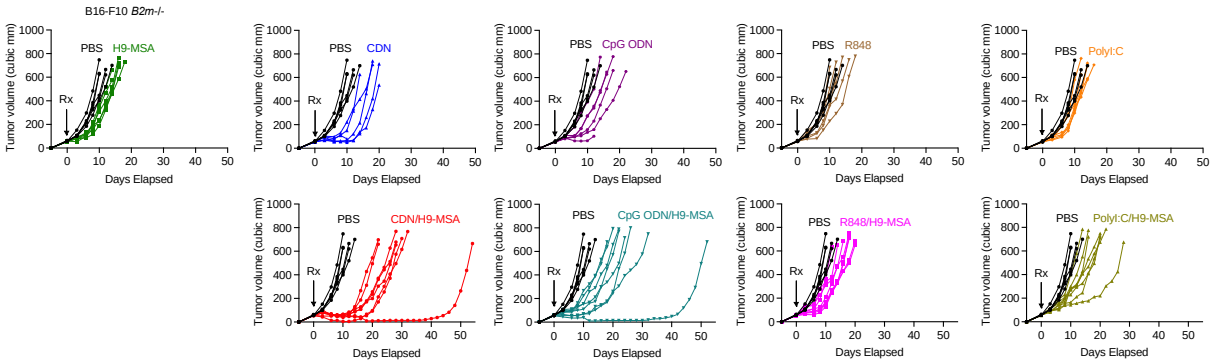

Figure 3.12. Spider plots showing growth of individual tumors from Figure 3.11. Spider plots for comparison of H9-MSA, CDN, CpG ODN, R848 and PolyI:C treatments.

Local CDNs and systemic H9-MSA synergized in creating a systemic NK cell mediated antitumor effect

To address whether CDN/H9-MSA therapy induces a systemic NK cell effect with the potential to reject metastases, we established a bilateral tumor model system. B16-F10-*B2m*-/- tumors were established on both flanks of syngeneic mice (Figure 3.13A). In order to focus on the NK-mediated effect, all the mice were depleted of CD4 and CD8 T cells before the start of treatment. Tumors on the right flank of each mouse were injected with either PBS or CDN. H9-MSA or PBS was then delivered intraperitoneally. As before, combination therapy was more effective than the single therapies in the CDN-injected tumors (Figure 3.13B, Figure 3.14A). Remarkably, the same was true in the contralateral tumors that were not injected with CDNs, corroborating that local CDN therapy by itself exerted a systemic effect (Nicolai et al., 2020), and demonstrating that CDNs synergized with H9-MSA in mobilizing greater systemic antitumor effects (Figure 3.13B, Figure 3.14A). Depletion of NK cells diminished the efficacy of combination therapy similarly in both the injected tumor and the uninjected tumor (Figure 3.13C, Figure 3.14). As these mice were depleted of CD4 and CD8 T cells, the data implicated NK cells as major antitumor effectors both locally and in the distant tumor. Some delay in tumor growth in both tumors was still evident after simultaneous depletion of NK cells, CD4 and CD8 cells. Part of the residual effects of therapy in these conditions may be due to systemic TNF and IFN, based on the findings within single tumor experiments (Figure 3.8).

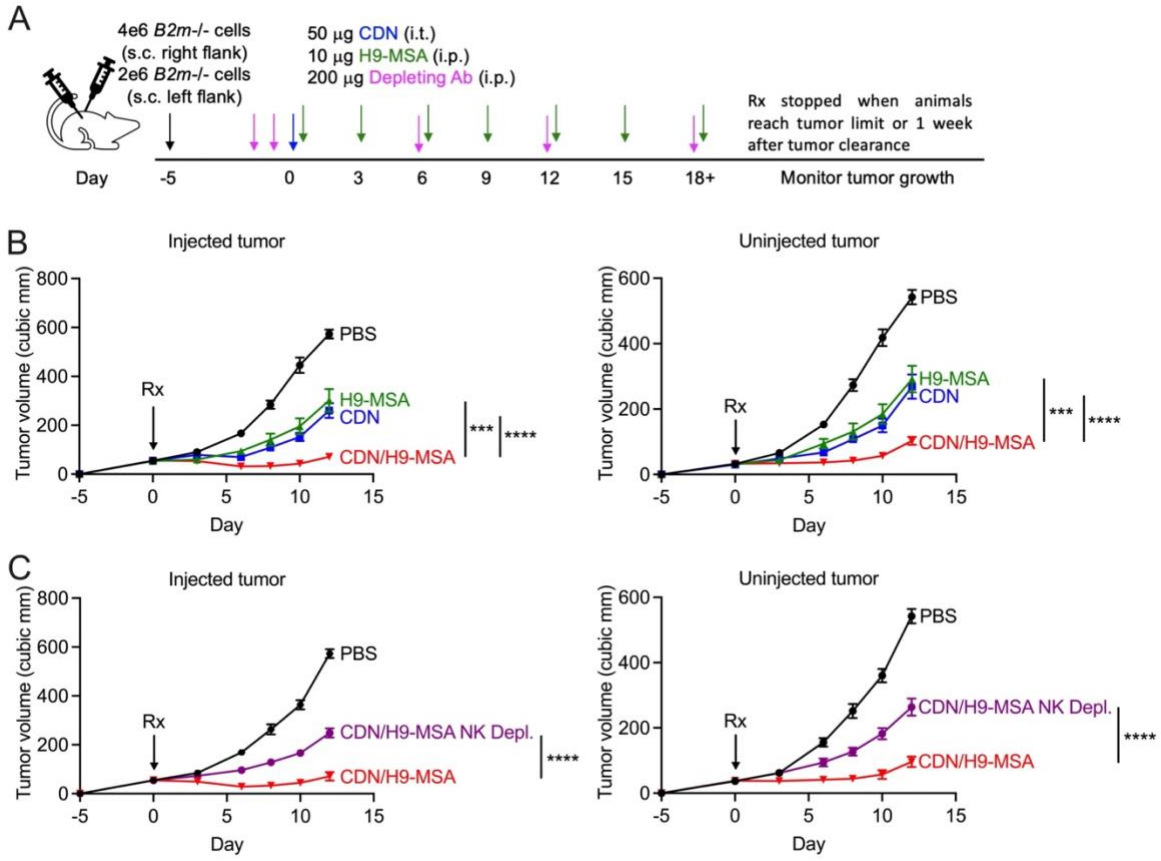

Figure 3.13. Intratumoral CDN injections combined with intraperitoneal H9-MSA injections synergized in creating a systemic NK cell-mediated antitumor effect. (A) Timeline of the bilateral tumor experiments. On day -5, B16-F10-*B2m*-/- tumor cells were injected s.c. on both flanks of C57BL/6J mice. Mice were depleted of CD4 cells and CD8 cells 2 days and 1 day before initiation of treatment. On day 0, right flank tumor was injected once i.t. with 50 µg CDN or PBS. The mice received i.p. injections of PBS or 10 µg H9-MSA starting on day 0. The cytokine or PBS injections were repeated every three days until mice were euthanized. **(B)** Growth of injected (left panel) vs contralateral uninjected tumors (right panel) receiving the indicated therapies. The data were combined from 3 experiments (n=18). **(C)** Tumor growth following CDN/H9-MSA therapy in mice from which NK cells were depleted or not (with the treatment schedule shown in panel A) as indicated. The data were combined from 2 experiments (n=12). Tumor growth data were analyzed by 2-way ANOVA. Error bars represent standard error of the mean (SEM). *P< 0.05, **P < 0.01, ***P < 0.001, ****P < 0.0001.

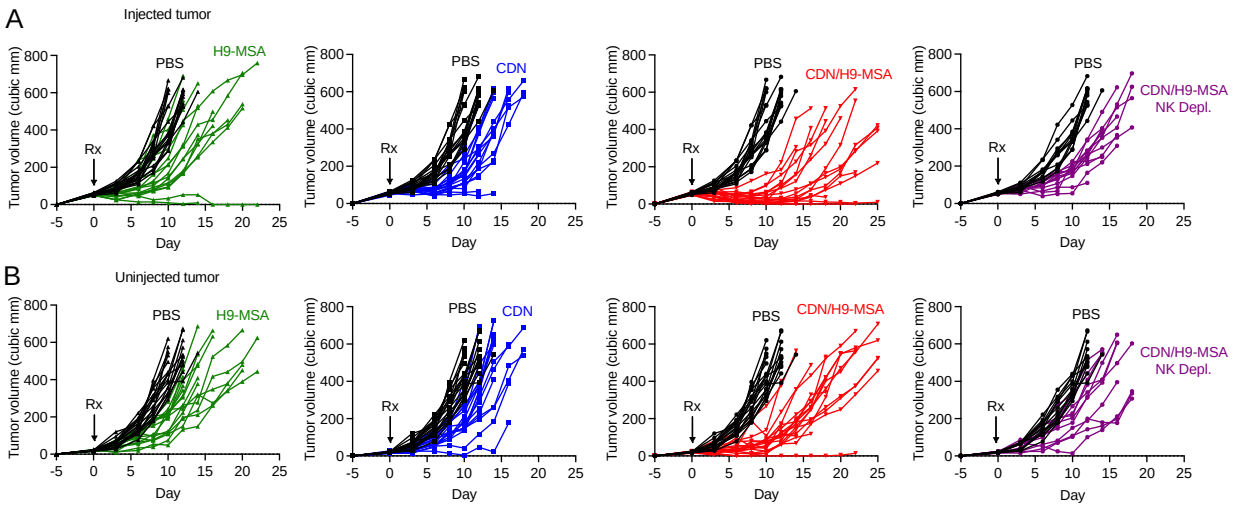

Figure 3.14. Spider plots showing growth of individual tumors from Figure 3.13. (A) Injected tumors and **(B)** Uninjected tumors from Fig. 3.13.

CDN/H9-MSA combination therapy mobilized more activated intratumoral NK cells with greater functional activity

To address the mechanisms underlying the synergy of CDN and H9-MSA in induction of antitumor NK cell responses, we employed the bilateral tumor system, and examined markers of activation on NK cells infiltrating both tumors 2 days and 5 days after treatment. The percentages of granzyme B+ NK cells in the tumors, and the levels of granzyme B per cell (mean fluorescence intensity of staining), were significantly elevated in mice treated with CDN/H9-MSA compared to mice treated with CDN alone (on day 5 for both injected or uninjected tumors), or compared to mice treated with H9-MSA alone (the levels of granzyme B/cell on day 2 for uninjected tumors and on day 5 for injected tumors) (Figure 3.15A, B, Figure 3.16, Figure 3.17). The percentages of CD69+ NK cells in the tumors were significantly elevated in mice treated with CDN/H9-MSA compared to mice treated with CDN alone (on day 5, and in uninjected tumors on day 2), or compared to mice treated with H9-MSA alone (on day 2) (Figure 3.15A, B, Figure 3.16, Figure 3.17). The percentages of NK cells expressing the activation marker Sca1 were also elevated in mice receiving combination therapy compared to mice receiving CDN therapy, and in uninjected tumors compared to mice receiving H9-MSA therapy (Figure 3.18A, B). On day 2, the percentages of NK cells among CD45+ cells were elevated in uninjected tumors in mice receiving combination therapy compared to mice receiving CDN therapy (Figure 3.15A, B, Figure 3.16, Figure 3.17). Overall, the combination therapy elicited NK cells showing higher levels of activation or granzyme B expression than did the individual therapies.

The greater activity of NK cells after combination therapy was evident when cytotoxic activity of splenic NK cells was tested ex vivo, despite there being no significant increase in NK cell numbers in the spleen (Figure 3.19). The lysis of B16-F10-*B2m*-/- tumor cells by splenic NK cells was highly elevated 24 or 72 hours after initiating treatment with the combination therapy, and was more sustained compared to separate treatments with CDN or H9-MSA (Figure 3.15C). NK depletion abrogated killing as expected (Figure 3.15D). In parallel, the percentages of splenic NK cells showing elevated granzyme B, CD69 or Sca1 were significantly elevated in mice two days after receiving the combination therapy compared to mice receiving the separate therapies (Figure 3.18C, D). These data demonstrated that the combination therapy had multiple impacts, maximizing NK cell activation and content of cytotoxic effector molecules (granzyme B), as well as cytotoxicity, and prolonging the NK response compared to each therapy separately.

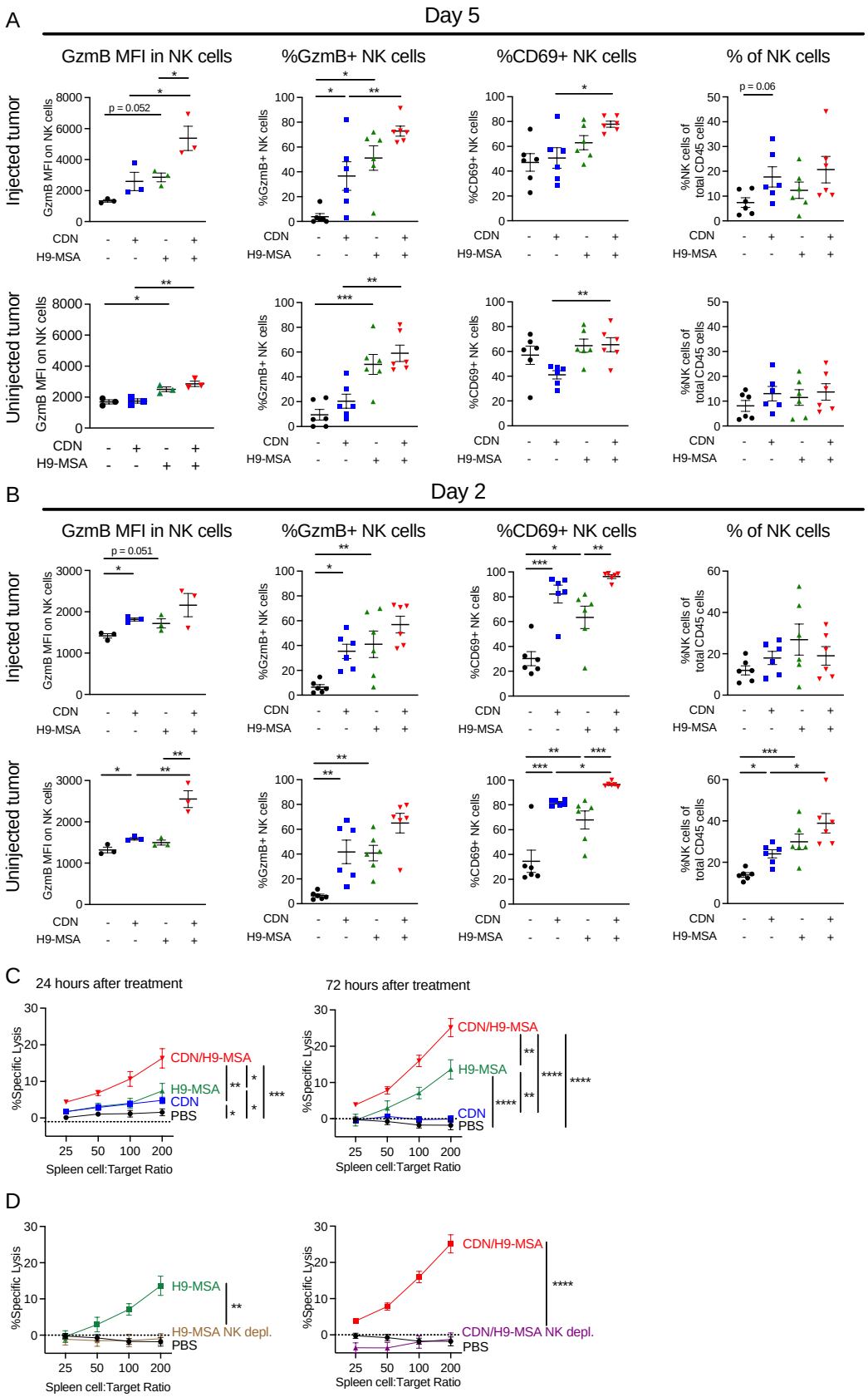
A
Day 5
GzmB MFI in NK cells
%GzmB+ NK cells
%CD69+ NK cells
% of NK cells
Injected tumor
Uninjected tumor
GzmB MFI on NK cells
%GzmB+ NK cells
%CD69+ NK cells
%NK cells of total CD45 cells
p = 0.052
p = 0.06
CDN
H9-MSA
B
Day 2
p = 0.051
C
24 hours after treatment
72 hours after treatment
%Specific Lysis
Spleen cell:Target Ratio
CDN/H9-MSA
H9-MSA
CDN
PBS
D
H9-MSA NK depl.
CDN/H9-MSA NK depl.

Figure 3.15. Activation, proliferation and cytotoxicity of NK cells in tumor bearing mice receiving CDN/H9-MSA immunotherapy. B16-F10-*B2m*-/- tumors were established on both flanks of C57BL/6J mice as in Figure 3.13. On d5 **(A)** or d2 **(B)** single cell suspensions of both tumors were examined for the intracellular or cell surface markers shown and the percentages of NK cells among viable CD45+ cells. n=3. GzmB MFI data are representative of at least 2 independent experiments (n=3) and all other data were combined from 2 independent experiments (n=6). Samples were analyzed by one-way ANOVA. **(C)** B16-F10-*B2m*-/- tumors were established and treated as described in Figure 3.13. 24 hr and 72 hr after treatment, splenocytes were tested for cytotoxicity of B16-F10-*B2m*-/- target cells. Spontaneous lysis of these target cells averaged 11%. Error bars are shown for biological replicates (n=8). **(D)** B16-F10-*B2m*-/- tumors were established, treated and tested as in panel C, 72 hrs after initiating H9-MSA therapy or combination therapy, as indicated. Additionally, mice in one group receiving each therapy were depleted of NK cells. n=8 biological replicates. Data in panels C and D were combined from 2 independent experiments and were analyzed by 2-way ANOVA. n=8. Error bars represent standard error of the mean (SEM). *P< 0.05, **P < 0.01, ***P < 0.001, ****P < 0.0001.

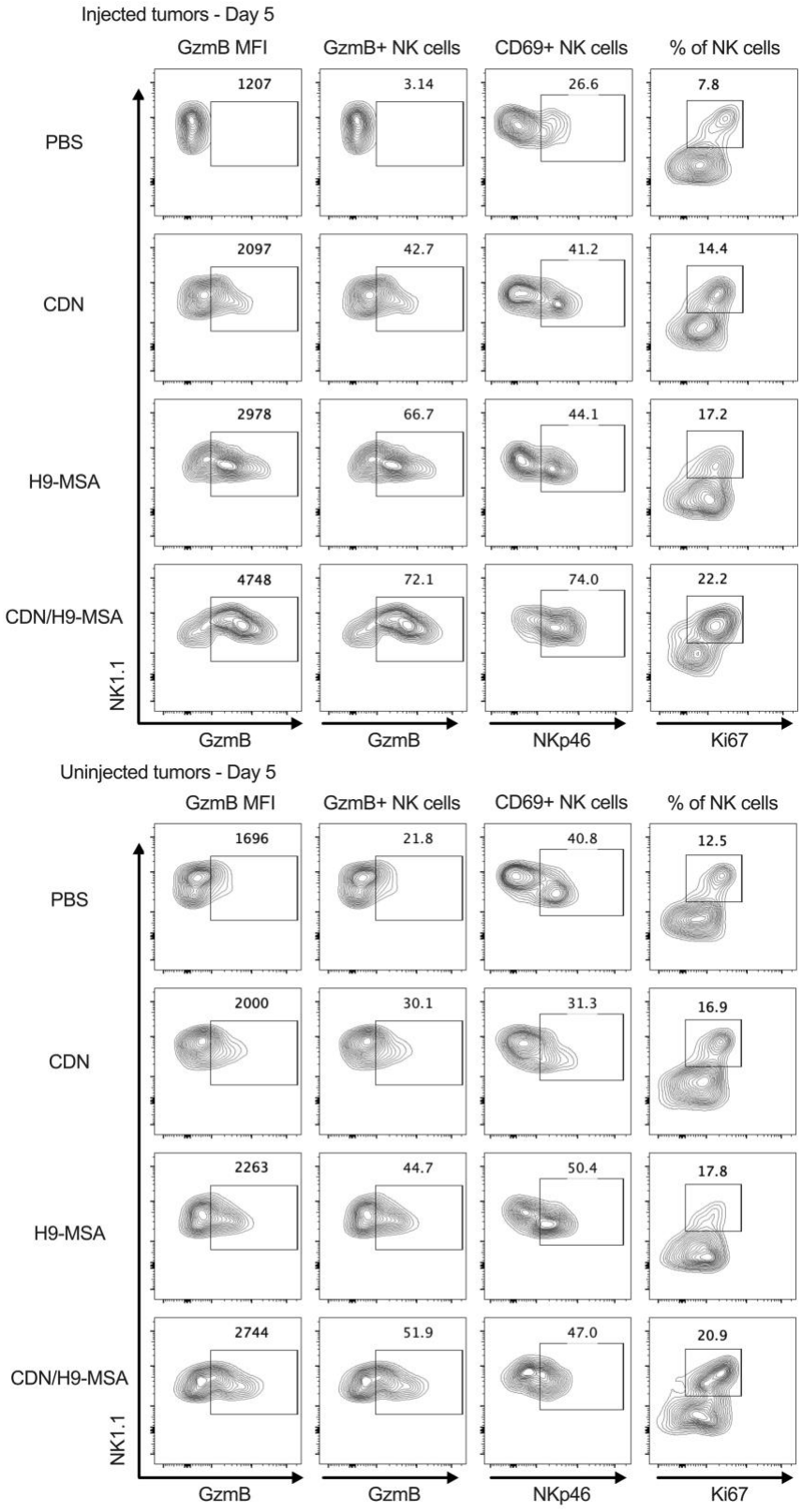

Figure 3.16. Representative gating strategies for flow cytometry data in Figure 3.13A. NK cells were gated as viable, $CD45^+$, $CD3^-$, $CD19^-$, $F4/80^-$, $Ter119^-$, $NK1.1^+$, $NKp46^+$ cells.

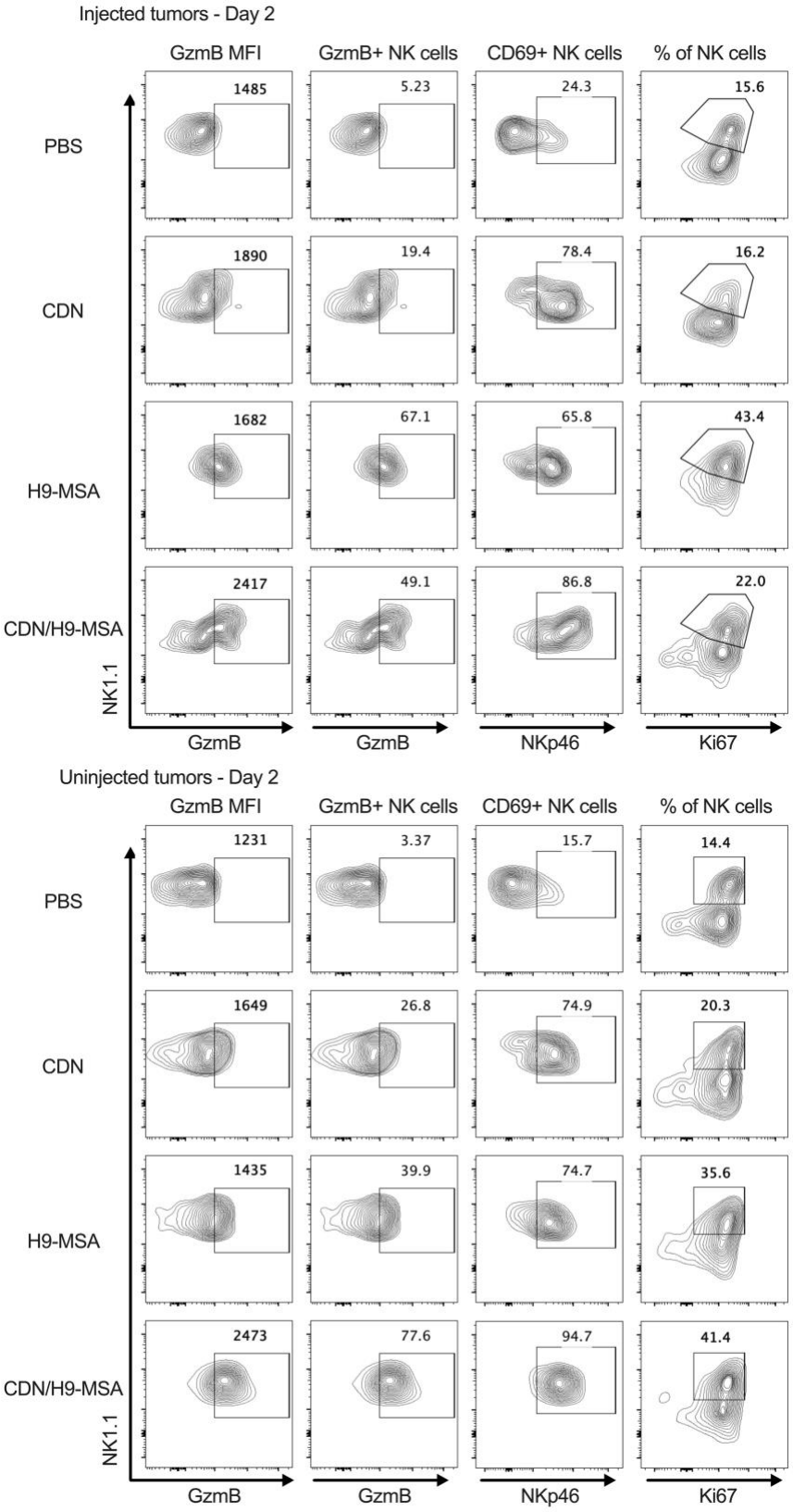
Injected tumors - Day 2
GzmB MFI
GzmB+ NK cells
CD69+ NK cells
% of NK cells
PBS
CDN
H9-MSA
CDN/H9-MSA
1485
5.23
24.3
15.6
1890
19.4
78.4
16.2
1682
67.1
65.8
43.4
2417
49.1
86.8
22.0
NK1.1
GzmB
GzmB
NKp46
Ki67
Uninjected tumors - Day 2
GzmB MFI
GzmB+ NK cells
CD69+ NK cells
% of NK cells
PBS
CDN
H9-MSA
CDN/H9-MSA
1231
3.37
15.7
14.4
1649
26.8
74.9
20.3
1435
39.9
74.7
35.6
2473
77.6
94.7
41.4
NK1.1
GzmB
GzmB
NKp46
Ki67

Figure 3.17. Representative gating strategies for flow cytometry data in Figure 3.13B. NK cells were gated as viable, CD45$^+$, CD3$^-$, CD19$^-$, F4/80$^-$, Ter119$^-$, NK1.1$^+$, NKp46$^+$ cells.

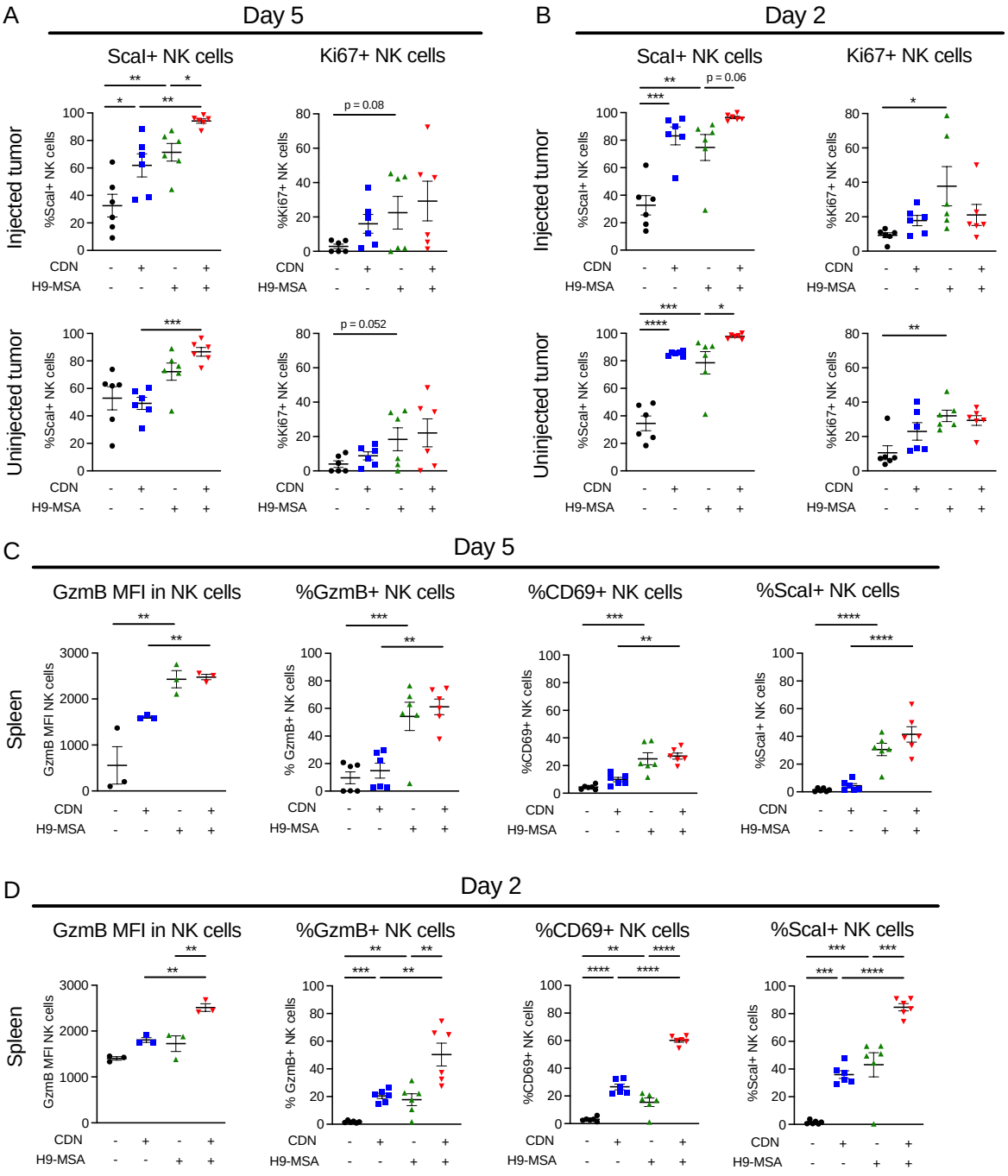

Figure 3.18. Induction of NK cell activation markers by CDN/H9-MSA treatments in tumors and spleens of mice. B16-F10-*B2m*-/- tumors were established on both flanks of C57BL/6J mice, treated and analyzed as in Figure 3.13. On d5 **(A)** or d2 **(B)** after initiating therapy, single cell suspension of both tumors were examined for Sca1 and Ki67 expression on NK cells in both injected and uninjected tumors. Splenocytes on d5 (C) or d2 (D) were examined for intracellular or cell surface markers on NK cells after CDN/H9-MSA

treatment. NK cells were gated as viable, CD45^{+}, CD3^{-}, CD19^{-}, F4/80^{-}, Ter119^{-}, NK1.1^{+}, NKp46^{+} cells. GzmB MFI data are representative of at least 2 independent experiments (n=3) and all other data were combined from 2 independent experiments (n=6). Samples were analyzed by one-way ANOVA. Error bars represent standard error of the mean (SEM). *P< 0.05, **P < 0.01, ***P < 0.001, ****P < 0.0001.

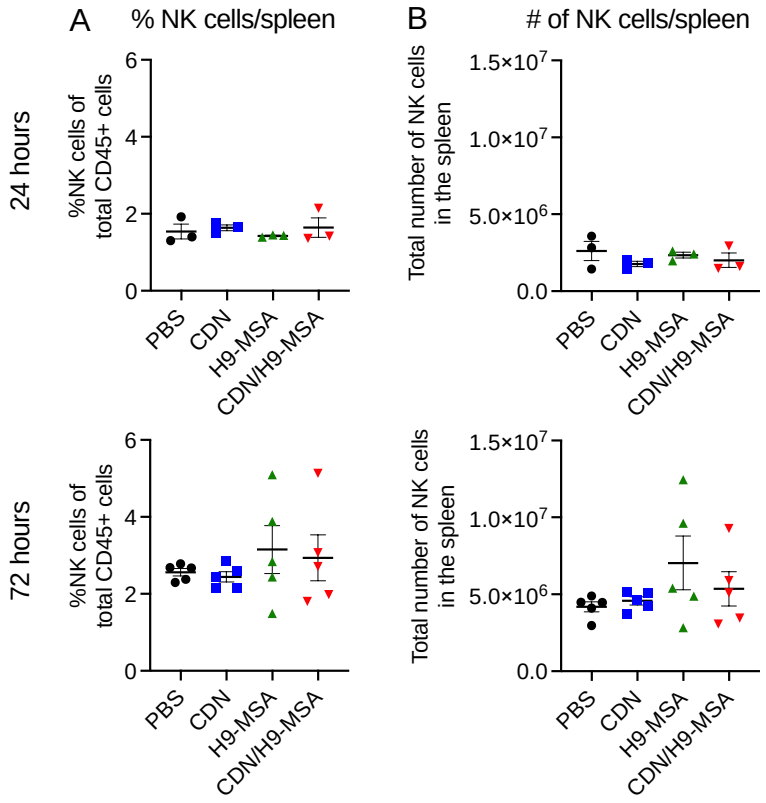

Figure 3.19. NK cell percentages and numbers in the spleen after CDN/H9-MSA treatment. NK cells were gated as viable, CD45^{+}, CD3^{-}, CD19^{-}, F4/80^{-}, Ter119^{-}, NK1.1^{+} cells. **(A)** Percentage of NK cells in the spleen. **(B)** Total number of NK cells in the spleen. Error bars represent standard error of the mean (SEM). *P< 0.05, **P < 0.01, ***P < 0.001, ****P < 0.0001.

CDN/H9-MSA combination therapy effectively treats tumors in mice with a complex microbiota

As new information about the microbiome is reported, it has become clear the efficacy of various therapies including checkpoint blockade is greatly influenced by the microbiota (Gopalakrishnan et al., 2018). To determine if changes in the microbiota would alter the efficacy of CDN/H9-MSA combination therapy, we turned to the "pet store mouse model" developed at the University of Minnesota. By co-housing C57BL/6J mice with mice from pet stores, the C57BL/6J mice take on a more complex microbiota and in turn, their immune systems better resemble an adult human (Beura et al., 2016). Using this system, we were able to test the combination of CDN/H9-MSA in treating MC38-*B2m*-/- tumors in co-housed animals versus specific pathogen free (SPF) animals. Tumors treated with the vehicle PBS grew significantly slower in co-housed mice than in SPF mice, but survival was not increased (Figure 3.20B, Figure 3.21). Co-housed mice treated with CDN or CDN/H9-MSA showed no difference in tumor growth or survival compared to SPF mice (Figure 3.20C, D). CDN and CDN/H9-MSA treatment in both SPF and co-housed mouse reduced tumor growth to a similar extent (Figure 3.20E). Overall, the CDN/H9-MSA combination therapy exhibited strong synergy against MHC I-deficient tumors in mice with a complex microbiota and immune system.

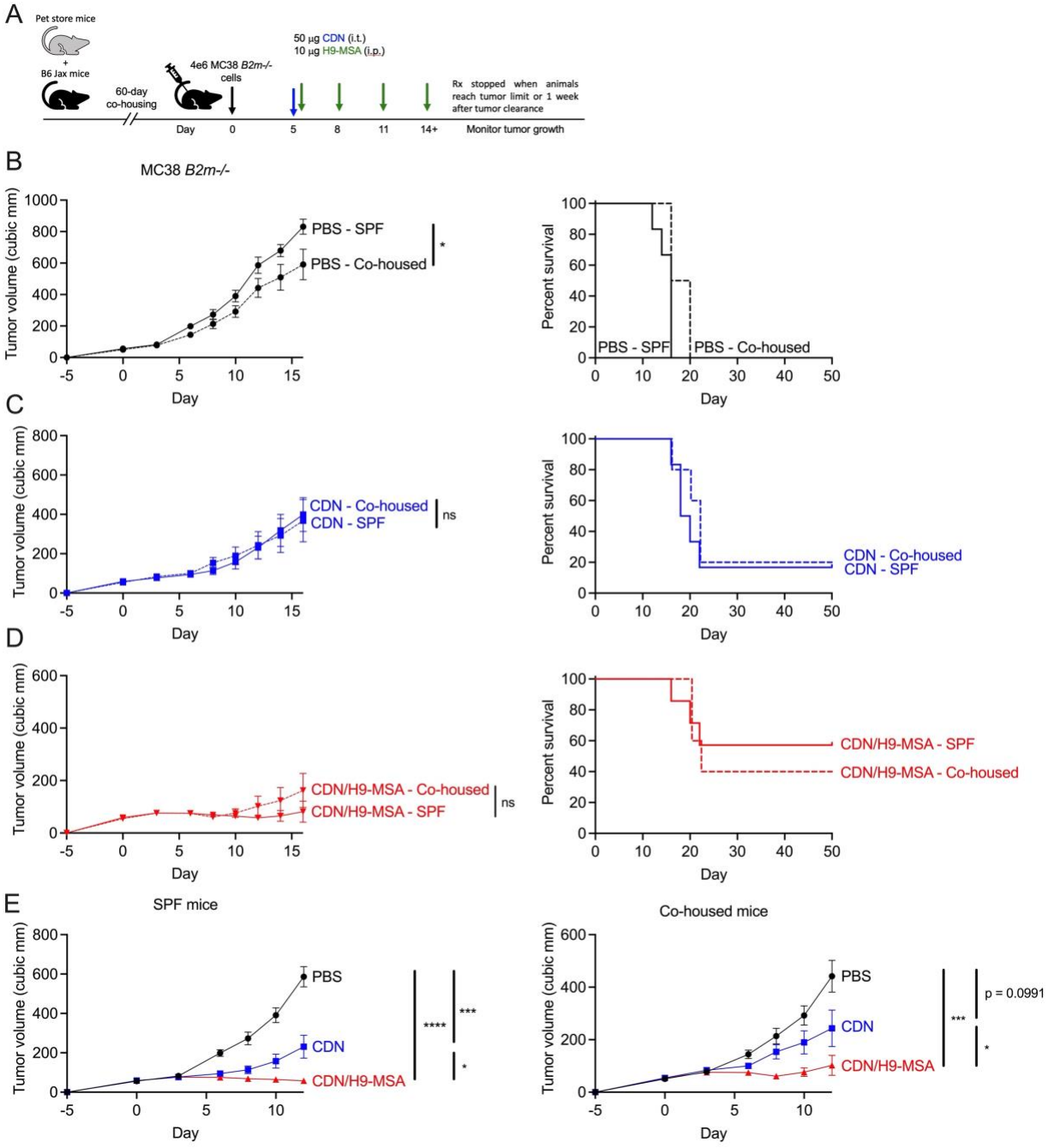

Figure 3.20. Co-housed mice with a complex microbiota exhibit synergy of CDN/H9-MSA therapy in treating MHC I-deficient tumors. (A) Timeline. C57BL/6J female mice and female pet-store were co-housed together for 60 days after which tumor cells were implanted s.c. in C57BL/6J mice and grown to approximately 50 mm^3 (day 0). Tumors were injected once i.t. with 50 µg of CDN or PBS. Mice were also injected i.p. with 10 µg H9-MSA or PBS on day 0. The cytokine or PBS injections were repeated every three days until euthanization or 1 week after tumor clearance. **(B, C, D)** Tumor growth curves and survival of mice treated with PBS (B), CDN (C) or CDN/H9-MSA (D). **(E)** Tumor growth curves and

survival of SPF mice (left) or co-housed mice (right) with various treatments. Tumor growth data was analyzed by 2-way ANOVA. Survival data was analyzed using log-rank (Mantel-Cox) tests. n=5-7 mice per group. All panels are from the same experiment. This experiment was only carried out once, so the results must be considered preliminary. Error bars represent standard error of the mean (SEM). *P< 0.05, **P < 0.01, ***P < 0.001, ****P < 0.0001

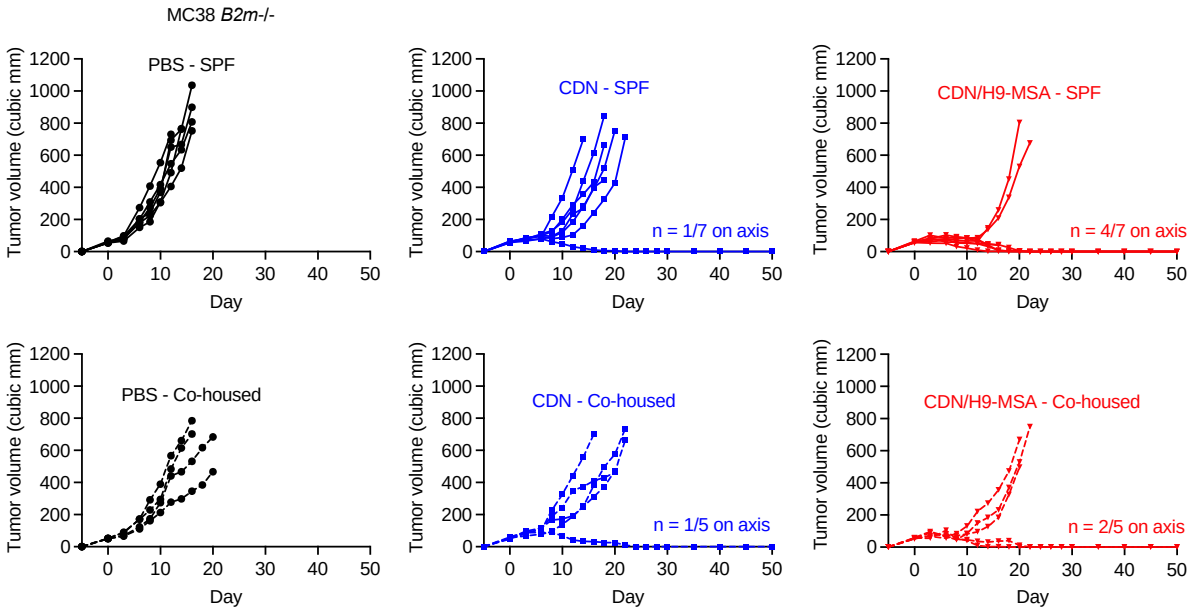

Figure 3.21. Spider plots showing growth of individual tumors from Figure 3.20. Spider plots for comparison of treated animals

CDN synergized with H9-MSA to induce regression of large MC38-B2m-/- tumors, but failed to cure mice

Mice bearing MC38-*B2m*-/- tumors treated with the CDN/H9-MSA combination therapy completely rejected their tumors when therapy was initiated when tumors were at a volume of 50 mm^3 (Figure 3.2). Because tumors can vary greatly in size at the time of patient diagnosis, we tested the efficacy of CDN/H9-MSA therapy when it was initiated with progressively larger tumors. Mice were injected s.c. with MC38-*B2m*-/- tumors and therapy was initiated when tumors reached volumes of 50 mm^3, 150 mm^3, 300 mm^3 or 450 mm^3 (Figure 3.22). All of the mice with the smallest tumors, 50 mm^3, completely rejected their tumors when treated with CDN/H9-MSA. In contrast, in mice with medium-sized (150 mm^3 or 300 mm^3) or large (450 mm^3) tumors, the CDN/H9-MSA combination therapy caused a substantial and significant delay in tumor growth, but all of the tumors eventually grew out. Of note, the CDN/H9-MSA treatments did cause an initial massive debulking of the medium- and large-sized tumors, similar to what we observed with small tumors.

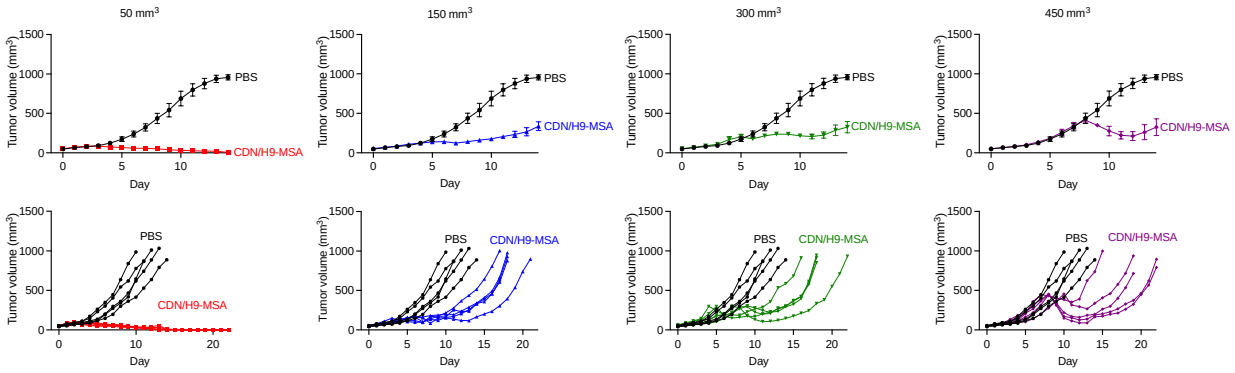

Figure 3.22. CDN/H9-MSA combination therapy effectively reduces MC38-*B2m*-/- medium- and large-sized tumor growth. MC38-*B2m*-/- tumor cells were implanted s.c. in C57BL/6J mice and grown to varying tumor sizes. When tumors reached the appropriate size, they were injected once i.t. with 50 μg of CDN or PBS. Mice were also injected i.p. with 10 μg H9-MSA or PBS on day 0. The cytokine or PBS injections were repeated every three days until 1 week after tumor clearance or the mice needed to be euthanized due to progressing tumors. Tumor growth curves and spider plots of individual mice with MC38-*B2m*-/- tumors of either 50mm^3, 150 mm^3, 300 mm^3, or 450mm^3 starting sized tumors. Tumor growth data was analyzed by 2-way ANOVA. The data in all panels are representative at least two independent experiments. n=5 mice per group. Error bars represent standard error of the mean (SEM).

Discussion

The CDN/H9-MSA therapy combination synergistically induced profound antitumor responses in several solid MHC I-deficient tumor transplant models of varying sizes. We suspect that the therapy combination would be very effective for hematologic malignancies as well, considering that such tumor cells are frequently highly sensitive to NK-mediated killing. It remains to be seen whether this therapy combination will be effective for larger tumors than tested here.

An important consideration for clinical applications is whether therapies elicit control of metastases distant from the site of a primary tumor, which are known to limit the efficacy of immunotherapies (Ribas and Wolchok, 2018; Sharma and Allison, 2015). We observed that local administration of CDN in a primary tumor, combined with systemic applications of H9-MSA, resulted in strong systemic activation of NK cells capable of limiting the growth of a second tumor on the opposite flank of the animals and mediating killing of tumor cells in ex vivo tests with splenic NK cells. In contrast, NK cell activation after a single treatment with CDN alone was short lived, as by 72 hours after treatment, cytotoxicity by splenic NK cells had subsided. Thus, the combination therapy sustained the systemic cytotoxicity of NK cells. We suspect that the impact of intratumoral injections of CDNs on NK cell activation in a distant second tumor or in the spleen is due to induced accumulation of systemic IFN which resulted in > 1 ng/ml of IFN-β detected in the serum after intratumoral CDN injections in a different tumor model (Nicolai et al., 2020). Systemic accumulation of other cytokines induced by intratumoral CDN injections and/or the leakage of small amounts of CDNs from the tumor into the general circulation (Sivick et al., 2018) may also play a role. We think it unlikely that the systemic effects are due to trafficking of NK cells activated at the site of treatment to other sites, because the percentage of activated NK cells in uninjected tumors was close to 100% as assessed by Sca1 expression (Figure 3.16A, B) and was nearly as high in the spleen two days after treatment with CDN/H9-MSA (Figure 3.16C, D). It is highly unlikely that such a high percentage of all NK cells trafficked through the site of treatment in this short period.

Another important consideration for clinical application is how or if the microbiome will affect the efficacy of the combination treatment. It has been shown the presence of specific bacteria in the intestines limits the effectiveness of anti-PD-1 therapy. Using the recently developed co-housing system, we were able to establish mice with a complex microbiota to evaluate how the presence of many different microbial species could influence the CDN/H9-MSA antitumor responses. To our surprise, co-housed mice exhibited a similar rate of tumor rejection compared to SPF mice, indicating that this therapy does not seem to be much affected by varying microbial species and therefore could translate very well into a clinical setting.

Mechanistically, the synergistic antitumor effects of CDNs and H9-MSA were manifested primarily by greater induction of NK cell activation, cytotoxicity and granzyme B expression, as well as some impact on NK cell proliferation. Type I IFNs induced by intratumoral injections of CDN act directly on NK cells to induce granzymes and cytotoxicity (Martinez et al., 2008; Nicolai et al., 2020) and protection from fratricide (Madera et al., 2016) and indirectly by inducing IL-15Rα/IL-15 complexes on DCs, which are trans-presented to NK cells (Lucas et al., 2007; Nicolai et al., 2020). The early bursts of IFN and IL-15 induced by administration of CDN

are not sustained, however, consistent with the rapid waning of NK activity we observed with CDN alone. NK cells that infiltrate MHC I-deficient tumors are also prone to enter a state of hyporesponsiveness or anergy, which can be delayed or reversed with injections of cytokines, including H9, or a mixture of IL-12 and IL-18 (Ardolino et al., 2014). Together, these mechanisms are likely to account for the synergistic effects of combining H9-MSA and CDN therapy.

In syngeneic tumor transplant models, H9-MSA acted synergistically with CDNs, but also with another agonist for the innate immune system, CpG ODN DS-L03, a TLR9 agonist optimized to stimulate high levels of type I IFN (Yang et al., 2013b). These findings show the promise of combining IL-2/IL-15 family cytokines with agents that induce IRF3 and NF-kB signaling. Clinical trials of TLR agonists and STING agonists as cancer therapies have thus far yielded mixed results but clinical development remains active (Harrington et al., 2018; McWhirter and Jefferies, 2020; Meric-Bernstam et al., 2019). Many engineered forms of IL-2 family cytokines, including pegylated IL-2, Fc-bound, and engineered partial agonists, are currently being investigated in many clinical and pre-clinical trials (Mullard, 2021). Our findings suggest that those variants should be tested in combination with innate agonists such as STING agonists or CpG ODN to improve overall outcomes. The greater challenges of treating human cancer versus mouse cancer models are well documented and may reflect later diagnosis, a relatively older population in the case of human patients, and the frequent use of transplantable mouse cancer models as opposed to primary cancer models, among other factors. Our results with primary sarcomas were encouraging, however, and suggest that the synergistic effects of combining innate agonists and IL-2 family cytokines may have considerable promise in clinical applications.

Compared to high dose IL-2, the H9 superkine was previously shown to provide greater antitumor efficacy yet lower toxicity with lower accumulation of Tregs (Levin et al., 2012). Published studies show greater efficacy of IL-2 and other cytokines with half-life extending modifications, such as fusion to albumin or Fc domains, or PEGylation (Mullard, 2021; Zhu et al., 2015). We observed that extended half-life H9 was more effective than extended half-life IL-2 in the context of combination therapy as well. We observed acceptable toxicity in mice receiving the combination therapy, generally maintaining a normal body score, but acknowledge further assessment of toxicity is needed. Considering these results, H9-MSA warrants consideration for clinical applications. Combining CDN therapy with other half-life extended IL-2 and IL-15 variants, several of which are undergoing clinical testing (Mullard, 2021), may also be effective.

The therapeutic effects of CDN/H9-MSA combination therapy were mediated by different effector cells depending on the tumor cell line studied and whether the tumor cells expressed MHC I molecules. In two difficult-to-treat MHC I-deficient tumor models NK cells were critical for tumor rejection after combination therapy. Remarkably, in the MC38-*B2m*-/- model the treatment effectively cured 100% of tumor-bearing *Rag2*-/- mice, which lack T cells. NK cells were essential for these dramatic effects. In the B16-F10-*B2m*-/- model, NK cells and CD4 T cells each caused weaker tumor rejection separately, but together resulted in long term survival in the large majority of the animals. The less effective NK cell responses in the B16-

F10-*B2m*-/- model could be related to the absence of NKG2D ligands, which are present on MC38 cells but not B16 cells (Jamieson et al., 2002).

In the absence of T cells and NK cells, the combination therapy still delayed tumor growth in all the tumor models studied but did not result in long-term remissions. Our data suggest that therapy-induced production of TNF-a, which alters the tumor vasculature, and type I IFNs, which inhibit cell proliferation, are partly responsible for the residual antitumor effects and is supported by the observation of increased serum IFN after a single intratumoral CDN injection (Nicolai et al., 2020). It remains possible that the therapy combination also induces other antitumor cytokines or other cell types that retard tumor growth, such as myeloid cells or other innate lymphoid cell subtypes.

In conclusion, our results show that CDN therapy combined with the IL-2 superkine, H9-MSA, effectively enhanced the rejection MHC I-deficient tumors. The CDN/H9-MSA treatments proved to be remarkably effective against difficult-to-treat tumors, mobilizing various effector cells depending on tumor cell type. These results provide compelling support for testing combinations of innate immune system agonists and IL-2 family superkines as potential next-generation immunotherapies for tumors that are resistant to currently approved immunotherapy regimens.

Chapter 4
CDN and H9-MSA combination therapy enhance T cell antitumor responses from against MHC I-deficient and MHC I+ tumors

Portions of this chapter were adapted and/or reprinted with permission from "Wolf, N.K., Blaj, C., Picton, L, Snyder, G., Zhang, L. Nicolai, C.J., Ndubaku, C.O., McWhirter, S.M. Garcia, K.C. and Raulet, D.H. Synergistic effects of a STING agonist and an IL-2 superkine in cancer immunotherapy against MHC I-deficient and MHC I+ tumors. *Proc Natl Acad Sci U S A*, In press (2022)."

Introduction

In chapter 3, the antitumor NK cell effects induced by the powerful synergy of a STING agonist and an IL-2 superkine were explored in the context of MHC I-deficient tumor models. A single intratumoral injection of CDN combined with periodic injections of the IL-2 superkine, H9-MSA, resulted in a dramatically increased percentage of animals with disease-free survival in very difficult-to-treat tumor transplant models. In the case of MHC I-deficient tumor lines, tumor rejection was mediated at least in part by NK cells.

In this chapter we investigate the capacity of this combination therapy to elicit potent T cell mediated tumor rejection. As described in chapter 3, in some models we tested CD4 T cells also contributed to tumor rejection after treating mice with CDN alone (RMA-*B2m-/-* tumors, as shown previously by Chris Nicolai in the laboratory (citation) or CDN/H9-MSA (B16-*B2m-/-* tumors, chapter 3). It is unknown how these CD4 T cells induced by CDN or CDN/H9-MSA therapy play a role in mediating tumor rejection in various MHC I-deficient tumor models.

The role for CD4 T cells is generally thought be in "helping" the CD8 T cell and B cell responses (Haabeth et al., 2014; Tay et al., 2021) . CD4 T cells activation occurs through recognition of peptide loaded MHC II on antigen presentation cells leading to the production of various cytokines, such as IFNγ and TNFα, that help to facilitate an antitumor immune response. However, there are reports supporting a role for CD4 T cells in eliminating tumor cells independently of CD8 T cells or antibody (Pardoll and Topalian, 1998). The mechanisms of tumor elimination by CD4+ T cells remain unclear, however.

Traditionally, CD8 T cells are considered the major mediators of antitumor immune responses and are the focus of most immunotherapies. CD8 T cells interact with MHC I, displaying peptides including neoantigens derived from mutated proteins or inappropriately expressed proteins in tumor cells, on the surface of antigen presenting cells (APCs) and the tumor cells themselves. This engagement causes activation of the CD8 T cells and subsequent killing of target cells (Raskov et al., 2021). Strong CD8 T cell responses have been shown to be induced by injection of STING agonists intratumorally, leading to primary regression of MHC I+ WT tumors (Corrales et al., 2015; Sivick et al., 2018).

However, many types of tumors evade CD8 T cell recognition by displaying few or no antigens, or losing expression of MHC I. In several models of MHC I-deficient tumors treated with CDN therapy, CD8 T cells played no role in tumor rejection (Figure 3.2) (Nicolai et al., 2020). In some models of this type, CD4 T cells were partially responsible for tumor rejection. Some MHC I+ tumors are very resistant to immunotherapies, however, including CDN therapy by itself. This may reflect a low abundance of tumor antigens or other features that reduce immunogenicity of such tumors.

This chapter explores various instances in which strong T cell mediated antitumor responses are induced by CDN therapy or CDN/H9-MSA therapy. In one such model, CDN treatment increased systemic levels of tumor specific CD4 T cells with a Th1-like phenotype. In another MHC I-deficient model, CDN alone failed to induce potent antitumor CD4 T cells, whereas treatments with CDN/H9-MSA induced potent CD4 T cell and CD4/CD8 T cell responses. The antitumor CD4 T cell response did not rely on MHC II expression on the tumor cells to elicit tumor rejection. Priming with tumor cells elicited cytokine producing CD4 T cells specific for antigens on tumor cells. Finally, this chapter documents that the CDN/H9-MSA combination therapy regimen synergistically mobilizes powerful CD8 T cell responses in the case of certain MHC I+ tumors, including a syngeneic tumor transfer model and a carcinogen-induced primary tumor model. Together, these findings suggest that the CDN/H9-MSA combination elicits potent antitumor effects by NK cells, CD4 T cells and CD8 T cells, indicating the generality of the approach.

Results

Myeloid depletions reveal these cells do not play a large role in mediating tumor rejection of RMA-B2m-/- tumors after treatment with CDN

In Chapter 3, I documented that CDN/H9-MSA therapy elicited potent CD4 T cell mediated rejection of B16-B2m-/- tumors, in addition to stimulating antitumor NK cells. Previously, a former member of the Raulet laboratory, Chris Nicolai, showed that CDN therapy alone elicited significant CD4 T cell mediated tumor rejection (as well as antitumor NK cells) using a different MHC I-deficient tumor model: RMA-*B2m*-/- tumors. His work revealed CD4 T cells did not rely on tumor expression of MHC II for direct recognition and did not kill through FAS. He found that IFNγ, produced by the CD4 T cells, was important for the antitumor response. Based on these findings, we considered that myeloid cells induced by IFNg (Boehm et al., 1997) may play a key role in tumor rejection. Nicolai tested whether tumor rejection induced by CDN in NK-deficient NK-DTA mice (which lack NK cells in order to focus on the CD4 mediated component of rejection) was impaired by depleting macrophages (Clodronate liposomes), neutrophils (anti-Ly6C and anti-GR-1), monocytes (anti-GR-1) or eosinophils (anti-IL-5). Each depletion had a small effect, but only GR-1 treatments (which deplete neutrophils and monocytes) had a statistically significant effect compared to PBS treatments (unpublished data).

To explore the effects of the myeloid cells further, we reasoned that each of several phagocytic cell types might be participating in tumor rejection. Therefore, I elected to test whether simultaneous depletion of neutrophils, monocytes and macrophages would have a greater impact on tumor rejection in this model. NK cell-deficient NK-DTA mice bearing RMA-*B2m*-/- tumors received therapy with CDN, followed by treatments with PBS or with a mixture of clodronate, anti-Ly6G and anti-GR-1. The triple depletion did not significantly impair tumor rejection, nor did treatments with each separately (Figure 4.1). Therefore, I was not able to confirm the role of phagocytes, separately or together, in CDN-induced tumor rejection dependent on CD4 T cells.

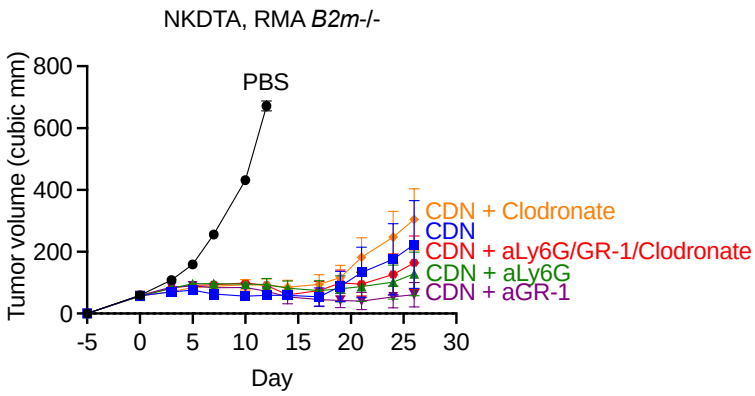

Figure 4.1. Myeloid cellular depletions of mice bearing RMA-*B2m*-/- tumors. RMA-*B2m*-/- tumor cells were implanted s.c. in C57BL/6J mice on day -5 and grown to approximately 50 mm^3. On day 0, tumors were injected once intratumorally with 50 μg of CDN or PBS. Additionally, some mice received 100 ug anti-GR-1 (clone RB6-8C5) and/or 100 μg anti-GR-1 (clone RB6-8C5) and/or 200 μg anti-Ly6G (clone 1A8) and/or 200 μl Clodronate Liposomes on day -2 and -1 and repeated every 3 days. Tumor growth curves shown. n=6-7 mice per group. Error bars represent standard error of the mean (SEM).

CDN therapy induced more tumor specific CD4 T cells, exhibiting an increased Th1 subset phenotype

In his investigation of the CD4 T cell response induced by CDN in mice with RMA-*B2m*-/- tumors, Nicolai was able to identify CD4 T cells specific for the gp70 tumor antigen those cells express using gp70 MHC II ($I\text{-}A^b$) tetramers. He discovered significantly more tetramer positive CD4 T cells in the spleens of CDN treated tumor bearing mice than in mice that received PBS instead of CDN. By stimulating the cells with the gp70 peptide, Nicolai found, showed that in mice receiving CDN therapy, more of the CD4+ tetramer positive T cells produced IFNγ, TNFα, and IL-2.

To further aid in classifying the subtype of the responding CD4 T cells, I repeated these tetramer stains on splenocytes as well as immune cells from the tumor draining lymph node (dLN). Mice were given RMA-*B2m*-/- tumors, which were treated with PBS or CDN. Six days later, splenocytes and dLN cells were collected and stained. CDN therapy induced significantly more gp70 tetramer positive CD4 T cells in the spleen compared to PBS treated or naïve mice (Figure 4.2A, Figure 4.3A). However, CDN and PBS treatments resulted in a similar percentage of gp70 tetramer positive CD4 T cells in the dLN (Figure 4.2A). Hence, CDN therapy caused an increase in the percentage of specific CD4 T cells in the spleen but not the draining LN.

To identify the T helper subset contributing to the antitumor response in CDN treated mice, tetramer positive cells were stained for the key transcription factor of each T helper subset (Figure 4.2B, C, Figure 4.3B). In the spleens of tumor bearing mice, percentage of $Tbet^+$ CD4 T cells increased from <10% in PBS treated mice to approximately 35% in CDN treated mice (Figure 4.2B, Figure 4.3B) indicating that Th1 cells were induced. The other Th subsets were generally decreased in the CDN-treated vs PBS treated animals, significantly so in the case of Th2 (GATA3+) and Tfh (Bcl-6+) cells. The decrease in Tregs was almost significant, consistent with Nicolai's unpublished data showing decreased Tregs after CDN therapy in this model. (Figure 4.2B, Figure 4.3B). The same trends were observed in the tumor dLN, with more $Tbet^+$ cells and fewer $GATA3^+$, $RORyt^+$, $FoxP3^+$ and $Bcl\text{-}6^+$ cells, induced by CDN therapy, though only the reduction in Bcl-6+ cells was statistically significant (Figure 4.2C). These data together with Nicolai's data showing that a larger proportion of these CD4 tetramer positive T cells produce Th1 cytokines, suggest CDN therapy induces a skew towards Th1 CD4 T cells in RMA-*B2m*-/- tumor bearing mice. Notably, approximately 50% of the CD4+ cells did not stain for any of the Th defining transcription factors.

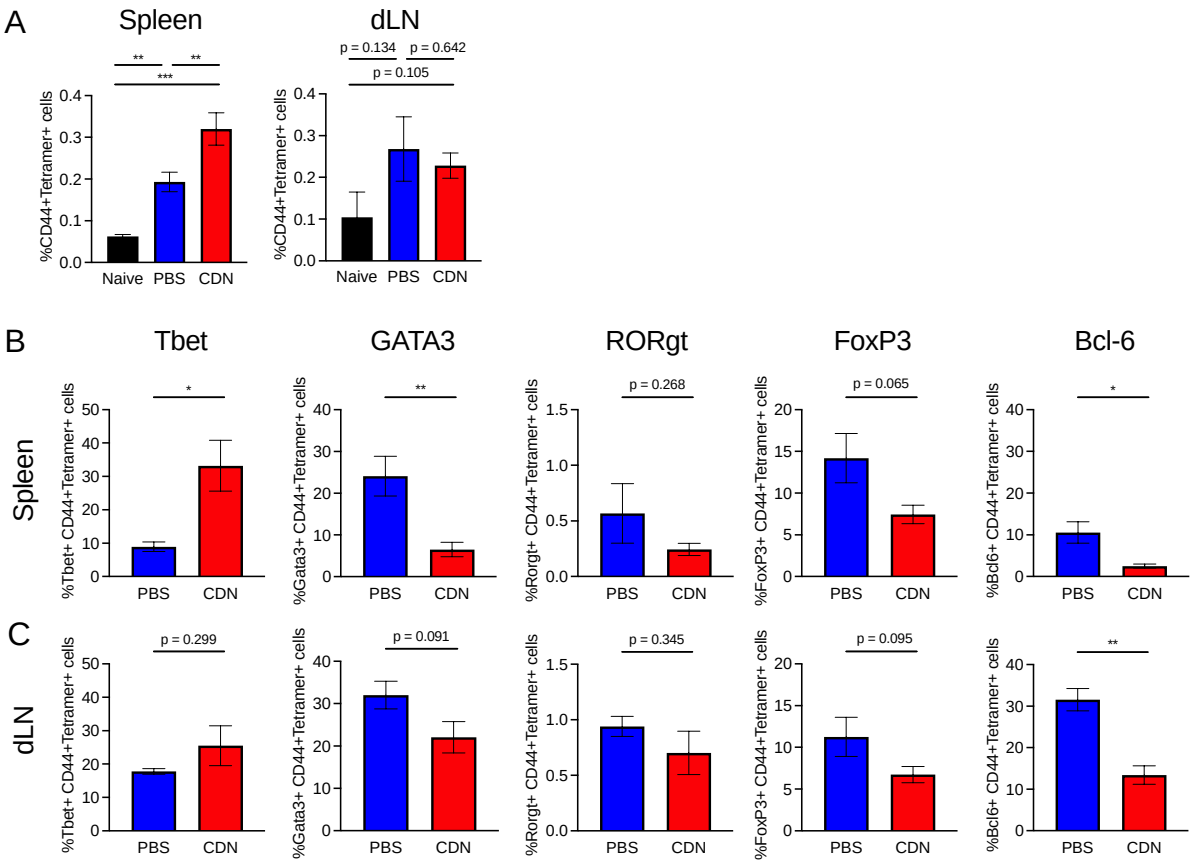

Figure 4.2. CDN therapy induced more tumor specific CD4 T cells, exhibiting an increased Th1 subset phenotype. RMA-*B2m-/-* tumor cells were implanted s.c. in C57BL/6J mice on day -5 and grown to approximately 50 mm^3. On d0, tumors were injected once intratumorally with 50 μg indicated CDN or PBS. Approximately a week later, splenocytes were stained with gp70 MHC II tetramer at 1:400 for 3 hr at 37C and then further stained for viability and surface/intracellular markers. **(A)** Percentage of gp70 MHC II tetramer positive CD4 T cells in the spleen (left) and tumor draining lymph node (dLN) (right). The data in all panels are representative of two independent experiments. **(B, C)** Tetramer positive CD4 T cells in the spleen (B) and dLN (C) stained for the T cell helper subset identifying transcription factors. CD4+ T cells were gated as viable, $CD45^+$, $NK1.1^-$, $CD19^-$, $Ter119^-$, $F4/80^-$, $CD3^+$, $CD4^+$. Fluorescence Minus One (FMO) samples were used for gating of the indicated transcription factor. n=4 mice per group. Data analyzed by 2-tailed unpaired Student's t-test. This experiment was only carried out once, so the results must be considered preliminary. Error bars represent standard error of the mean (SEM). *P< 0.05, **P < 0.01, ***P < 0.001, ****P < 0.0001.

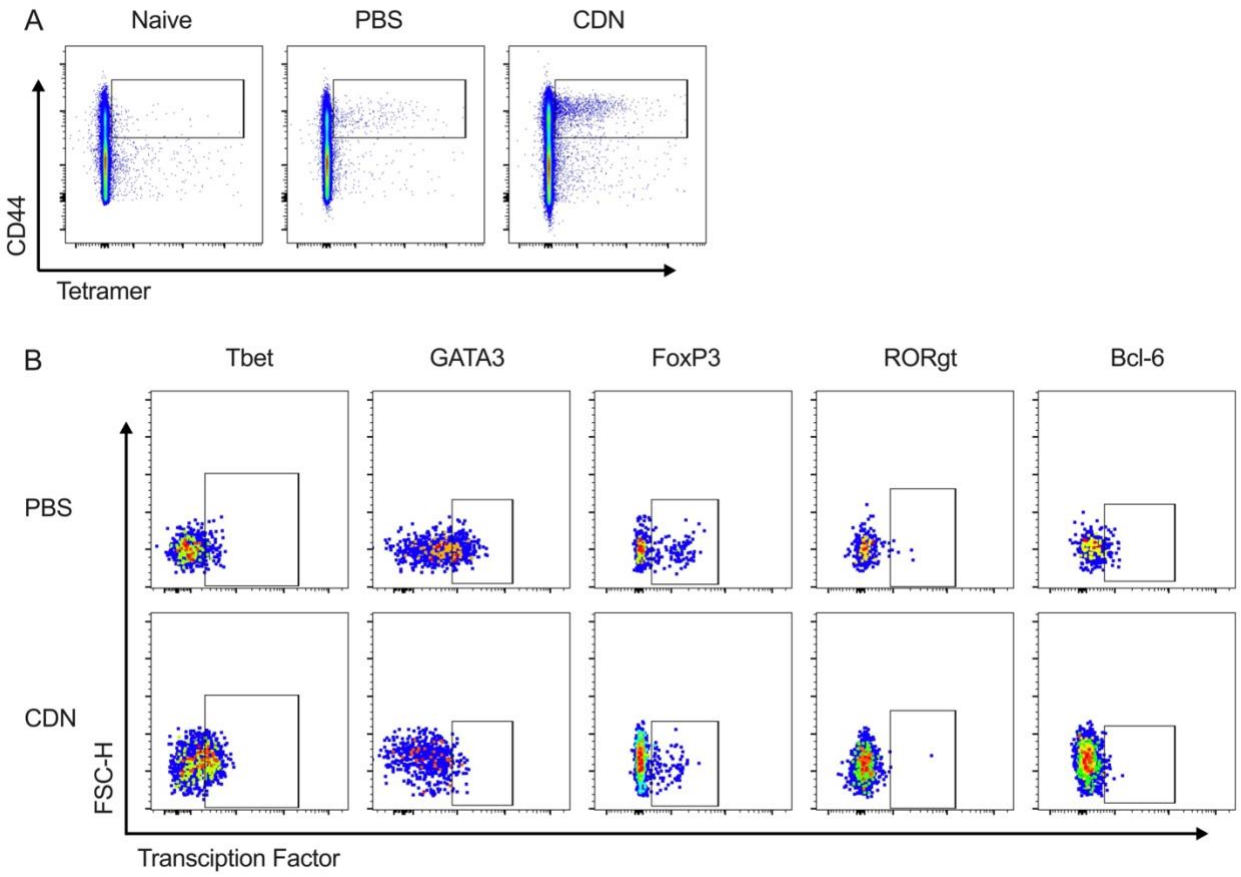

Figure 4.3. Representative flow plots of tetramer-stained cells from Figure 4.2. (A) Representative flow plots of splenocytes from RMA-*B2m*-/- tumor bearing mice stained with gp70 tetramer. **(B)** Representative flow plots of tetramer+ splenocytes stained for the various CD4 T helper subsets.

CDN/H9-MSA therapy stimulated CD4 T cell antitumor responses to B16-F10-B2m-/- tumors, independently of MHC II tumor expression

In Chapter 3, In Chapter 3, I showed evidence of powerful synergy between a STING agonist, CDN, and the IL-2 superkine, H9-MSA, in improving long-term survival in mice bearing B16-F10-*B2m*-/- tumors. The antitumor effects were mediated by both NK cells and CD4 T cells. To explore the role of antitumor CD4 effects induced by the combination therapy in B16-F10-*B2m*-/- tumor rejection, we utilized NK cell-deficient NK-DTA mice. NK-DTA mice bearing B16-F10-*B2m*-/- tumors treated with H9-MSA alone showed a small, but significant, decrease in tumor growth, with effect on survival of mice compared to PBS (Figure 4.4A, Figure 4.5A). Mice treated with CDN resulted in a significant decrease in tumor growth and prolonged survival (Figure 4.4A, Figure 4.5A). Treatment with both CDN and H9-MSA resulted in a further significant decrease in tumor growth and significantly extended median survival compared to either treatment alone (Figure 4.4A, Figure 4.5A).

To determine whether CD4 or CD8 T cells were mediating rejection of B16-F10-*B2m*-/- tumor cells in NK-deficient NK-DTA mice, we performed cellular depletions after establishing of tumors, and just before initiating CDN/H9-MSA therapy. Depletion of CD4 T cells led to a significant acceleration in tumor growth, supporting the conclusion that CD4 T cells are necessary therapy induced responses against these tumors (Figure 4.4B, Figure 4.5B). Depletion of CD8 T cells alone trended towards an increase in tumor growth, albeit the difference was not statistically significant compared to undepleted mice (Figure 4.4B, Figure 4.5B). Depletion of both CD4 T cells and CD8 T cells significantly increased tumor growth compared to mice that were depleted of only CD4 cells, suggesting that CD8 T cells can play a role in restricting growth of the MHC deficient B16-F10-*B2m*-/- tumors in mice lacking both NK cells and CD4 cells (Figure 4.4B, Figure 4.5B).

Because we have engineered our tumor cells to lack *B2m*-/- and therefore MHC I, the CD8 T cells are not able to recognize MHC I on the tumor cells, suggesting that they act indirectly. It remained unclear whether the CD4 T cells recognized MHC II on the tumor cells, because it has been previously shown that B16 tumor cells can upregulate MHC II when exposed to IFN-γ (Londei et al., 1984). We therefore tested whether MHC II expression by B16-F10-*B2m*-/- cells was essential for CD4 cell-mediated tumor rejection. Starting with B16-F10-*B2m*-/- cells we used transient CRISPR/Cas9 targeting of the MHC II *Ab1* gene, which encodes a subunit of the A^b MHC II protein. After transiently transfecting the CIITA MHC II transcriptional coactivator (Devaiah and Singer, 2013), we sorted MHC II-negative cells (see Chapter 2). Subsequent transient transfection with CIITA failed to induce A^b expression by these tumor cells (Figure 4.6A). The resulting tumor cells, lacking both MHC I and MHC II, were designated B16-F10-*B2m*-/-*Ab1*-/- cells.

B16-F10-*B2m*-/- or B16-F10-*B2m*-/-*Ab1*-/- tumors were established in NK cell-deficient NK-DTA mice, and treated with combination therapy as in Figure 3.2. The growth of both types of tumors was similarly restricted as a result of therapy (Figure 4.6B). The impaired growth of B16-F10-*B2m*-/-*Ab1*-/- tumors after therapy was partially reversed when CD4 T cells were depleted. These data indicated that the antitumor effects of CD4 T cells after combination

therapy were not dependent on direct recognition of MHC II or MHC I on the B16-F10 tumor cells.

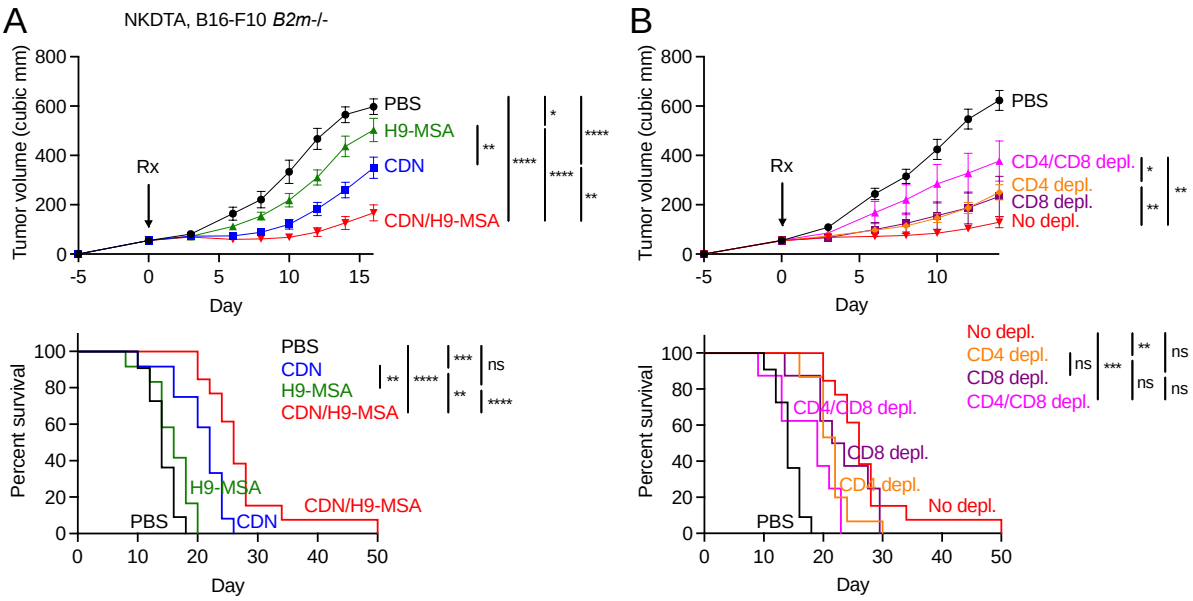

Figure 4.4. CDN/H9-MSA therapy induced potent antitumor effects against MHC I-deficient tumors in mice lacking NK cells tumors, mediated by CD4 T cells. (A, B) Experiments were carried out as in Figure 3.2 except NK-DTA mice were employed. **(A)** Impact of CDN, H9-MSA or combination therapy. **(B)** Antitumor effects were reversed by depleting CD4 T cells and to an even greater extent by depleting both CD4 and CD8 T cells. Tumor growth data were analyzed by 2-way ANOVA. Survival data were analyzed using log-rank (Mantel-Cox) test. The data in all panels are representative of two independent experiments, except for the CD8 and CD4/CD8 depletion which was performed only once. n=6-7 mice per group. Error bars represent standard error of the mean (SEM). *P< 0.05, **P < 0.01, ***P < 0.001, ****P < 0.0001.

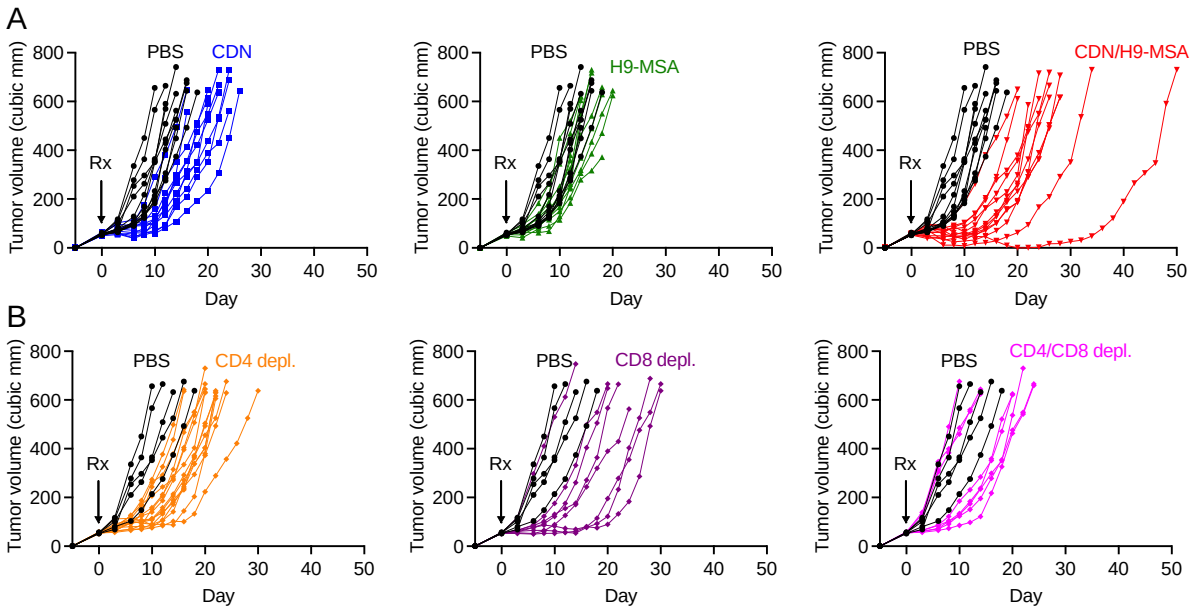

Figure 4.5. Spider plots showing growth of individual tumors from Figure 4.4. (A) Individual growth curves from NK-DTA mice with B16-F10-*B2m*-/- tumors and **(B)** NK-DTA mice with B16-F10-*B2m*-/- tumors subjected to cellular depletions.

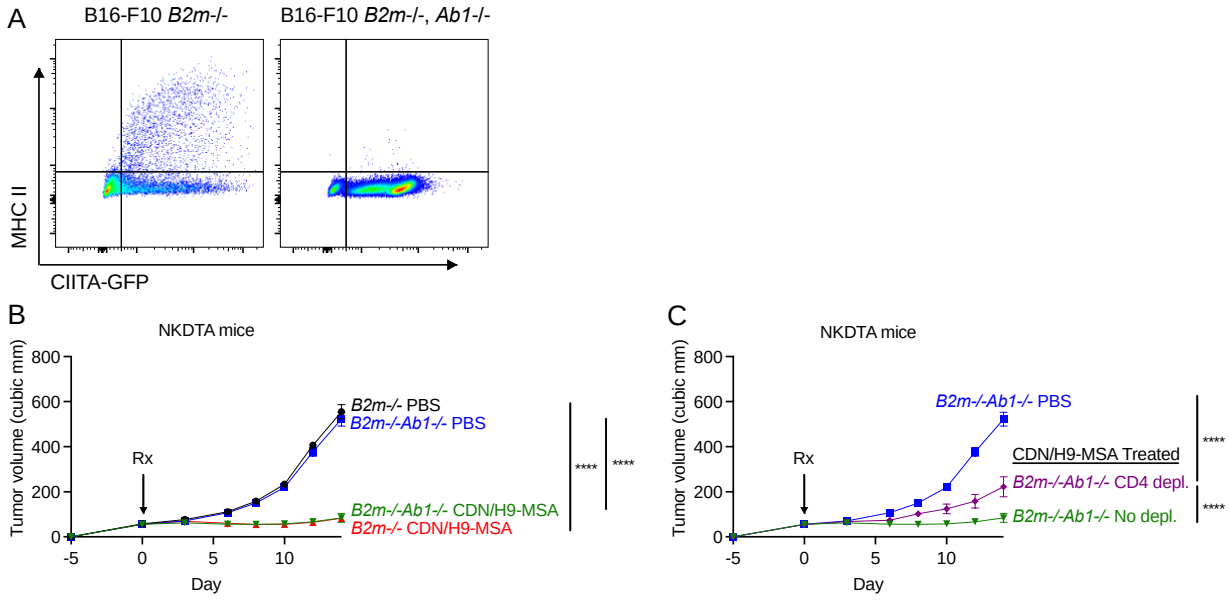

Figure 4.6. CD4 T cells mediated antitumor effects after CDN/H9-MSA combination therapy independently of MHC II expression by tumor cells. (A) MHC II knockout B16-F10-*B2m*-/- tumor cells (B16-F10-*B2m*-/-*Ab*-/- cells) were generated by the CRISPR-Cas9 system by transient transfection with a plasmid containing Cas9 and an sgRNA targeting *H2-Ab1*. One week after transient transfection, the cells were transiently transfected with a plasmid containing CIITA-GFP to induce the expression of MHC II. Cells were then stained for MHC II and sorted for MHC II-, GFP+ cells using a FACSAria sorter, before returning

the cells to culture. One week later cells were again transiently transfected with the same plasmid containing CIITA-GFP and stained for MHC II. Cells were analyzed for knockout efficiency by flow cytometry, examining the percentage of MHC II-, GFP+ cells. (B) The indicated types of tumors were established in NK-DTA mice, and subjected to the indicated therapy, as in Figure 3.2. Growth of B16-F10-*B2m*-/- vs B16-F10-*B2m*-/-*Ab1*-/- tumors with and without therapy is shown. (C) Antitumor effects of combination therapy were partially reversed in mice depleted of CD4 T cells. Tumor growth data were analyzed by 2-way ANOVA. Survival data were analyzed using log-rank (Mantel-Cox) test. The data in all panels are representative of two independent experiments. n=6 mice per group. Error bars represent standard error of the mean (SEM). *P< 0.05, **P < 0.01, ***P < 0.001, ****P < 0.0001.

Tumor-specific CD4 T cells responses promoted by CDN and H9-MSA combination therapy

To characterize the CD4 T cell response elicited by CDN/H9-MSA therapy against B16-F10-*B2m*-/- tumors, we first tested the functionality of the tumor specific CD4 T cells. Mice with established B16-F10-*B2m*-/- tumors were treated with CDN and/or H9-MSA twice, three days apart. Approximately one week after the start of therapy, splenocytes were collected, stimulated with the tumor specific peptide, Trp1, and examined for cytokine production by CD4 T cells. When given two doses of H9-MSA, a significantly higher percentage of splenic CD4 T cells from mice treated with CDN/H9-MSA or H9-MSA, versus mice treated with CDN or PBS, produced IFNγ, TNFα or IL-2 (Figure 4.7A). However, production of these cytokines also occurred to a significant extent even when peptide was not added to the cultures, suggesting that some of the response was directly induced by the therapy. When the mice were given only one dose of H9-MSA, the background response was considerably reduced. Under those conditions, there was a weak IFNg response to peptide without therapy, but surprisingly, this occurred even with naïve splenocytes, suggesting that these effects were nonspecific. On the whole, these data failed to demonstrate a specific splenic CD4 T cell response to a tumor antigen.

To further characterize the CD4 T cell antitumor responses, we wanted to specific identify these T cells in mice treated with the combination therapy. In order to do so, we had the National Institutes of Health (NIH) Tetramer Core Facility (TCF) produce MHC II (I-A^b) Trp1 tetramers, which have been shown to identify B16-F10 Trp1 tumor specific peptide CD4 T cells (Sharbi-Yunger et al., 2019). Mice were established with B16-F10-*B2m*-/- tumors, treated with CDN and/or H9-MSA and approximately one week later, splenocytes were stained with the Trp1 tetramer to identify tumor specific CD4 T cells. The percentage of tetramer positive CD4+ T cells was very low in the spleen of naïve mice, as expected, but was not increased significantly in tumor bearing mice, whether or not they received therapy. In fact the percentages of tetramer positive CD4+ T cells trended lower in mice receiving H9-MSA or CDN/H9-MSA therapy, albeit the difference was not significant. The results with tetramer staining and peptide stimulation suggest either that few antigen specific CD4 T cells were induced, or that the responding cells had trafficked out of the spleen to another site in the animals. We did note that the percentage of tetramer positive cells that expressed the transcription factor $FoxP3^+$ was reduced in mice treated with CDN/H9-MSA combination therapy> These data raise the possibility that the combination therapy reduces the number of regulatory T cells with the potential to suppress the response.

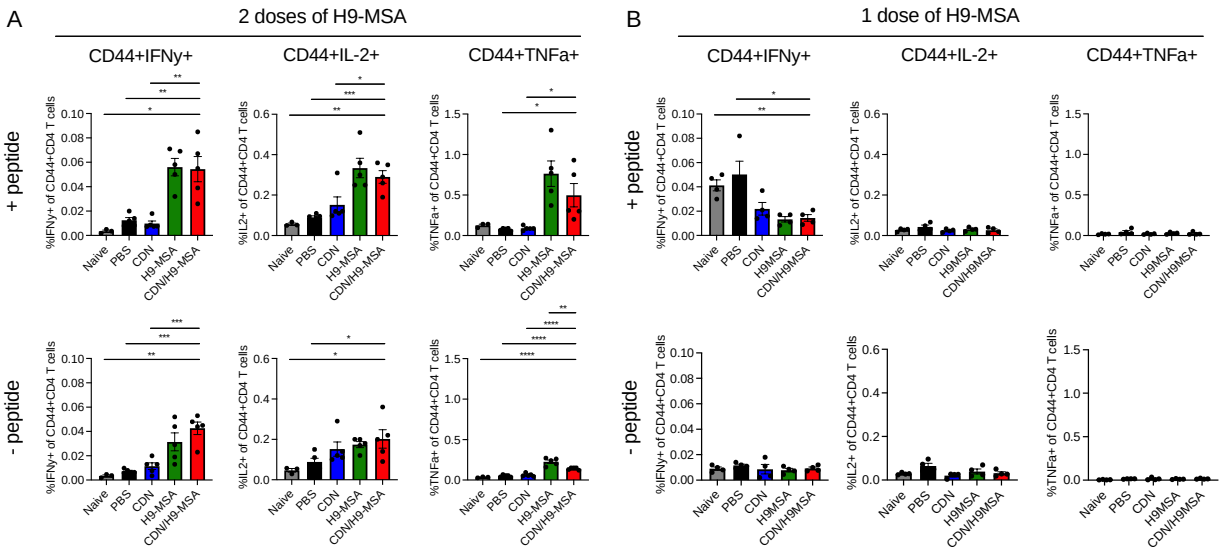

Figure 4.7. B16-F10-*B2m*-/- peptide, Trp1, stimulated CD4 T cells responses in splenocytes from CDN/H9-MSA combination therapy treated mice. B16-F10-*B2m*-/- tumor cells were implanted s.c. in C57BL/6J mice on day -5 and grown to approximately 50 mm^3. On d0, tumors were injected once intratumorally with 50 μg of CDN or PBS, and/or i.p. with 10 μg of H9-MSA or PBS. Additionally, some mice received a second dose of H9-MSA three days later. Approximately a week later, splenocytes were stimulated with tumor-specific peptide, Trp1, for 5 hours and then stained for intracellular markers of CD4 T cells. **(A)** Trp1 peptide stimulation of CD4 T cells, after mice received 2 doses of H9-MSA, induced cytokine production. (B) Trp1 peptide stimulation of CD4 T cells from mice which received a single dose of H9-MSA, did not induce cytokine production. CD4+ T cells were gated as viable, $CD45^+$, $NK1.1^-$, $CD19^-$, $Ter119^-$, $F4/80^-$, $CD3^+$, $CD4^+$. The data in all panels are representative at least two independent experiments. n=4-7 mice per group. Data analyzed by 2-tailed unpaired Student's t-test. Error bars represent standard error of the mean (SEM). *P< 0.05, **P < 0.01, ***P < 0.001, ****P < 0.0001.

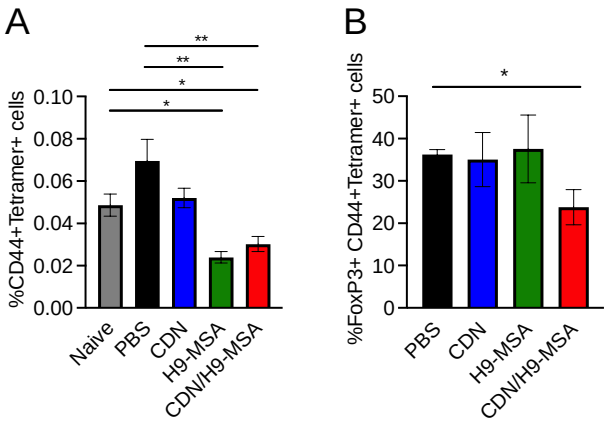

Figure 4.8. Tumor specific CD4 T cells identified in combination therapy treatment mice. B16-F10-*B2m-/-* tumor cells were implanted s.c. in C57BL/6J mice on day -5 and grown to approximately 50 mm^3. On d0, tumors were injected once intratumorally with 50 μg indicated innate agonist or PBS, and/or i.p. with 10 μg of H9-MSA or PBS. Approximately a week later, splenocytes were stained with Trp1 MHC II tetramer at 1:200 for 3 hr at 37C and then further stained for viability and surface/intracellular markers. **(A)** Percentage of Trp1 MHC II tetramer positive CD4 T cells induced in mice treated with CDN and/or H9-MSA therapy. The reduced percentage of tetramer positive CD4 T cells in H9-MSA or CDN/H9-MSA mice was significant compared to PBS or naïve controls. **(B)** Tetramer positive CD4 T cells showed reduced FoxP3 expression in CDN/H9-MSA treated mice. CD4+ T cells were gated as viable, $CD45^+$, $NK1.1^-$, $CD19^-$, $Ter119^-$, $F4/80^-$, $CD3^+$, $CD4^+$. n=4 mice per group. Data analyzed by 2-tailed unpaired Student's t-test. Error bars represent standard error of the mean (SEM). *P< 0.05, **P < 0.01, ***P < 0.001, ****P < 0.0001.

CDN/H9-MSA therapy activated CD8 T cells to reject MHC I$^+$ tumors

In Chapter 3, the STING agonist, CDN, and the IL-2 superkine, H9-MSA, were shown to synergize in treating two hard-to-treat s.c. models, B16-F10-*B2m*-/- and MC38-*B2m*-/-. The rejection was dependent on NK cells, and in one case by CD4 T cells, but was independent of CD8 T cells. This impact of combination therapy on NK cell-dependent and CD4 T cell dependent tumor rejection prompted us to ask whether this approach has broader applicability, including against MHC I$^+$ tumors. Therefore, we tested whether the CDN/H9-MSA therapy combination is effective with "wildtype" MHC I$^+$ B16-F10 tumors, a model that is poorly responsive to most therapies including checkpoint therapy. B6 mice with established MHC I$^+$ B16-F10 tumors treated separately with CDN or H9-MSA showed delays in tumor growth, but very poor long-term survival, whereas the combination of CDN/H9-MSA showed synergistic tumor rejection and disease-free survival of most of the mice for > 100 days (Figure 4.9A, Figure 4.10).

Cellular depletion experiments demonstrated that CD8 T cells were essential for rejection of the MHC I$^+$ tumors, whereas CD4 cells and NK cells were largely dispensable (Figure 4.9B). Elimination of all three populations was no more impactful than CD8 depletion alone. Therefore, CD8 T cells are very effectively mobilized against MHC I$^+$ tumors by this combination therapy. Thus, combining an innate agonist and IL-2 superkine synergistically mobilized T cells or NK cells against tumors, depending on the MHC expression status of the tumor cells.

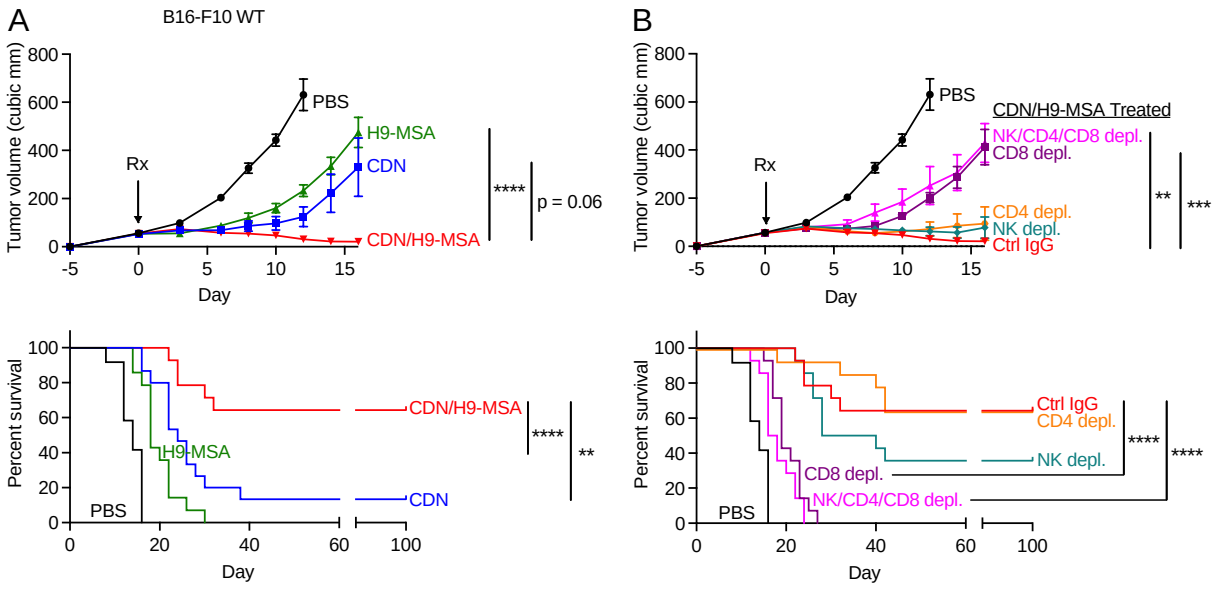

Figure 4.9. CDN/H9-MSA therapy induced potent antitumor effects with MHC I+ tumors, mediated by CD8 T cells. (A, B) Experiments were carried out as in Figure 3.2 except MHC I+ B16-F10 wildtype cells were employed. **(A)** Impact of CDN, H9-MSA or combination therapy. **(B)** Antitumor effects were reversed by depleting CD8 T cells ($p<0.0001$), with no significant impacts of depleting NK cells or CD4 T cells (p=ns). Tumor growth data were analyzed by 2-way ANOVA. Survival data were analyzed using log-rank (Mantel-Cox) test. The data in all panels are representative of two independent experiments.

n=6-7 mice per group. Error bars represent standard error of the mean (SEM). *P< 0.05, **P < 0.01, ***P < 0.001, ****P < 0.0001.

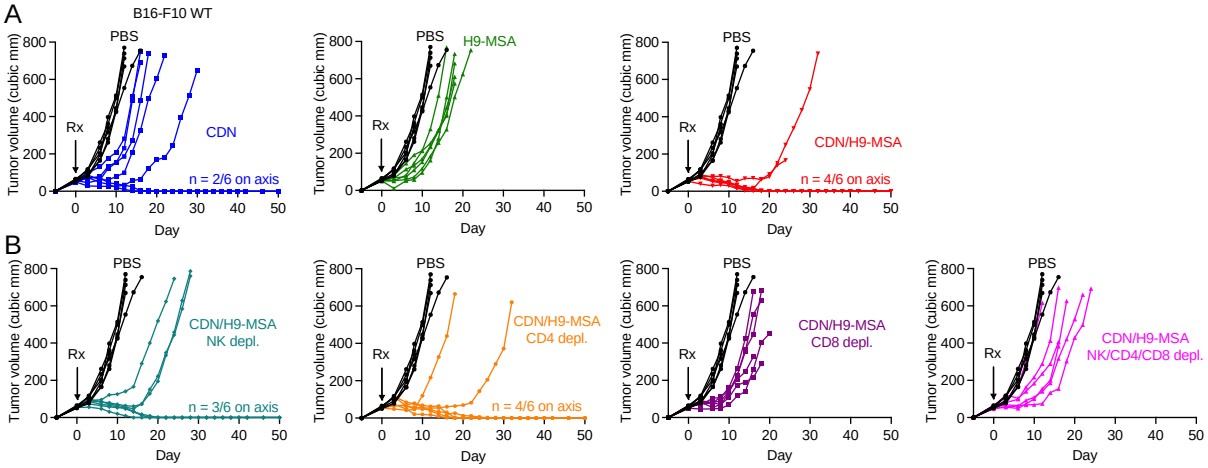

Figure 4.10. Spider plots showing growth of individual tumors from Figure 4.9. (A) B16-F10 WT tumors and **(B)** B16-F10 WT tumors subjected to cellular depletions.

Efficacy of combination therapy in the methylcholanthrene induced sarcoma model

Subcutaneous tumor models are generally easier to treat than autochthonous tumor models, which are more similar to human cancers. In collaboration with Cristina Blaj, a postdoctoral fellow in the lab, we chose to utilize the methylcholanthrene (MCA)-induced sarcoma model to address the efficacy of the CDN/H9-MSA combination in a primary autochthonous cancer model, a very "high bar" model in tests of effective therapies. MCA was injected s.c. on the right flanks and mice were monitored frequently for palpable tumors, which arose 8-10 weeks after carcinogen administration in 80% of the treated animals. When a tumor reached a volume of approximately 50 mm^3, that mouse was treated individually. Mice were initially injected with three doses of CDNs i.t. every three days followed by weekly injections. Some mice received H9-MSA i.p. applied every three days (Figure 4.11A, Figure 4.12A). H9-MSA alone had a minor, albeit significant effect on tumor growth and terminal morbidity of the animals, whereas CDN therapy caused a substantial delay in both tumor progression and terminal morbidity (Figure 4.11B, Figure 4.12A). The CDN/H9-MSA combination was significantly more effective than CDNs alone in prolonging survival, with a small percentage of animals surviving after 160 days.

Some toxicity of the CDN/H9-MSA combination was evident in this model, including the appearance of chronic granulomatous histiocytic inflammation in some mice, that arose in the leg muscle on the same side of the mouse as the treated tumor. When treated with topical diphenhydramine (Benadryl), the inflammation was partially controlled, and mice were continued in the experiment.

The initial antitumor effects were significantly diminished when either NK cells, CD8 cells or, to a lesser extent, CD4 cells were depleted from the animals before initiating therapy (Figure 4.11C, Figure 4.12B). Depleting NK cells accelerated the demise of a fraction of the animals, whereas depleting CD8 or CD4 cells accelerated the demise of all the animals. Depleting all three populations simultaneously had a modestly greater effect than depleting CD8 or CD4 cells separately, suggesting some separate impacts of these lymphocyte populations, though some cooperative interactions between the populations are fully consistent with the data. Thus, NK cells, CD8 T cells and CD4 T cells all contribute to the therapeutic effects in this tumor model.

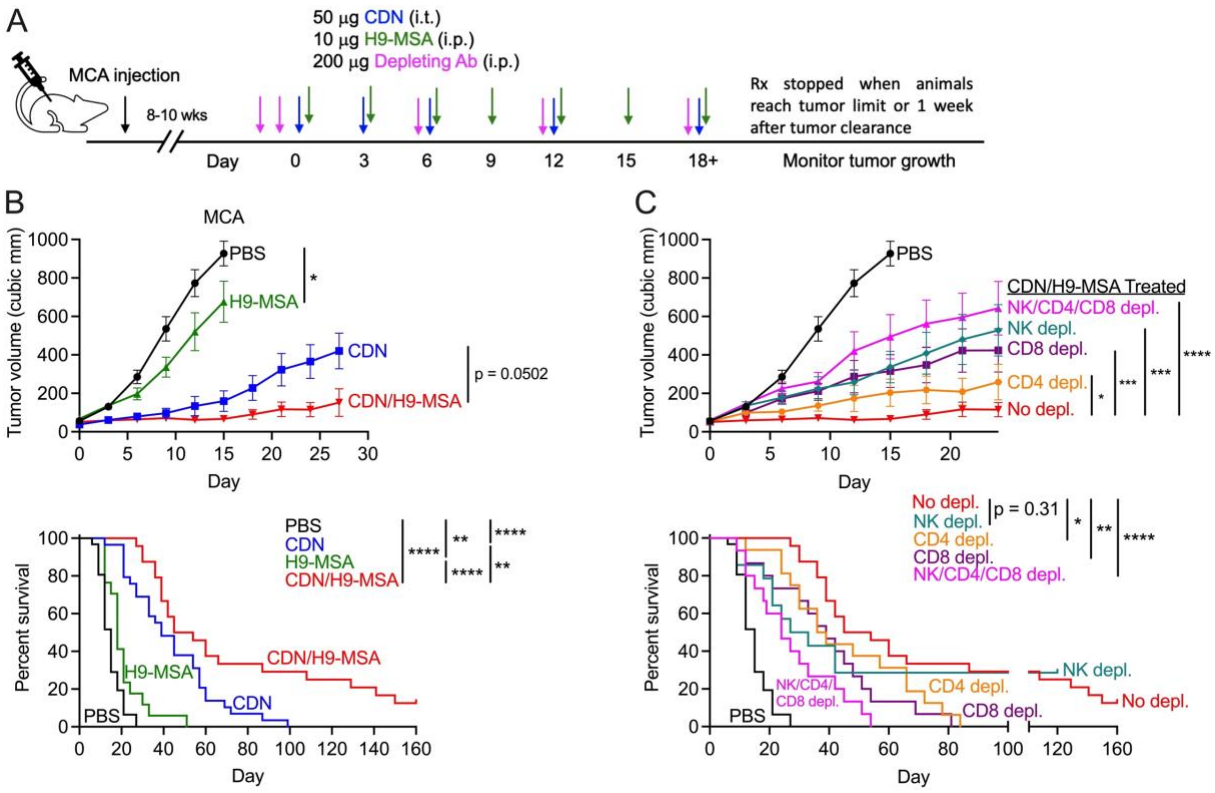

Figure 4.11. CDN/H9-MSA therapy induced potent antitumor activity in methylcholanthrene-induced sarcoma tumors, mediated by CD8 T cells, CD4 T cells and NK cells. (A) Timeline for MCA-induced tumors. When MCA-induced tumors reached ~50 mm^3 in size they were injected i.t. with PBS or 50 μg CDN on days 0, 3, and 6 and repeated every 6 six days, thereafter. Mice were also injected i.p. with PBS or 10 μg H9-MSA starting on day 0. The cytokine or PBS injections were repeated every two days until mice were euthanized or until 1 week after a mouse completely cleared a tumor. In some groups, mice were depleted of NK cells, CD8 T cells, or CD4 T cells, or injected with control IgG. **(B)** Tumor growth curves and survival of mice. **(C)** Tumor growth curves and survival of depleted mice. Data in these panels are a combination of multiple experiments, such that some of the data (e.g. CDN/H9-MSA) are shared in different panels. n=11-24. Data were analyzed by 2-way ANOVA. Error bars represent standard error of the mean (SEM). *P< 0.05, **P < 0.01, ***P < 0.001, ****P < 0.0001.

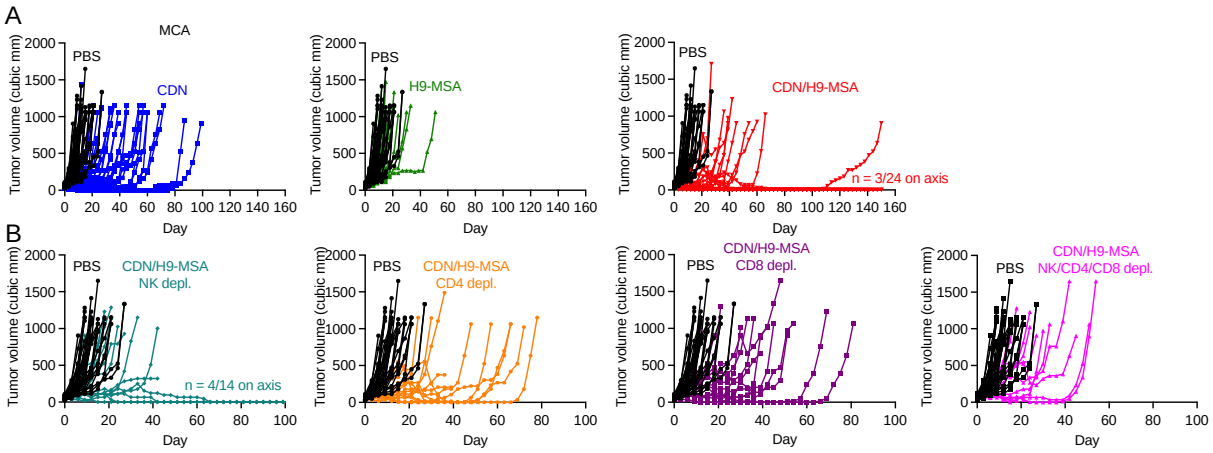

Figure 4.12. Spider plots showing growth of individual tumors from Figure 4.11. (A) MCA tumors and **(B)** MCA tumors subjected to cellular depletions.

Discussion

Adding to our findings that CDN and CDN/H9-MSA therapy induce antitumor NK cells, the data in this chapter demonstrate induction of potent antitumor T cell responses by T cells. We corroborated earlier findings that CDN therapy induces antitumor CD4 T cells against RMA-*B2m-/-* tumors, and showed that CDN/H9-MSA combination therapy synergistically induced CD4 mediated antitumor responses in the B16-F10-*B2m-/-* model. In addition, we showed that the therapy combination synergistically mobilized CD8 T cell-mediated tumor rejection in MHC I+ B16-F10 cells and in primary methylcholanthrene induced sarcomas.

In the RMA-*B2m-/-* model, we showed that CD4 T cells induced by CDN therapy alone increased the number of CD4 T cells specific for an MHC II-presented tumor antigen, and that many of these T cells were Th1 type CD4 T cells, with Th2 cells and Th17 cells being much less abundant.

In the B16-F10-*B2m-/-* model, CD4 T cells induced by CDN/H9-MSA therapy showed significant antitumor effects in mice lacking NK cells. In light of previous findings in the RMA-*B2m-/-* model that CDN therapy amplified the number of functional CD4 T cells specific for an MHC II-presented tumor antigen [cite Nicolai thesis], we tested whether therapy amplified the percentage of CD4 T cells specific for an MHC II-presented tumor antigen expressed by B16-F10-*B2m-/-* cells. However, we failed to detect significantly expanded CD4 T cells staining with an MHC II tetramer in the spleen, nor did we detect a significant increase in functional CD4 T cells producing cytokines in response to an MHC II-presented tumor antigen peptide in the spleen. It remains possible that the tumor antigen specific CD4 T cells have trafficked out of secondary lymphoid organs such as the spleen. Further studies will be necessary to assess whether MHC II-restricted, tumor antigen-specific, CD4 T cell responses were induced.

We considered the possibility that MHC II was induced on B16-F10-*B2m-/-* tumor cells and subject to direct recognition by tumor antigen specific CD4+ T cells (Haabeth et al., 2014; Quezada et al., 2010; Xie et al., 2010).. Interestingly, however, by disrupting the MHC II gene in

B16 tumor cells, we showed that the antitumor effects did not require MHC II expression by B16-F10 cells. Chris Nicolai had previously generated data indicating that rejection of RMA-*B2m-/-* tumor cells by CD4 T cells elicited by CDN monotherapy similarly does not require MHC II expression by tumor cells [cite Nicolai thesis?].

The mechanisms of tumor elimination by CD4+ T cells are unknown. Given the absence of direct MHC II (or MHC I) recognition, the possibilities include cytokine action, mobilization of effector myeloid cells or possibly direct recognition by the CD4+ T cells of some non-MHC ligand on tumor cells. In the case of the RMA-*B2m*-/- model, I tested whether tumor rejection by CD4 T cells required neutrophils and/or macrophages. Simultaneous elimination of these cells using clodronate liposomes, anti-GR1 and anti-Ly6G failed to significantly diminish tumor rejection, arguing against the possibility that phagocytes mobilized by CD4 T cells play a major role in tumor elimination.

In sum, with respect to the mechanisms of tumor elimination by therapy induced CD4+ T cells, we have shown that in one model Th1 cells are the predominant CD4 T cell subtype induced, but that there is no indication that rejection is mediated by phagocytes activated by the CD4+ T cells. Hence the mechanisms of tumor elimination remain uncertain.

In the context of MHC I+ B16-F10 tumors, a "cold" tumor model that is resistant to checkpoint therapy and other experimental monotherapies (Lechner et al., 2013), CDN/H9-MSA therapy induced a highly effective CD8 T cell mediated antitumor response, with no evidence for roles of NK cells or CD4 T cells. The impressive impact of CDN/H9-MSA therapy shown here is notable considering that durable antitumor responses in this model has required combining 3-4 agents in past studies (Moynihan et al., 2016; Sivick et al., 2018). The absence of effective antitumor NK cells in this model with CDN/H9-MSA therapy may be explained by the inhibitory effects of MHC I, but it remains unclear why effective antitumor CD4 T cells were not elicited.

The finding that CDN/H9-MSA therapy worked well for both MHC I+ cold tumors and MHC I-deficient tumor variants suggests the promise of this approach both for tumor types that are resistant to checkpoint therapy and for preventing the emergence of MHC I-deficient tumor variants during immunotherapy. The loss of MHC I expression may occur before or during immunotherapy and is increasingly recognized as a significant mechanism of acquired resistance of tumors to checkpoint therapy (Garrido et al., 2016; Maleno et al., 2011; McGranahan et al., 2017; Sade-Feldman et al., 2017; Zaretsky et al., 2016).

In conclusion, our results show that CDN therapy combined with the IL-2 superkine, H9-MSA, effectively enhanced CD4 T cell mediated rejection MHC I-deficient tumors and CD8 T cell mediated rejection of MHC I WT tumors. The CDN/H9-MSA treatments proved to be remarkably effective against difficult-to-treat tumors, mobilizing various effector cells depending on tumor cell type. These results provide compelling support for testing combinations of innate immune system agonists and IL-2 family superkines as potential next-generation immunotherapies for tumors that are resistant to currently approved immunotherapy regimens.

Chapter 5
Additional therapies to improve anti-tumor responses in STING agonist and IL-2 superkine treated mice

Portions of this chapter were adapted and/or reprinted with permission from "Wolf, N.K., Blaj, C., Picton, L, Snyder, G., Zhang, L. Nicolai, C.J., Ndubaku, C.O., McWhirter, S.M. Garcia, K.C. and Raulet, D.H. Synergistic effects of a STING agonist and an IL-2 superkine in cancer immunotherapy against MHC I-deficient and MHC I+ tumors. *Proc Natl Acad Sci U S A*, In press (2022)."

Introduction

In Chapters 3 and 4, the antitumor NK cell and T cell effects induced by the powerful synergy of a STING agonist and an IL-2 superkine were explored in the context of MHC I-deficient and MHC I+ tumor models. A single intratumoral injection of CDN combined with periodic injections of the IL-2 superkine, H9-MSA, resulted in a dramatically increased percentage of animals with disease-free survival in three very difficult-to-treat tumor transplant models, two of which were MHC I-deficient and refractory to CD8 T cell recognition. In primary MCA-induced sarcomas, the combination therapy prolonged the survival of mice. Depending on the tumor model, tumor rejection depended on NK cells, both NK cells and CD4 T cells, CD8 T cells, or all three populations. The results using this combination are impressive, but the therapy failed with larger tumors, indicating that there is still room for improvement.

The tumor microenvironment (TME) consists of many different factors that play a role in tumor development. The TME is populated by many different cell types including immune cells, stromal cells and tumor cells, and various molecules produced by each that influence the tumor development (Binnewies et al., 2018; Labani-Motlagh et al., 2020). Interactions between various cell types and molecules in the TME can lead to the suppression of immune cell activation through engagement of receptors/ligands, such as checkpoint molecules and NKG2D ligands, and through the production of immunosuppressive metabolites. To improve the efficacy of CDN/H9-MSA therapy, we endeavored to amplify the impact of tumor infiltrating NK cells and T cells through various forms of activation or through the inhibition of suppressive factors found in the TME.

Among various metabolites found in the TME, extracellular adenosine is notably immunosuppresive. The majority of intratumoral extracellular adenosine is thought to arise from the conversion of extracellular ATP, released from cells undergoing hypoxia and other forms of stress, to AMP and further into adenosine through the cancer associated ectoenzymes CD39 (ENPP1) and CD73 (Vigano et al., 2019). Cells undergoing hypoxia and inflammation-associated cytokines also induce overexpression of CD39 and CD73 in many cancers (Wang and Matosevic, 2018). The resulting extracellular adenosine can bind to any of four G protein-coupled adenosine receptors, A_1, A_{2a}, A_{2b}, and A_3. These four receptors are found on many immune cells, including NK cells (Wang and Matosevic, 2018). Stimulation of A_{2a} and A_{2b} receptors by adenosine has been shown to impart immunosuppression of immune cells (Carozza et al., 2020; Chambers et al., 2018). Stimulation of adenosine receptor A_{2a} on NK cells has been shown to limit maturation and cytotoxic functions (Chambers et al., 2018; Young et al., 2018). Gene targeting of A_{2a}R led to improved tumor control by NK cells (Young et al., 2018). We employed AB928 designed by Arcus Biosciences, a dual adenosine receptor inhibitor that inhibits A_{2a}R and A_{2b}R, to inhibit the immunosuppression of NK cells mediated by adenosine

(Seitz et al., 2019). In this chapter, we report that AB928 did not augment tumor control induced by CDN or H9-MSA therapy, at least in the MHC I-deficient tumor model studied.

Prostaglandins, also found in the TME, promote cancer cell growth and survival, by acting directly to promote tumorigenesis and through imparting immunosuppression on numerous tumor infiltrating immune cells (Wang and Dubois, 2010; Zelenay et al., 2015). Prostaglandin E2 (PGE2) is produced by cyclooxygenase (COX)-1 and 2 enzymes and signals through four receptors, EP1-4. PGE2 is the most abundant prostaglandin found in many tumors and has been linked to immunosuppression through the engagement of EP2 and EP4 on T cells, myeloid-derived suppressor cells (MDSCs) and NK cells (Bonavita et al., 2020; Wang and Dubois, 2010; Zelenay et al., 2015). Inhibition of COX enzymes by non-steroidal anti-inflammatory drugs (NSAIDs) has been correlated with reduced risk of development of various cancers, including colon cancer. However, clinical trials have shown little chemopreventative effects and prolonged treatment with non-selective NSAIDs is known to cause adverse side effects (Wang and Dubois, 2010). Using a novel dual EP2/EP4 PGE2 receptor antagonist, TPST-1495 developed by Tempest Therapeutics, we examined the effects of blocking prostaglandins in the TME, alone or in combination with CDN/H9-MSA. In this chapter, we show that while TPST-1495 had single agent efficacy in the MHC I-deficient tumor model studied, it did not synergize with CDN and/or H9-MSA to further inhibit tumor control of MHC I-deficient tumors.

With respect to tumor cell recognition, most of the relevant activating NK cell receptors recognize host gene-encoded ligands that are induced by cell stress pathways. Thus, NK cells are dedicated, in part, to eliminating stressed cells, such as cancer cells. Recognition of this type has been called ‘induced-self recognition’ and is best studied in the case of the NKG2D receptor. NKG2D recognizes numerous ligands, all of which are distant relatives of MHC I proteins. In mice the ligands include the RAE-1 family members (RAE-1α-RAE-1ε), MULT1, and three H60 isoforms (Raulet et al., 2013). Previously, the lab demonstrated that a steady-state interaction between NKG2D on NK cells and RAE-1ε constitutively expressed on lymph node endothelial cells leads to partial desensitization of NK cells and diminished NK cell antitumor responses and rejection (Thompson et al., 2017). To test the impact of blocking this interaction in order to prevent desensitization of NK cells, we employed an anti-RAE-1ε antibody. In this chapter, we report that anti-RAE-1ε did not synergize with CDN and/or H9-MSA to further inhibit immune control of MHC I-deficient tumors, at least in the model studied.

Another strategy to improve NK cell responses is through the addition of other cytokines (beyond IL-2 family cytokines) known to activate NK cells. IL-12 and IL-18 cytokines are known to potently enhance NK cell (and T cell) functional activities. Each cytokine alone exhibits antitumor effects in mouse tumor models (Nguyen et al., 2020; Smyth et al., 2000; Srivastava et al., 2010), but only limited efficacy in patients with cancer (Motzer et al., 1998; Weiss et al., 2003). The combination of IL-12 and IL-18 is more potent in stimulating IFNγ production by NK cells in vitro and, when injected in vivo, sustained the survival of mice with certain tumors (Coughlin et al., 1998; Osaki et al., 1998). Furthermore, combined IL-12 and IL-18 treatment increased the long-term survival of mice with MHC I^{low} tumors and reversed NK cell desensitization (Ardolino et al., 2014). While potent, the IL-12 and IL-18 combination is associated with augmented toxicity, sometimes fatal, due to elevated serum levels of inflammatory cytokines such as IFN-γ (Carson et al., 2000). In this chapter, we show the addition

of IL-12 and IL-12 modestly synergize with CDN and/or H9-MSA to further augment immune control of MHC I-deficient tumors.

Our final attempt to improve NK cell responses was through the addition of checkpoint blockade. Checkpoint therapy has shown remarkable results and changed the standard of treatment for many patients with the first checkpoint targeting agent receiving FDA approval in 2011 (Sharma et al., 2021). The success of PD-1 and PD-L1 immune checkpoint blockade therapy is mainly interpreted in the context of amplifying T cell responses. However, evidence has accumulated that NK cells also upregulate the inhibitory receptor PD-1 in certain cancers and that PD-1 engagement can inhibit NK cells in some instances (Beldi-Ferchiou et al., 2016; Benson et al., 2010; Hsu et al., 2018; Liu et al., 2017; Vari et al., 2018). TIGIT is an inhibitory receptor expressed on both T cells and NK cells that has been shown to inhibit both types of lymphocytes, through interactions with its ligand, CD155, on antigen presenting cells or on tumour cells (Bi et al., 2014; Stanietsky et al., 2009). Blockade of TIGIT with antibodies amplified NK cell activity in multiple tumor models. In some of the models studied, NK cells were indispensable for the therapeutic effects of TIGIT blockade alone or when anti-TIGIT was combined with anti-PD-1/anti-PD-L1 (Zhang et al., 2018b), and in other cases $CD8^+$ T cells played a central role (Johnston et al., 2014). In this chapter, we examined the impacts of checkpoint blockade with anti-CD137, anti-PD-1, anti-CTLA4 and/or anti-TIGIT in enhancing antitumor NK cell and T cell effects induced by CDN and/or H9-MSA in controlling MHC I-deficient and MHC I+ tumors. Little synergy was observed in the MHC I-deficient tumor transfer model we examined, but a substantial synergy was observed in a spontaneous MHC I+ sarcoma model.

Results

The adenosine receptor inhibitor, AB928, in combination with CDN and/or H9-MSA did not enhance tumor rejection

Extracellular adenosine present in the TME binds to adenosine receptors, A2aR and A2bR, present on various immune cells, resulting in immunosuppression (Carozza et al., 2020; Chambers et al., 2018). AB928, a novel dual A2aR/A2bR antagonist, blocks the immunosuppressive effects of adenosine (Seitz et al., 2019). We examined the impact of blocking adenosine action of transplanted MHC I-deficient B16-F10-*B2m-/-* tumors by employing AB928 alone or in combination with CDN and/or H9-MSA. Treatment with AB928 alone (Figure 5.1, Figure 5.2) or in combination with CDN (Figure 5.1A), H9-MSA (Figure 5.1B) or CDN/H9-MSA (Figure 5.1C) did not significantly decrease tumor growth or prolong survival of mice compared to CDN and/or H9-MSA alone. These findings indicated that in this MHC I-deficient model, adenosine blockade by AB928, did not mediate significant single agent activity nor did it significantly enhance anti-tumor effects of CDN and/or H9-MSA.

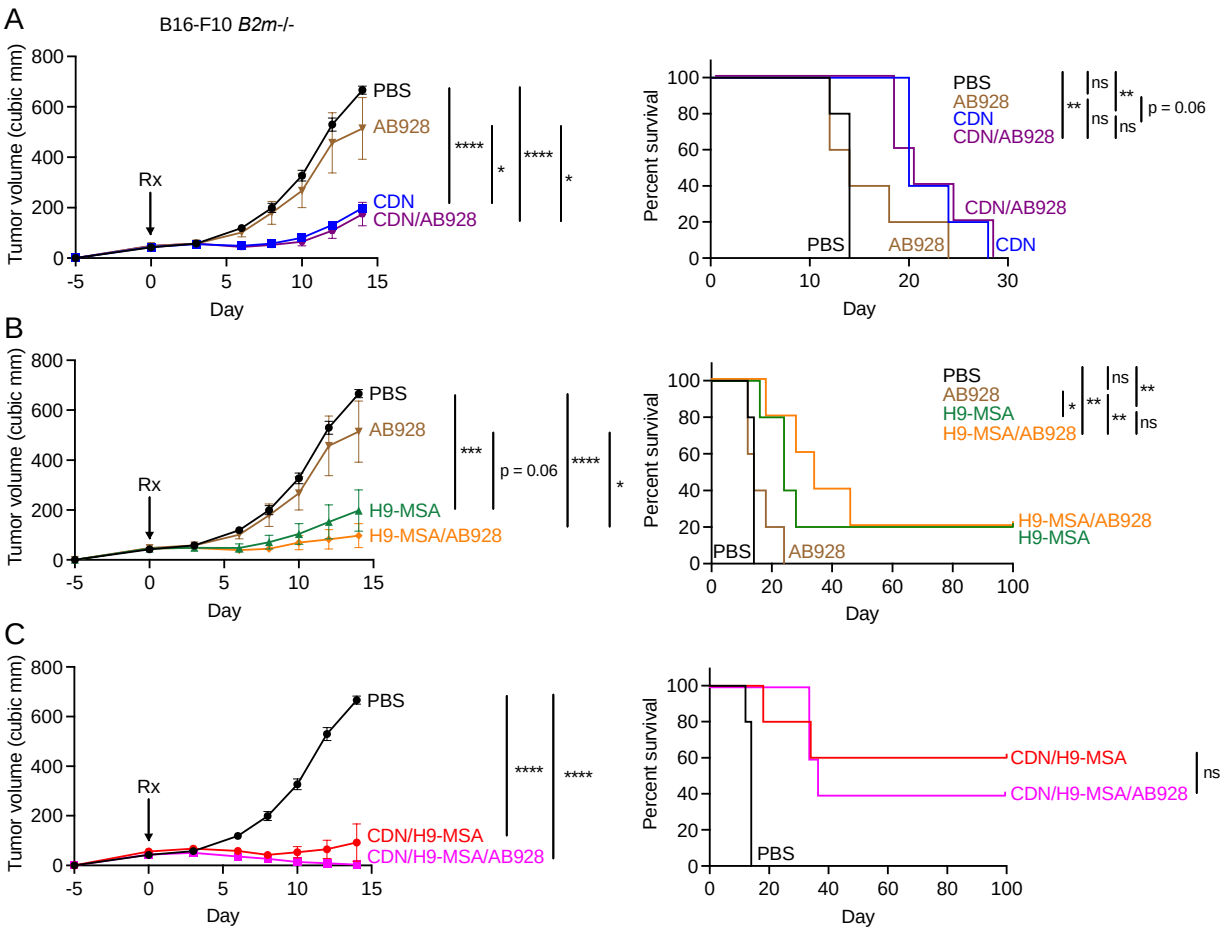

Figure 5.1. AB928 does not enhance tumor alone or in combination with CDN and H9-MSA rejection in an MHC I-deficient tumor model. B16-F10-*B2m-/-* tumor cells were implanted s.c. in C57BL/6J mice on day -5 and grown to approximately 50 mm^3. On d0, tumors were injected once intratumorally with 50 μg CDN or PBS, and/or i.p. with 10 μg H9-MSA or PBS. The cytokine or PBS injections were repeated every three days until euthanization or 1 week after tumor clearance. Additionally, some mice received 100 mg/kg AB928 twice daily by oral gavage. **(A-C)** AB928 did not enhance tumor rejection or survival of tumor bearing mice when combined with **(A)** CDN, **(B)** H9-MSA or **(C)** CDN/H9-MSA. Tumor growth data were analyzed by 2-way ANOVA. Survival data were analyzed using log-rank (Mantel-Cox) test. The data in all panels are representative at least two independent experiments. n=5-7 mice per group. Error bars represent standard error of the mean (SEM). *P< 0.05, **P < 0.01, ***P < 0.001, ****P < 0.0001. Any unmarked comparison in the tumor growth data was not statistically significant.

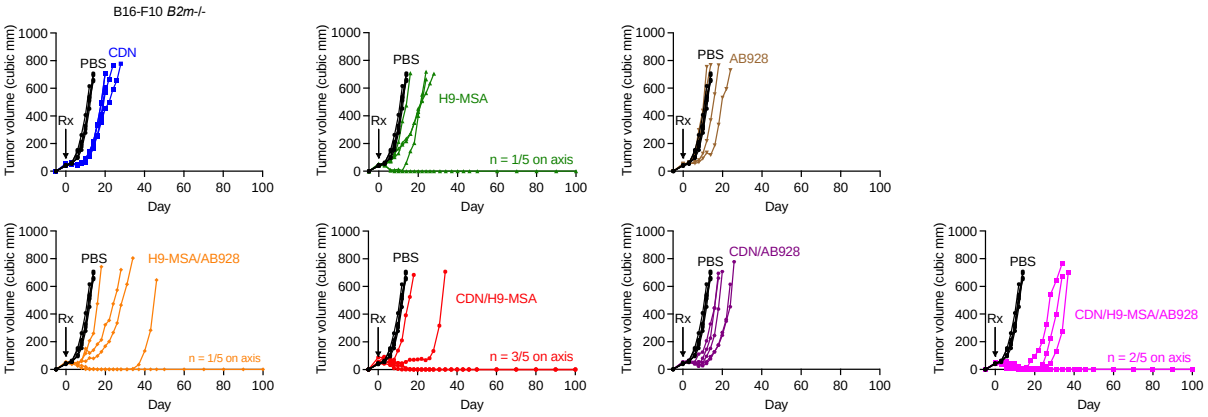

Figure 5.2. Spider plots showing growth of individual tumors from Figure 5.1. Spider plots for AB928 treated animals.

Prostaglandin inhibitor, TPST-1495, exhibited significant single agent efficacy but did not enhance tumor rejection mediated by CDN or H9-MSA

Extracellular prostaglandins, PGE_2, present in the TME, promote immunosuppression by binding to receptors EP2 and EP4 on various effector immune cells (Bonavita et al., 2020; Zelenay et al., 2015). TPST-1495, a novel EP2/EP4 dual receptor antagonist, blocks the immunosuppressive effects of prostaglandins. We examined the role for prostaglandins in rejection of MHC I-deficient tumor models by employing TPST-1495 in combination with CDN or H9-MSA. Treatment with TPST-1495 alone (Figure 5.3, Figure 5.4) showed significant single agent efficacy similar to the single agent efficacy of CDN or H9-MSA. However, no synergy was observed by when TPST-1495 was combined with CDN (Figure 5.3A) or H9-MSA (Figure 5.3B). These findings indicated that in this MHC I-deficient model, prostaglandin blockade by TPST-1495 showed single agent efficacy but did not significantly enhance the anti-tumor effects of CDN or H9-MSA. Note that it could not be ascertained whether TPST-1495 might increase the effectiveness of CDN/H9-MSA therapy, since the CDN/H9-MSA combination cured all the animals. The addition of TPST-1495 to the mix similarly cured all the mice (data not shown).

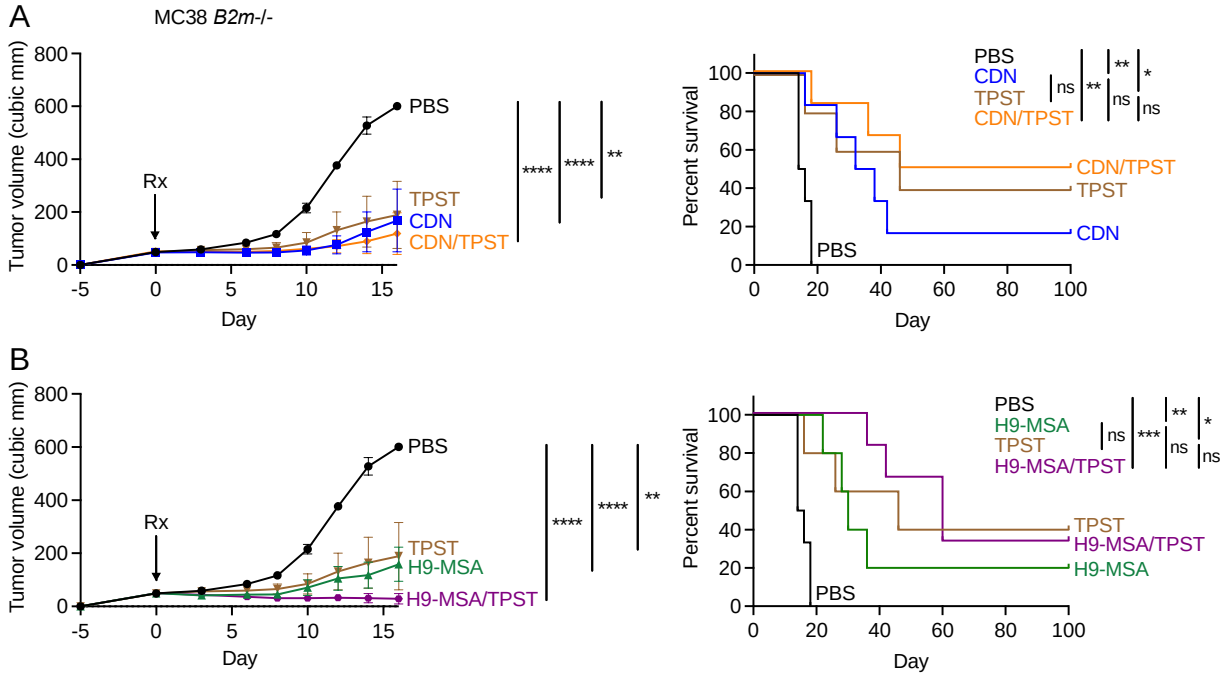

Figure 5.3. TPST-1495 showed single agent efficacy but does not enhance tumor rejection in combination with CDN or H9-MSA in an MHC I-deficient tumor model. MC38 *B2m-/-* tumor cells were implanted s.c. in C57BL/6J mice on day -5 and grown to approximately 50 mm^3. On d0, tumors were injected once intratumorally with 50 μg CDN or PBS, and/or i.p. with 10 μg H9-MSA or PBS. The cytokine or PBS injections were repeated every three days until euthanization or 1 week after tumor clearance. Additionally, some mice received 100 mg/kg TPST-1495 twice daily by oral gavage. **(A)** Treatment with CDN and TPST-1495 did not enhance tumor rejection or overall survival. **(B)** Treatment with H9-MSA and TPST-1495 did not enhance tumor rejection or overall survival. Tumor growth

data were analyzed by 2-way ANOVA. Survival data were analyzed using log-rank (Mantel-Cox) test. n=5-7 mice per group. This experiment was only carried out once, so the results must be considered preliminary. Error bars represent standard error of the mean (SEM). *P< 0.05, **P < 0.01, ***P < 0.001, ****P < 0.0001. Any unmarked comparison in the tumor growth data was not statistically significant.

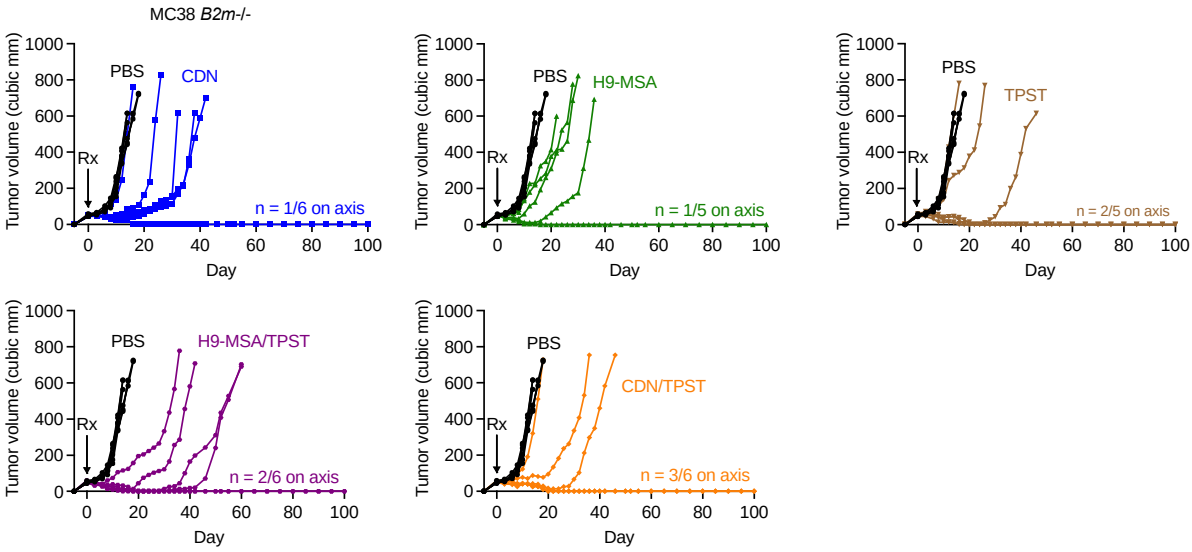

Figure 5.4. Spider plots showing growth of individual tumors from Figure 5.3. Spider plots for TPST-1495 treated animals.

Blockade of NKG2D ligand, RAE-1ε, in combination with CDN and H9-MSA did not enhance tumor rejection

It has previously been shown preventing NKG2D interactions with host RAE-1ε enhances NK cell antitumor responses *in vivo* (Deng et al., 2015; Thompson et al., 2017). We reasoned that blocking RAE-1ε in combination with CDN/H9-MSA therapy might therefore improve rejection of MHC I-deficient tumors. To focus on rejection mediated by NK cells, mice were depleted of CD4 and CD8 T cells. Treatment with anti-RAE-1ε alone did not show significant single agent effects or increase tumor rejection in combination with CDN (Figure 5.5A, Figure 5.6). Combining anti-RAE-1ε blockade with CDN/H9-MSA (Figure 5.5B) did not enhance the antitumor effects compared to CDN/H9-MSA therapy, and did not prolong the survival of the mice. These findings indicated that in this MHC I-deficient model, blockade of RAE-1ε did not enhance anti-tumor effects of CDN or CDN+H9-MSA.

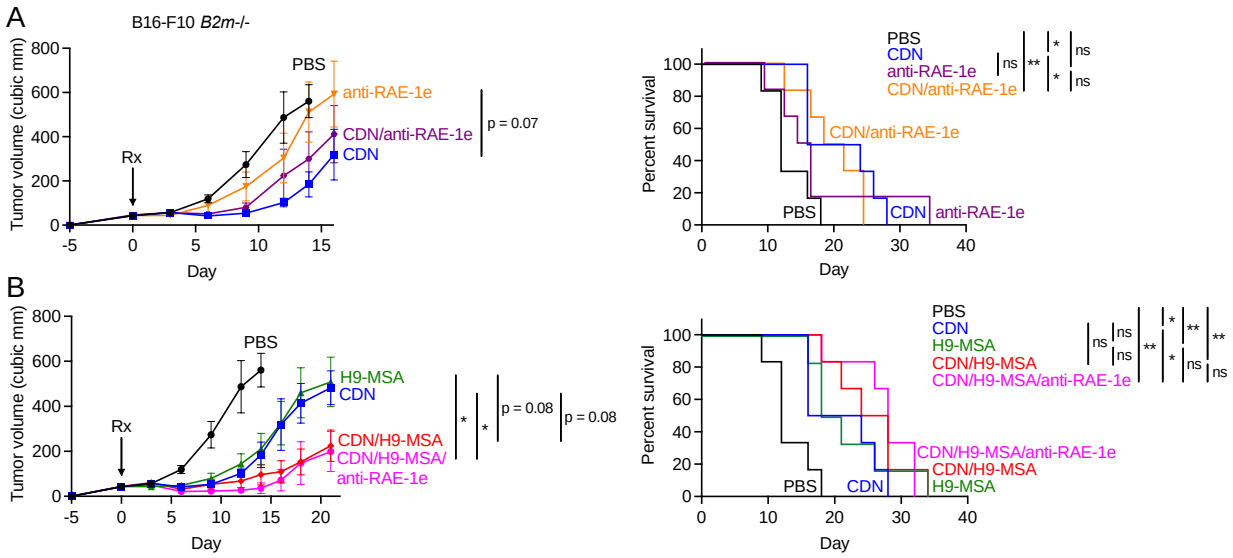

Figure 5.5. Anti-RAE-1ε, in combination with CDN and H9-MSA does not enhance tumor rejection. B16-F10 *B2m-/-* tumor cells were implanted s.c. in C57BL/6J mice on day -5 and grown to approximately 50 mm^3. On d0, tumors were injected once intratumorally with 50 μg CDN or PBS, and/or i.p. with 10 μg H9-MSA or PBS. The cytokine or PBS injections were repeated every three days until euthanization or 1 week after tumor clearance. Additionally, some mice were injected i.p. with 200 μg anti-RAE-1ε. In all panels, the mice were depleted of both CD4 and CD8 T cells before initiating therapy. **(A)** Treatment with CDN and anti-RAE-1ε did not enhance tumor rejection or survival. **(B)** Treatments with anti-RAE-1ε plus CDN/H9-MSA did not enhance tumor rejection or survival. Tumor growth data were analyzed by 2-way ANOVA. Survival data were analyzed using log-rank (Mantel-Cox) test. n=5-7 mice per group. This experiment was only carried out once, so the results must be considered preliminary. Error bars represent standard error of the mean (SEM). *P< 0.05, **P < 0.01, ***P < 0.001, ****P < 0.0001. Any unmarked comparison in the tumor growth data was not statistically significant.

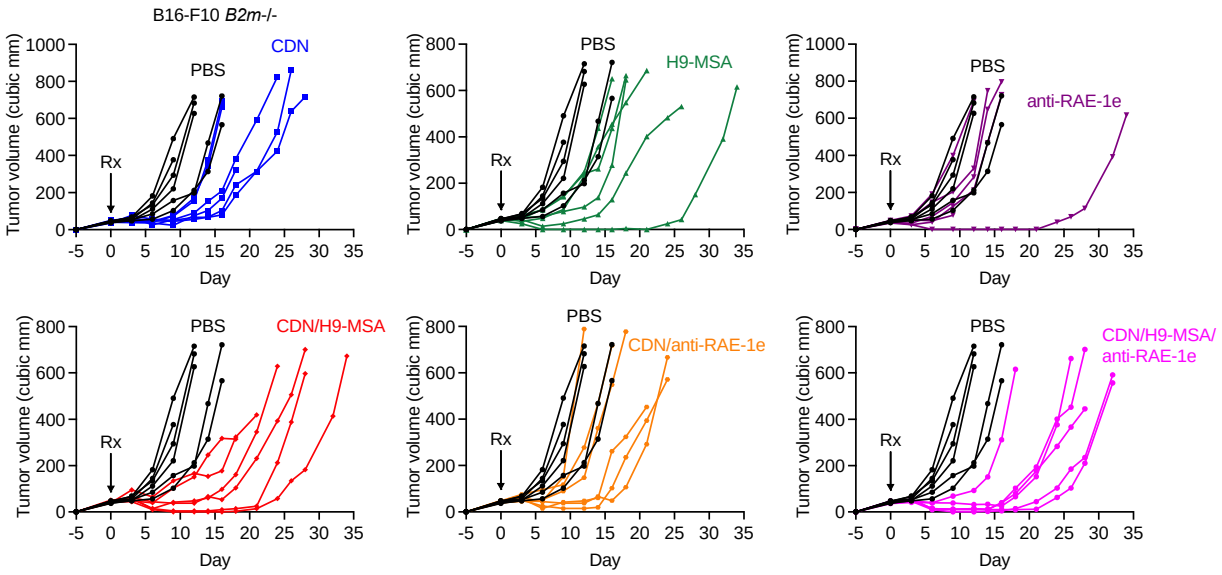

Figure 5.6. Spider plots showing growth of individual tumors from Figure 5.5. Spider plots for anti-RAE-1ε treated animals.

Cytokines, IL-12 and IL-18, in combination with CDN and H9-MSA modestly enhanced anti-tumor responses in MHC I-deficient tumors

IL-12 and IL-18 cytokines are known to potently enhance NK cell functional activities (Nguyen et al., 2020; Smyth et al., 2000; Srivastava et al., 2010). To test whether NK cell anti-tumor responses could be further amplified in CDN/H9-MSA treated mice, we tested the addition of IL-12 and IL-18 in mice depleted of CD4 and CD8 T cells. IL-12/18 therapy by itself had modest, statistically insignificant, effects on tumor growth and survival in this study. IL-12/18 therapy in combination with H9-MSA resulted in a significant decrease in tumor growth compared to IL-12/18 alone, and a nearly significant decrease in tumor growth compared to H9-MSA, and modest, but not significant, increase in survival (Figure 5.7A, Figure 5.8). Combining CDN and IL-12/18 did not enhance tumor rejection or survival compared to CDN alone (Figure 5.7B). Addition of IL-12/18 to the CDN/H9-MSA combination resulted in slightly slower tumor growth and tumor free survival of one mouse, but these improvements compared to CDN/H9-MSA therapy did not reach statistical significance (Figure 5.7C). This was, however, the first time we achieved a cure in mice bearing B16-F10-*B2m*-/- tumors that had been depleted of CD4 and CD8 T cells.

In addition to enhancing NK cell function, IL-12 and IL-18 are also known to enhance T cell functions. We therefore tested IL-12/18 in combination with CDN/H9-MSA in the B16-F10-*B2m*-/- model with no cellular depletions, where both NK cells and CD4 T cells were shown to contribute to tumor rejection (Figure 3.2). IL-12/18 therapy by itself had no significant antitumor effects, nor did it enhance the antitumor effects of H9-MSA therapy (Figure 5.9A, Figure 5.10) or CDN therapy (Figure 5.9B). When CDN/H9-MSA and IL-12/18 were combined, the survival rate increased to ~70% compared to 50% with CDN/H9-MSA, but this difference did not reach statistical significance (Figure 5.10C). The group sizes were small in this experiment, so it is possible that a more powered study with larger groups could document a significant difference. These data raise the possibility that the addition of IL-12/18 to CDN/H9-MSA therapy in the B16-F10-*B2m-/-* tumor model may modestly enhance antitumor responses.

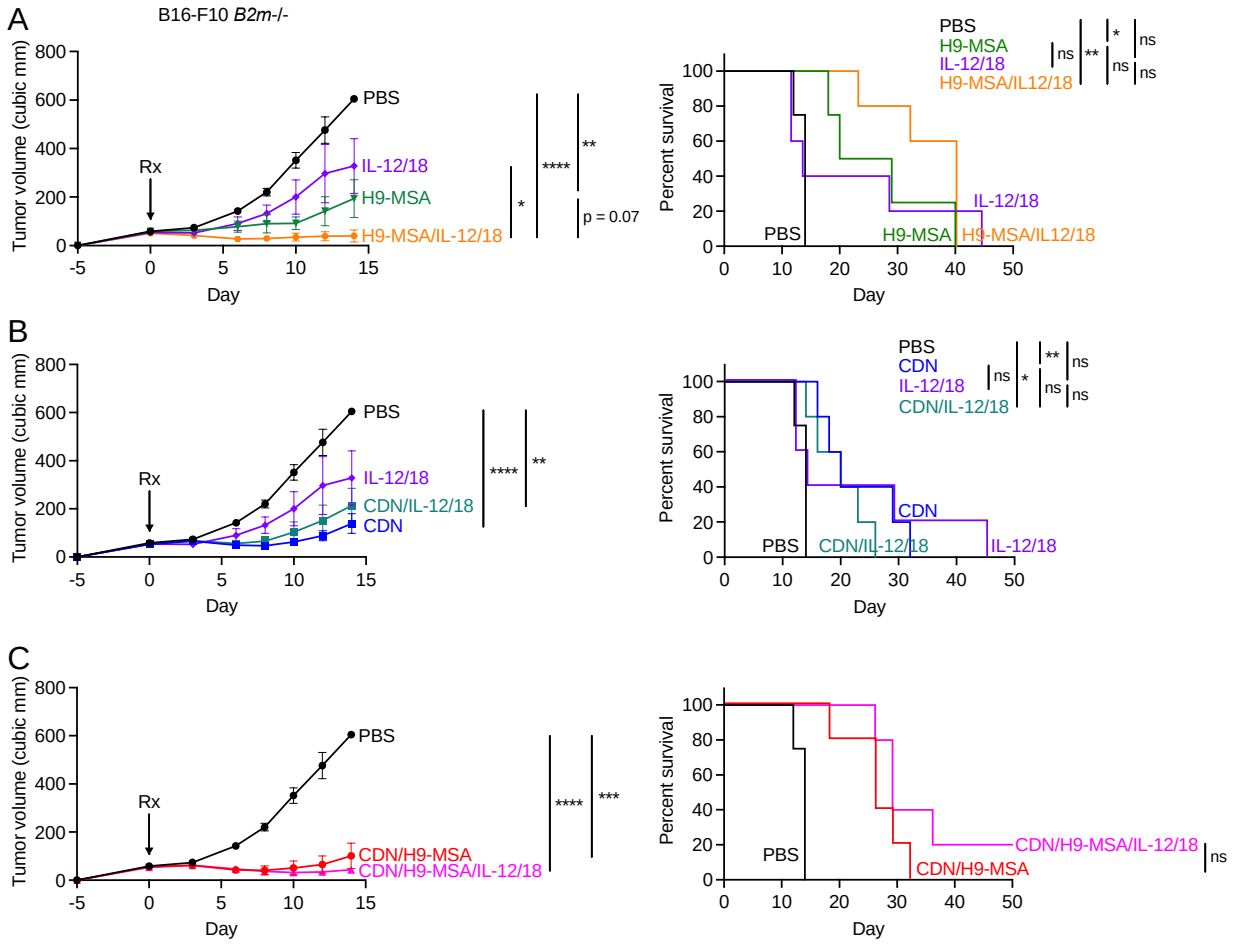

Figure 5.7. IL-12 and IL-18 in combination with CDN and H9-MSA modestly augmented antitumor effects of each separately in the absence of T cells. B16-F10-*B2m*-/- tumor cells were implanted s.c. in C57BL/6J mice on day -5 and grown to approximately 50 mm^3, which occurred 5 days later (labeled as day 0), before initiating therapy. In all panels, the mice were depleted of both CD4 and CD8 T cells before initiating therapy starting on day -2 and -1 and repeated every 6 days. On d0, tumors were injected once intratumorally with 50 μg CDN or PBS, and/or i.p. with 10 μg H9-MSA or PBS. The cytokine or PBS injections were repeated every three days until euthanization or 1 week after tumor clearance. Additionally, some mice were injected i.p. with 100 ng IL-12 and 100 ng IL-18. **(A)** Tumor growth and survival of mice treated with H9-MSA and IL-12/18. **(B)** Tumor growth and survival of mice treated with IL-12/18 and CDN therapy. **(C)** Tumor growth and survival of mice treated with IL-12/18 and CDN/H9-MSA. Tumor growth data were analyzed by 2-way ANOVA. Survival data were analyzed using log-rank (Mantel-Cox) test. n=5-7 mice per group. This experiment was only carried out once, so the results must be considered preliminary. Error bars represent standard error of the mean (SEM). *P< 0.05, **P < 0.01, ***P < 0.001, ****P < 0.0001. Any unmarked comparison in the tumor growth data was not statistically significant.

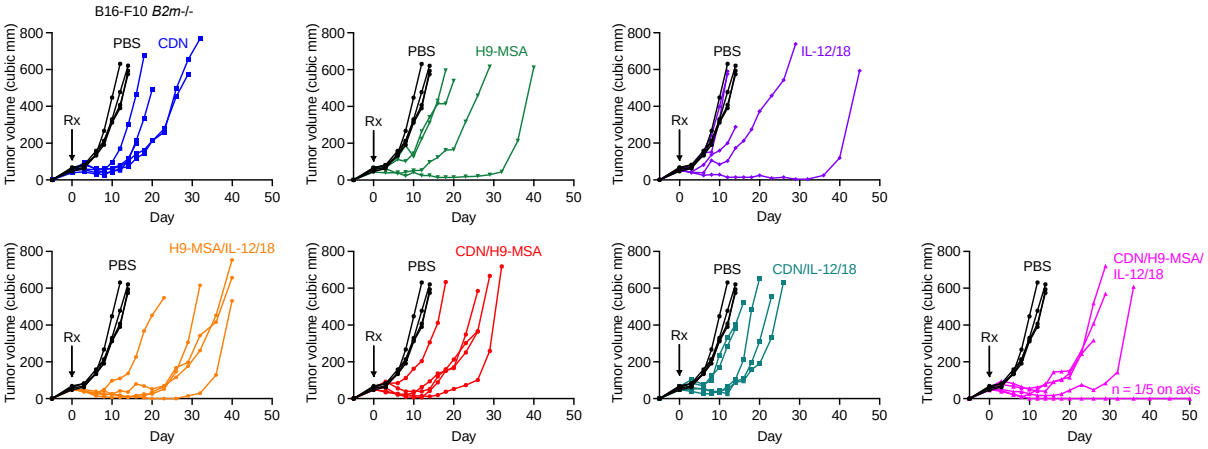

Figure 5.8. Spider plots showing growth of individual tumors from Figure 5.7. Spider plots for IL-12/18 treated animals in mice containing MHC I-deficient tumors depleted of CD4 and CD8 T cells.

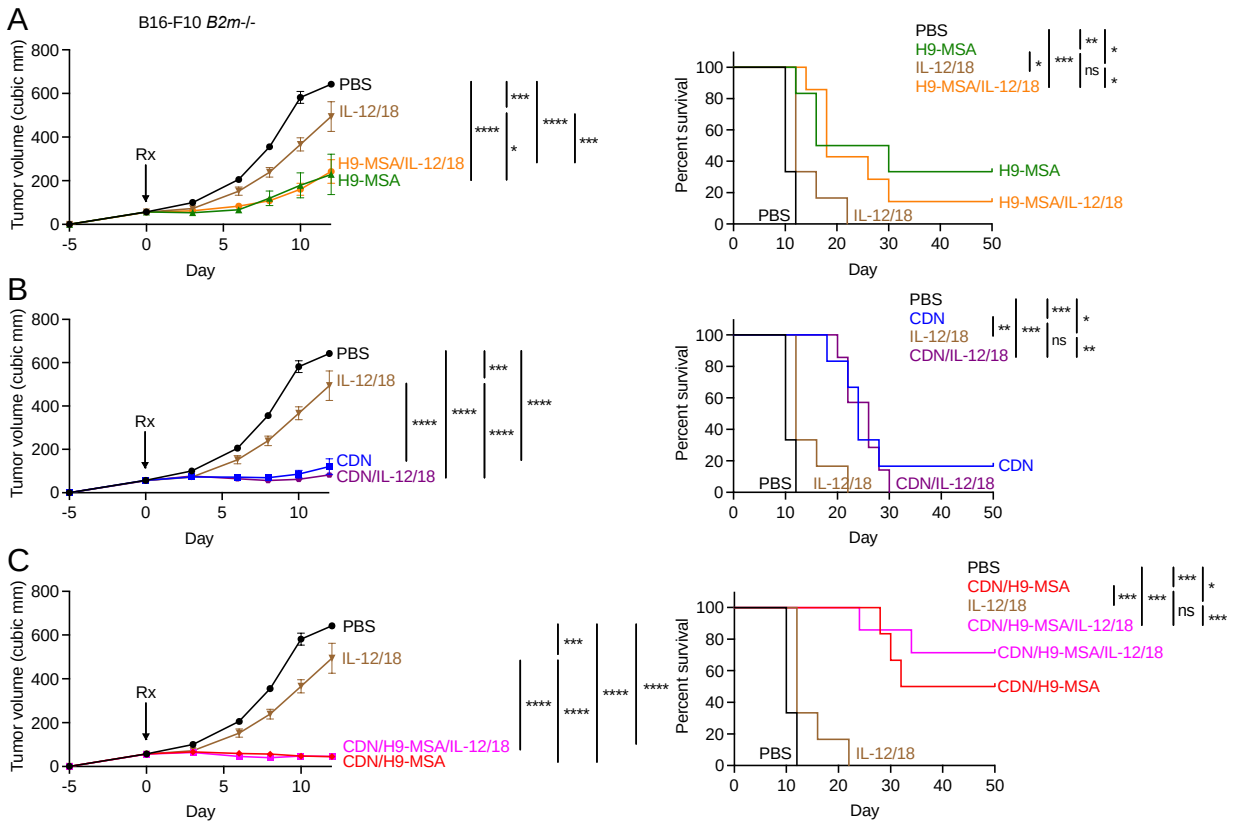

Figure 5.9. Addition of IL-12 and IL-18 in combination with CDN and H9-MSA modestly increased survival of mice compared to CDN/H9-MSA in the presence of T cells and NK cells. B16-F10-*B2m-/-* tumor cells were implanted s.c. in C57BL/6J mice on day -5 and grown to approximately 50 mm^3. On d0, tumors were injected once intratumorally with 50 μg CDN or PBS, and/or i.p. with 10 μg H9-MSA or PBS. The cytokine or PBS injections were repeated every three days until euthanization or 1 week after tumor clearance. Additionally, some mice were injected i.p. with 100 ng IL-12 and 100 ng IL-18. **(A)** Tumor growth and survival of mice treated with H9-MSA and IL-12/18. (B) Tumor growth and survival of mice treated with IL-12/18 and CDN therapy. **(C)** Tumor growth and survival of mice treated with IL-12/18 and CDN/H9-MSA. Tumor growth data were analyzed by 2-way ANOVA. Survival data were analyzed using log-rank (Mantel-Cox) test. n=5-7 mice per group. This experiment was only carried out once, so the results must be considered preliminary. Error bars represent standard error of the mean (SEM). *P< 0.05, **P < 0.01, ***P < 0.001, ****P < 0.0001. Any unmarked comparison in the tumor growth data was not statistically significant.

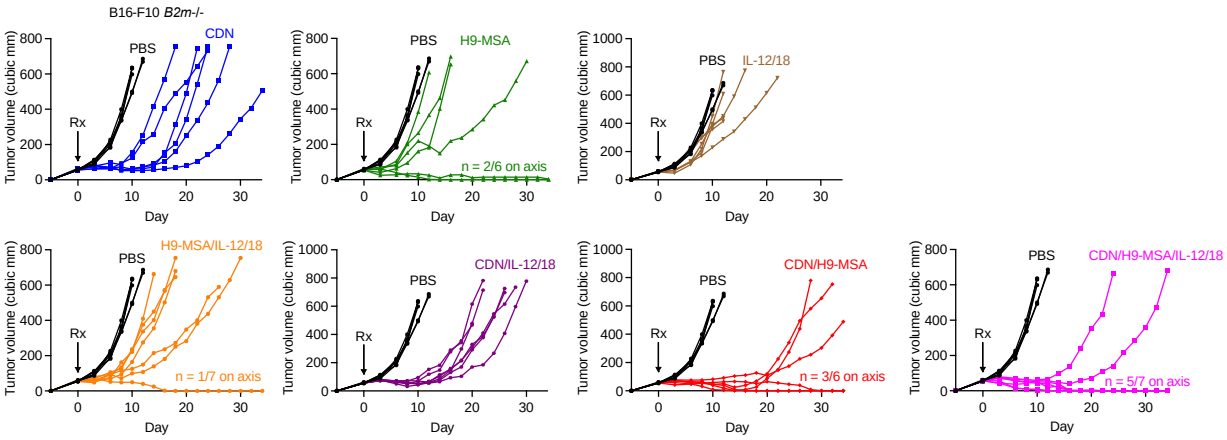

Figure 5.10. Spider plots showing growth of individual tumors from Figure 5.9. Spider plots for IL-12/18 treated animals in mice containing MHC I-deficient tumors.

Checkpoint blockade with anti-CD137 did not enhance NK cell mediated rejection of MHC I-deficient tumors

In our search to find new therapeutic combinations, we reasoned that CDN/H9-MSA combination therapy would lead to changes of cell surface markers that could influence antitumor responses and suggest combination therapies to try. Therefore, we employed our bilateral tumor system (Figure 3.11) and examined markers of activation and inhibition on tumor infiltrating NK cells following treatment.

We observed that CDN/H9-MSA therapy significantly increased the expression level of CD137 (also known as 4-1BB), a well-known co-stimulatory checkpoint molecule, on NK cells infiltrating B16-F10-*B2m*-/- tumors (Figure 5.11). To test the effects of blocking CD137 in combination with CDN and/or H9-MSA in the setting of NK cell mediated antitumor responses, mice were injected s.c. with B16-F10-*B2m*-/- tumors and depleted of CD4 and CD8 T cells to focus on NK cell effects. Anti-CD137 alone did not have single agent efficacy (Figure 5.12A, Figure 5.13). Combining anti-CD137 with CDN or CDN/H9-MSA did not significantly augment the antitumor effects of the latter agents in tumor growth or increase overall survival (Figure 5.12B). Therefore, although an increase in expression of CD137 was observed on tumor infiltrating NK cells in CDN-H9-MSA treated mice, the addition of anti-CD137 led to no discernable augmentation of the antitumor effects.

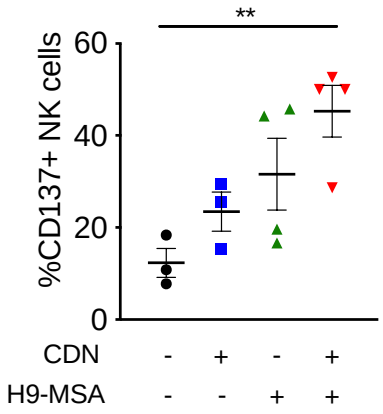

Figure 5.11. The co-stimulatory molecule, CD137, expression increased on NK cells in tumors after CDN/H9MSA treatment. B16-F10 *B2m*-/- tumor cells were implanted s.c. in C57BL/6J mice on day -5 and grown to approximately 50 mm^3. On d0, tumors were injected once intratumorally with 50 μg CDN or PBS, and/or i.p. with the with 10 μg H9-MSA or PBS on day 0. On d2, single cell suspensions of tumors were examined for the expression of CD137 on NK cells among viable CD45+ cells. Samples were analyzed by one-way ANOVA. n=3-4 mice per group. This experiment was only carried out once, so the results must be considered preliminary. Error bars represent standard error of the mean (SEM). *P< 0.05, **P < 0.01, ***P < 0.001, ****P < 0.0001.

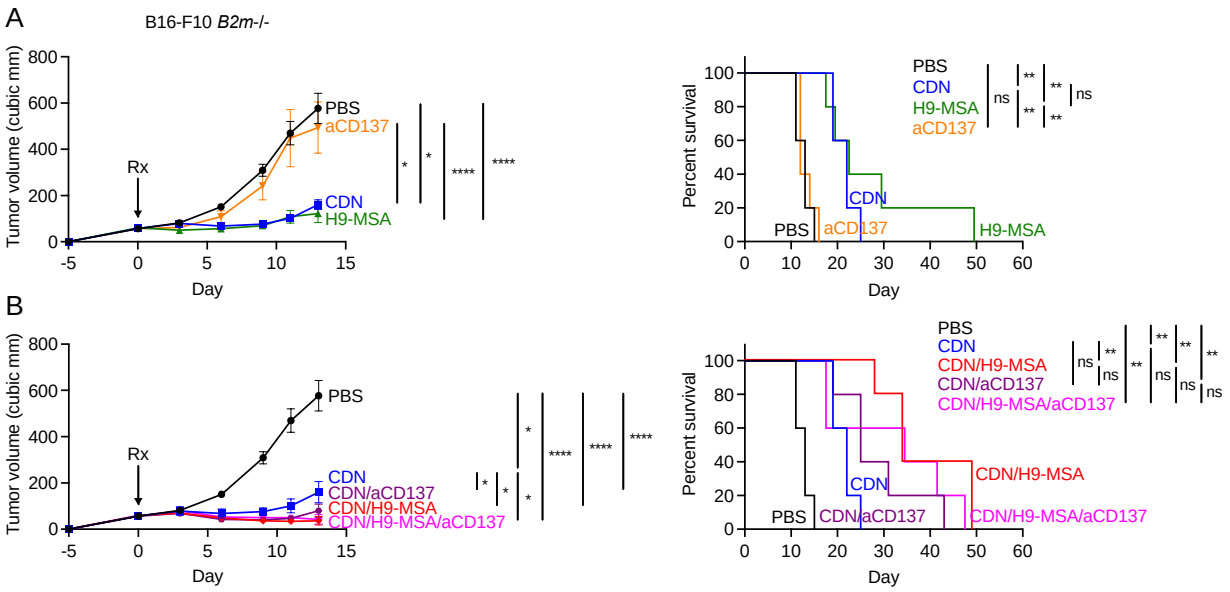

Figure 5.12. Anti-CD137 in combination with CDN and H9-MSA did not boost NK cell antitumor responses in an MHC I-deficient tumor model. B16-F10-*B2m-/-* tumor cells were implanted s.c. in C57BL/6J mice on day -5 and grown to approximately 50 mm^3. On d0, tumors were injected once intratumorally with 50 μg CDN or PBS, and/or i.p. with 10 μg H9-MSA or PBS. The cytokine or PBS injections were repeated every three days until euthanization or 1 week after tumor clearance. Additionally, some mice were injected i.p. with 200 μg anti-CD137. In all panels, the mice were depleted of both CD4 and CD8 T cells before initiating therapy. **(A)** Tumor growth and survival of mice was not affected by anti-CD137 therapy. **(B)** Tumor growth and survival of CDN or CDN/H9-MSA therapy was not enhanced by the addition of anti-CD137. Tumor growth data were analyzed by 2-way ANOVA. Survival data were analyzed using log-rank (Mantel-Cox) test. This experiment was only carried out once, so the results must be considered preliminary. n=5-7 mice per group. Error bars represent standard error of the mean (SEM). *P< 0.05, **P < 0.01, ***P < 0.001, ****P < 0.0001. Any unmarked comparison in the tumor growth data was not statistically significant.

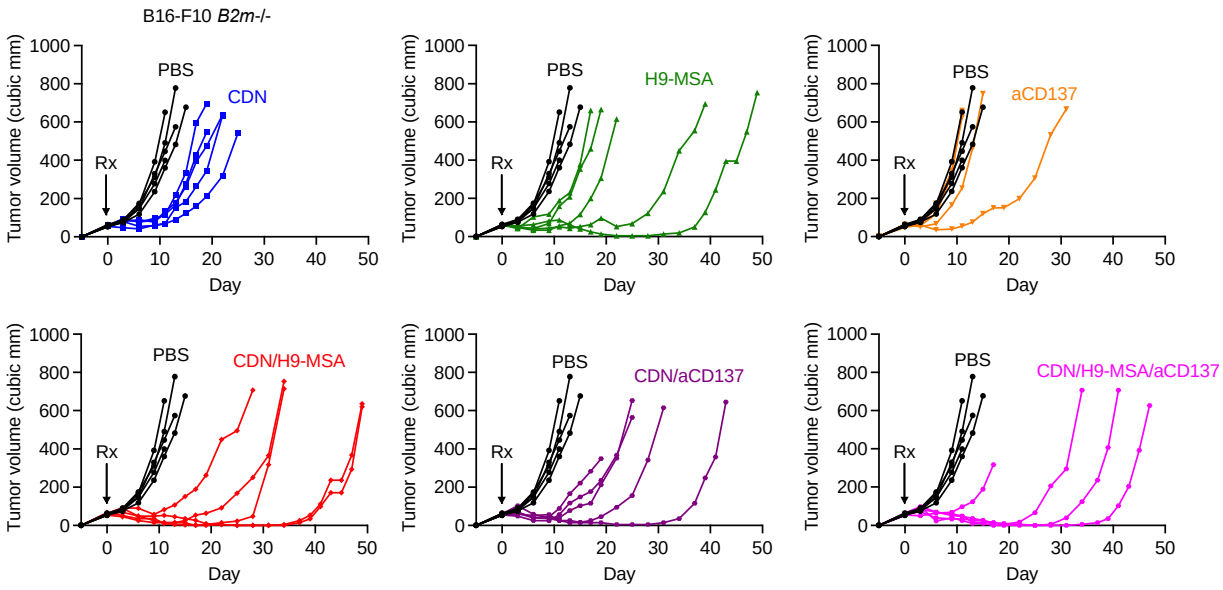

Figure 5.13. Spider plots showing growth of individual tumors from Figure 5.12. Spider plots for anti-CD137 treated animals.

Checkpoint blockade of PD-1, CTLA4 or TIGIT, did not enhance NK cell mediated rejection of B16-F10 MHC I-deficient tumors

Continuing our search for additional therapies to combine with CDN/H9-MSA therapy, we employed our bilateral tumor system (Figure 3.11) and observed that CDN/H9-MSA therapy increased the percentages among infiltrating cells in B16-F10 *B2m*-/- tumors of CD4 T cells or NK cells expressing PD-1, a well-known checkpoint molecule (Figure 5.14A, B). The impact on CD4 T cells was pronounced and statistically significant in the injected tumors but less pronounced in the bilateral tumor. The impacts on NK cells were more modest and did not reach statistical significance. To test the effects of PD-1 blockade in combination with CDN and H9-MSA, mice were injected s.c. with B16-F10-*B2m*-/- tumors and treated as in Figure 3.2. Due to the antitumor effects of both NK cells and CD4 T cells in this model, anti-CTLA4 was additionally tested as anti-PD-1 and anti-CTLA4 synergize in various tumor models (Hellmann et al., 2019). Survival of mice treated with CDN/H9-MSA was not prolonged by adding anti-PD-1 or anti-CTLA4 separately or together (Figure 5.15). In all cases the survival rate of mice was ~70%. Admittedly, there was relatively little room for improvement over the CDN/H9-MSA combination, but to the extent that differences could be discerned, we failed to observe improved antitumor effects by adding PD-1 and/or CTLA4 checkpoint therapy to the mix.

In addition to the upregulation of PD-1, the checkpoint molecule TIGIT was also systemically upregulated on NK cells in the uninjected tumors (Figure 5.16B) and in spleens (Figure 5.16C) of mice bearing two B16-F10 *B2m-/-* tumors following CDN/H9-MSA therapy. To test the effects of blocking TIGIT in combination with CDN and H9-MSA, mice were injected s.c. with B16-F10 *B2m*-/- tumors and treated as in Figure 3.2. Anti-TIGIT treatments showed significant single agent activity in reducing tumor growth, comparable to the single agent effects of CDN (Figure 5.17A, Figure 5.18) or H9-MSA (Figure 5.17B). However, combining anti-TIGIT with CDN or H9-MSA did not significantly augment the anti-tumor effects. The percentage of surviving mice treated with CDN/H9-MSA was not prolonged with the addition of anti-TIGIT (Figure 5.17C), albeit there was relatively little room for improvement compared to CDN/H9-MSA alone. Therefore, while an increase in expression of TIGIT was observed on NK cells in mice receiving CDN/H9-MSA therapy, the addition of anti-TIGIT blocking TIGIT did not greatly improve the efficacy of the therapy.

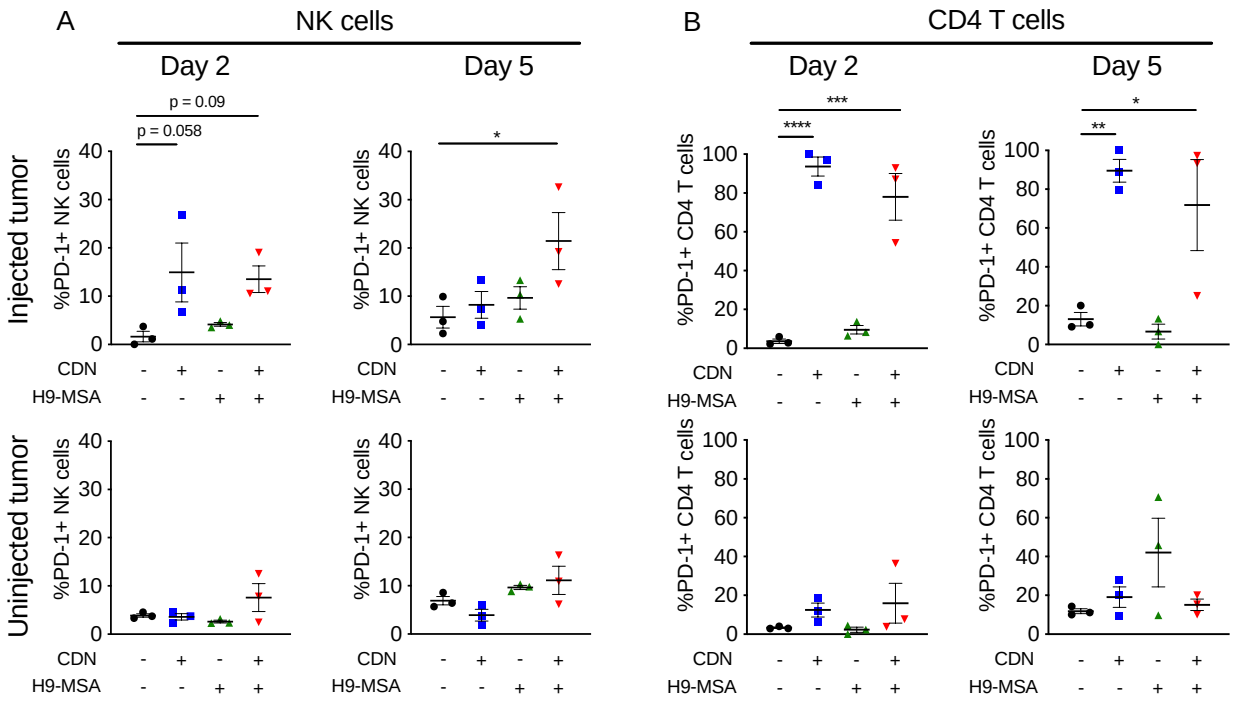

Figure 5.14. NK cells and T cells upregulate the checkpoint receptor PD-1 following CDN/H9-MSA therapy. B16-F10 *B2m-/-* tumor cells were implanted s.c. in C57BL/6J mice on day -5 and grown to approximately 50 mm^3. On d0, tumors were injected once intratumorally with 50 μg CDN or PBS, and/or i.p. with 10 μg H9-MSA or PBS on day 0 and again on day 3. On d2 and d5, single cell suspensions of tumors were examined for the expression of PD-1 on NK cells and CD4 T cells among viable CD45+ cells. Samples were analyzed by one-way ANOVA. The data in all panels are representative at least two independent experiments. n=3-4 mice per group. Error bars represent standard error of the mean (SEM). *P< 0.05, **P < 0.01, ***P < 0.001, ****P < 0.0001. Any unmarked comparison in the tumor growth data was not statistically significant.

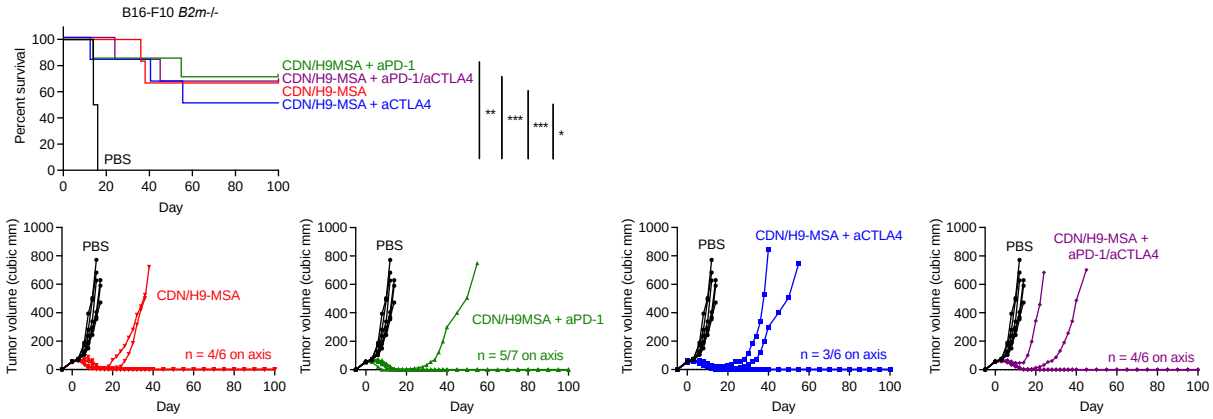

Figure 5.15. Anti-PD-1 and anti-CTLA4 did not boost antitumor responses against B16-F10-B2m-/- tumors when combined with CDN/H9-MSA therapy. B16-F10-*B2m-/-* tumor cells were implanted s.c. in C57BL/6J mice on day -5 and grown to approximately 50 mm^3. On d0, tumors were injected once intratumorally with 50 μg CDN or PBS, and/or i.p. with 10 μg H9-MSA or PBS. The cytokine or PBS injections were repeated every three days until euthanization or 1 week after tumor clearance. Additionally, some mice were treated i.p. with 200 μg anti-PD-1 (clone RMP1-14) and/or 200 μg anti-CTLA4 (clone 3H10) and repeated every three days. Survival data were analyzed using log-rank (Mantel-Cox) test. This experiment was only carried out once, so the results must be considered preliminary. n=5-7 mice per group. *P< 0.05, **P < 0.01, ***P < 0.001, ****P < 0.0001. Any unmarked comparison in the tumor growth data was not statistically significant.

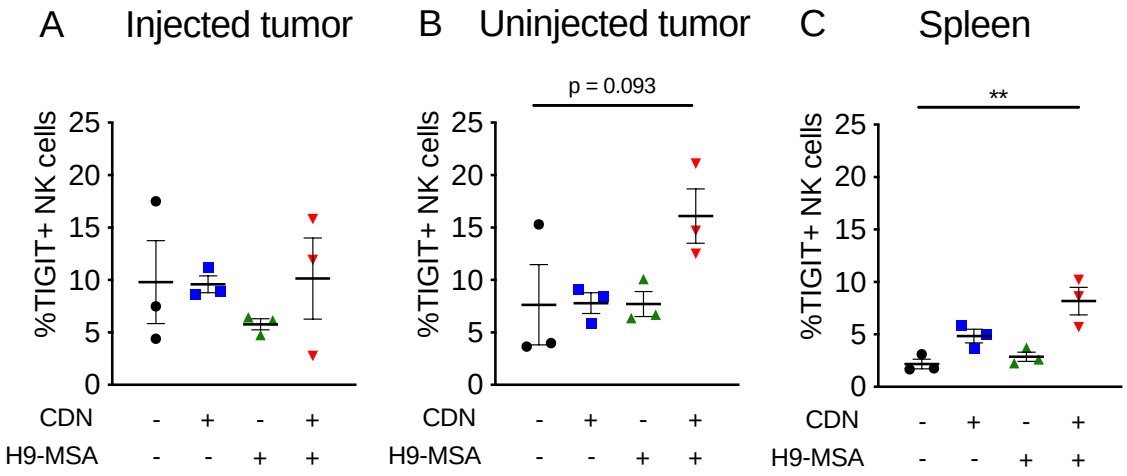

Figure 5.16. Following CDN/H9-MSA therapy, NK cells systemically upregulated the checkpoint receptor, TIGIT. B16-F10-*B2m-/-* tumor cells were implanted s.c. in C57BL/6J mice on day -5 and grown to approximately 50 mm^3. On d0, tumors were injected once intratumorally with 50 μg CDN or PBS, and/or i.p. with the with 10 μg H9-MSA or PBS on day 0. On d2 single cell suspensions of tumors and spleens were examined for the expression of TIGIT on NK cells among viable CD45+ cells. Samples were analyzed by one-way ANOVA. The data in all panels are representative at least two independent experiments. n=3-

4 mice per group. Error bars represent standard error of the mean (SEM). *P< 0.05, **P < 0.01, ***P < 0.001, ****P < 0.0001. Any unmarked comparison in the tumor growth data was not statistically significant.

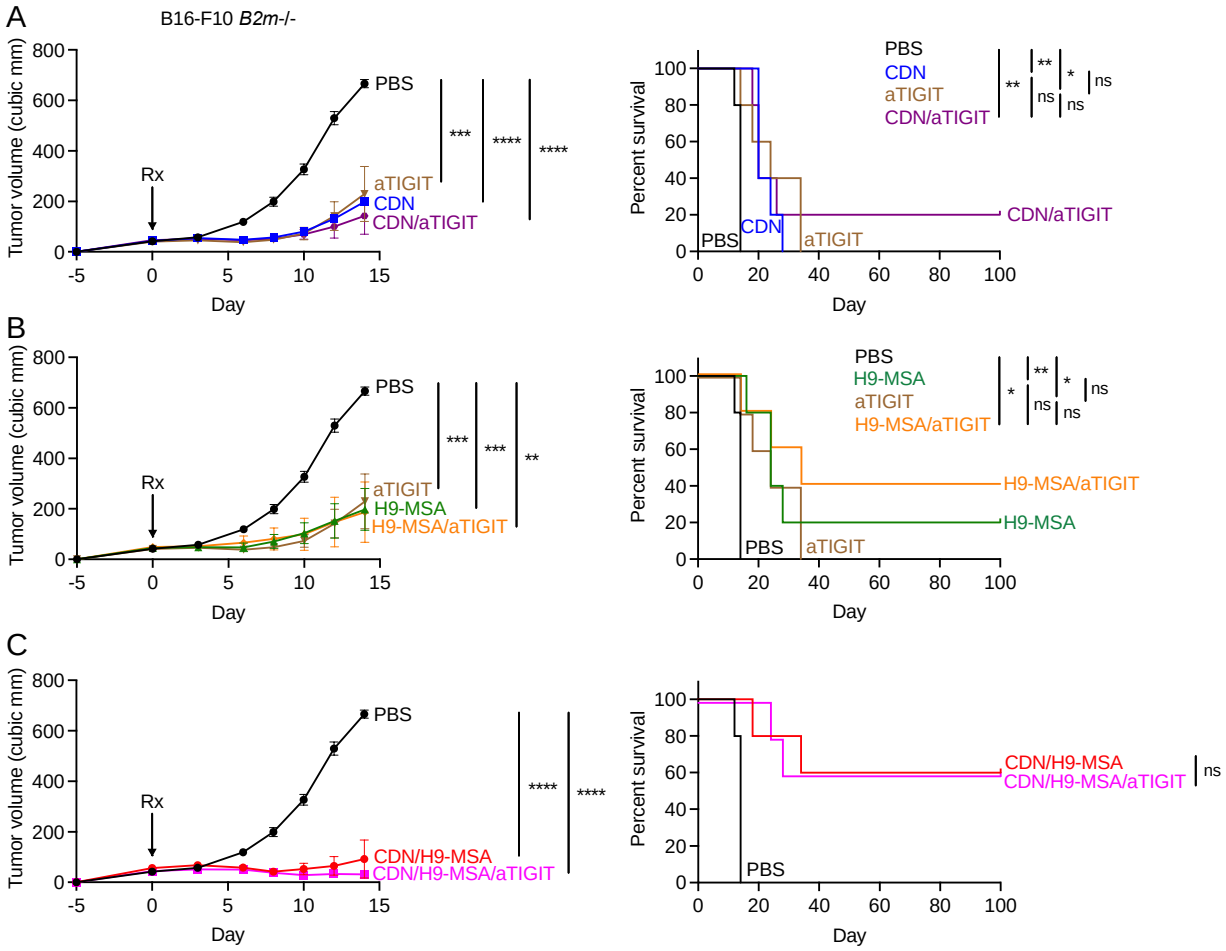

Figure 5.17. Anti-TIGIT alone reduced tumor growth in an MHC I-deficient tumor model but did not augment the therapeutic effects of CDN and/ or H9-MSA. B16-F10-*B2m-/-* tumor cells were implanted s.c. in C57BL/6J mice on day -5 and grown to approximately 50 mm^3. On d0, tumors were injected once intratumorally with 50 μg CDN or PBS, and/or i.p. with 10 μg H9-MSA or PBS. The cytokine or PBS injections were repeated every three days until euthanization or 1 week after tumor clearance. Additionally, some mice were treated i.p. with 200 μg anti-TIGIT (clone MUR10A), which was repeated every three days. **(A,B)** Tumor growth and survival of mice treated with anti-TIGIT in combination with CDN **(A)** or H9-MSA **(B)**. **(C)** Tumor growth and survival of mice treated with anti-TIGIT combined with CDN/H9-MSA was not enhanced compared to CDN/H9-MSA alone. Tumor growth data were analyzed by 2-way ANOVA. Survival data were analyzed using log-rank (Mantel-Cox) test. The data in all panels are representative at least two independent experiments. n=5-7 mice per group. Error bars represent standard error of the mean (SEM). *P< 0.05, **P < 0.01, ***P < 0.001, ****P < 0.0001. Any unmarked comparison in the tumor growth data was not statistically significant.

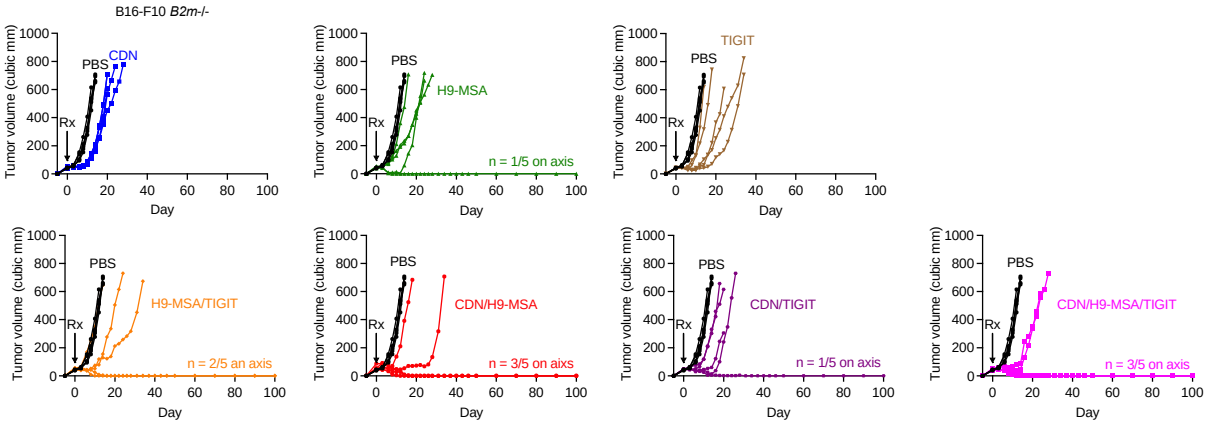

Figure 5.18. Spider plots showing growth of individual tumors from Figure 5.17. Spider plots for anti-TIGIT treated animals.

Checkpoint blockade with anti-PD-1 and anti-TIGIT did not enhance NK cell mediated rejection of larger MC38 MHC I-deficient tumors

To further explore whether checkpoint therapy can improve antitumor effects of NK cells elicited by the CDN/H9-MSA combination therapy, we turned to the MC38-*B2m-/-* tumor model, in which rejection is mediated by NK cells but not T cells. In this model, however, the CDN/H9-MSA combination cures 100% of mice when tumors are small (50 mm^3) at the time of treatment initiation. Therefore, we allowed the tumors to grow to 150 mm^3 or 450 mm^3 before initiating treatment, a situation in which CDN/H9-MSA therapy failed to result in prolonged tumor remissions (Figure 3.20). In this situation we could determine whether adding checkpoint therapy improved the outcomes. We first employed the bilateral tumor system to show that, similar to what we observed in the B16-*B2m-/-* tumor model, CDN/H9-MSA therapy increased the expression of PD-1 (Figure 5.19A) and TIGIT (Figure 5.19B) on NK cells infiltrating the tumors, in at least some of the comparisons.

Mice were injected s.c. with MC38-*B2m*-/- tumors and treated as in Figure 3.2 when tumors reached ~150 mm^3. The addition of anti-PD-1 or anti-TIGIT to the CDN/H9-MSA treatment led to slight, though not significant, decreases in tumor growth small, but statistically insignificant extensions in survival time (Figure 5.20). When combined separately with CDN/H9-MSA, Neither of these treatments led to complete tumor clearance in any of the treated mice. When anti-PD-1 and anti-TIGIT were added together to the therapy regimen, there was not much additional improvement in tumor rejection, except that one mouse cleared the primary tumor and remained tumor free long-term. Again, these improvements were not significant.

When these combinations were tested in mice with large tumors (450 mm^3) similar outcomes were observed (Figure 5.21). Adding anti-PD-1 to the combination had little effect, whereas adding anti-TIGIT potentially had a small, albeit insignificant, effect, although one mouse cleared the tumor altogether. When both anti-PD-1 and anti-TIGIT were added, there was no detectable improvement compared to CDN/H9-MSA alone.

Thus, in both the medium sized and large sized tumors, the addition of anti-PD-1 and anti-TIGIT did not greatly enhance the antitumor response of NK cells in the MC38 MHC I-deficient tumor model. A caveat to this conclusion is that relatively small numbers of animals were tested, and it is possible that some of the differences would be significant if the experiments were more highly powered.

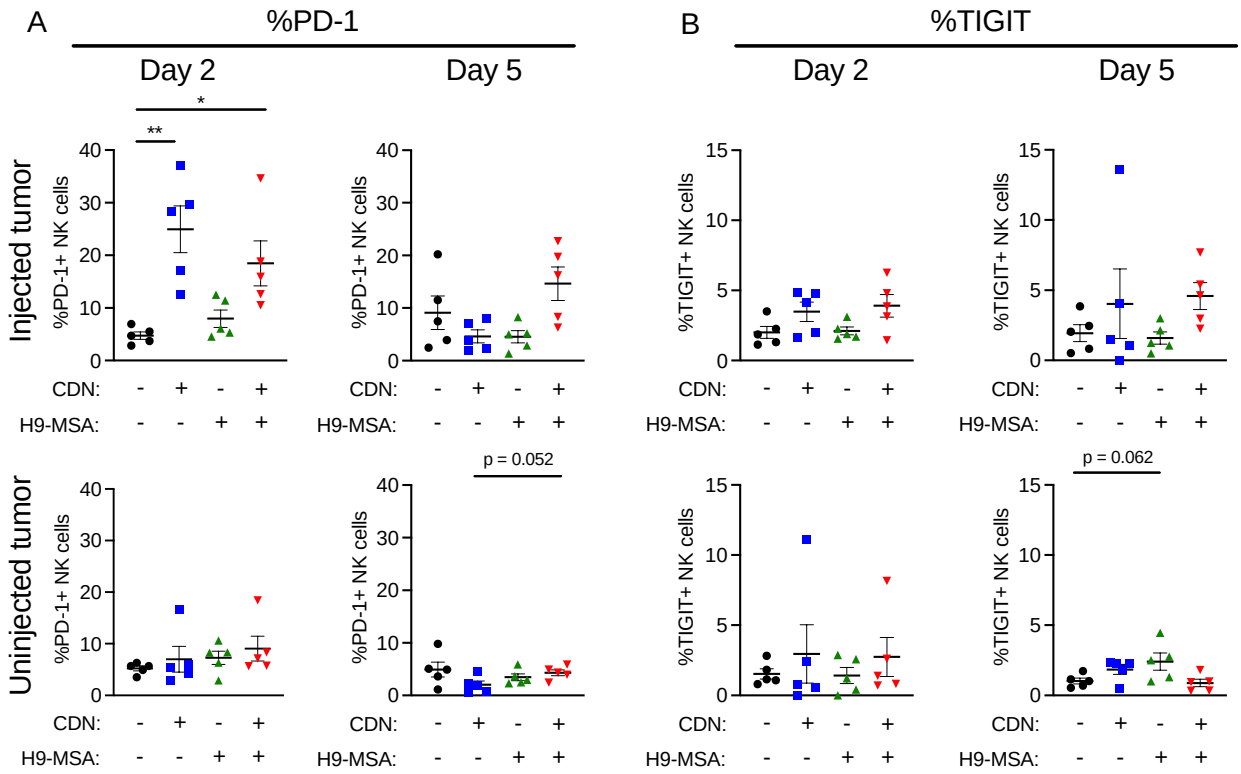

Figure 5.19. Tumor infiltrating NK cells upregulate the checkpoint molecules, PD-1 and TIGIT, following CDN/H9-MSA therapy. MC38 *B2m-/-* tumor cells were implanted s.c. in C57BL/6J mice on day -5 and grown to approximately 50 mm^3. On d0, tumors were injected once intratumorally with 50 μg CDN or PBS, and/or i.p. with 10 μg H9-MSA or PBS on day 0 and again on day 3. On d2 and d5, single cell suspensions of tumors were examined for the expression of PD-1 and TIGIT on NK cells among viable CD45+ cells. Samples were analyzed by one-way ANOVA. The data in all panels are representative at least two independent experiments. n=5 mice per group. Error bars represent standard error of the mean (SEM). *P< 0.05, **P < 0.01, ***P < 0.001, ****P < 0.0001. Any unmarked comparison in the tumor growth data was not statistically significant.

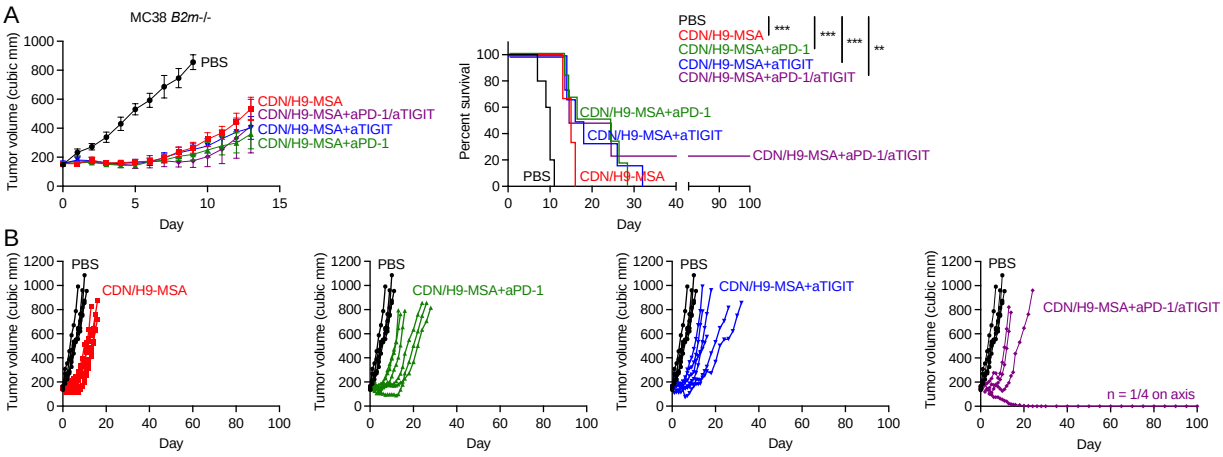

Figure 5.20. Checkpoint blockade with anti-PD-1 and/or anti-TIGIT, did not augment antitumor effects of CDN/H9-MSA in mice with medium sized tumors. MC38-*B2m-/-* tumor cells were implanted s.c. in C57BL/6J mice on day 0 and grown to approximately 150 mm^3. Then tumors were injected once intratumorally with 50 μg CDN or PBS, and/or i.p. with 10 μg H9-MSA or PBS. The cytokine or PBS injections were repeated every three days until euthanization or 1 week after tumor clearance. Additionally, some mice were treated i.p. with 200 μg anti-PD-1 (clone RMP1-14) and/or 200 μg anti-TIGIT (clone MUR10A), which was repeated every three days. **(A)** Tumor growth and survival data of anti-PD-1 and/or anti-TIGIT treatments combined with CDN/H9-MSA therapy. **(B)** Spider plots showing individual growth curves for treated animals in A. Tumor growth data were analyzed by 2-way ANOVA. Survival data were analyzed using log-rank (Mantel-Cox) test. n=5-7 mice per group. This experiment was only carried out once, so the results must be considered preliminary. Error bars represent standard error of the mean (SEM). *P< 0.05, **P < 0.01, ***P < 0.001, ****P < 0.0001. Any unmarked comparison in the tumor growth data was not statistically significant.

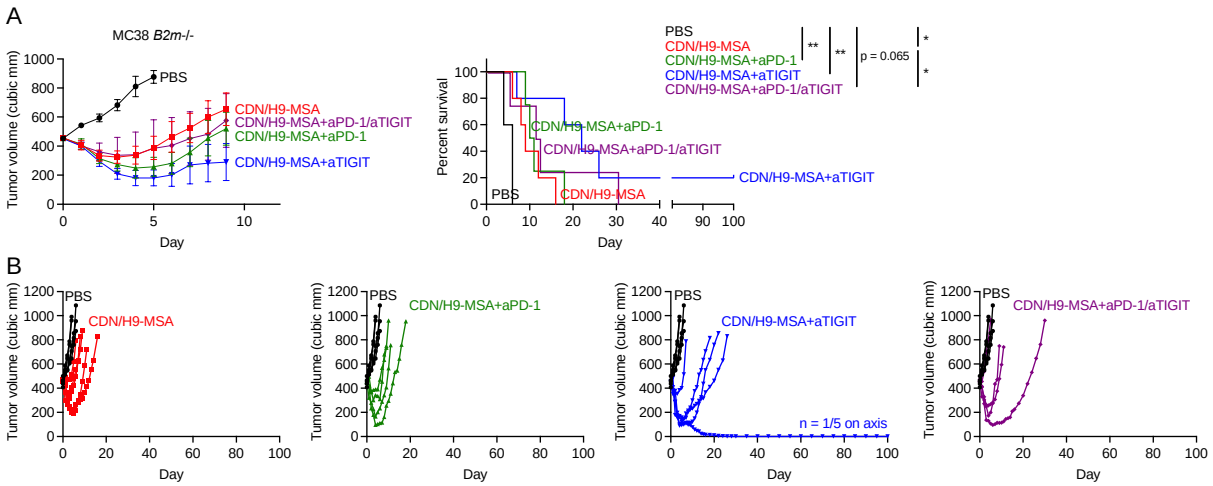

Figure 5.21. Checkpoint blockade with anti-PD-1 and/or anti-TIGIT did not augment antitumor effects of CDN/H9-MSA in mice with large sized tumors. MC38-*B2m-/-* tumor cells were implanted s.c. in C57BL/6J mice on day 0 and grown to approximately 450 mm^3. Then tumors were injected once intratumorally with 50 μg CDN or PBS, and/or i.p. with 10 μg H9-MSA or PBS. The cytokine or PBS injections were repeated every three days until euthanization or 1 week after tumor clearance. Additionally, some mice were treated i.p. with 200 μg anti-PD-1 (clone RMP1-14) and/or 200 μg anti-TIGIT (clone MUR10A), which was repeated every three days. **(A)** Tumor growth and survival data of anti-PD-1 and/or anti-TIGIT treatments combined with CDN/H9-MSA therapy. **(B)** Spider plots showing individual growth curves for treated animals in A. Tumor growth data were analyzed by 2-way ANOVA. Survival data were analyzed using log-rank (Mantel-Cox) test. This experiment was only carried out once, so the results must be considered preliminary. Error bars represent standard errors of the mean (SEM). *P< 0.05, **P < 0.01, ***P < 0.001, ****P < 0.0001. Any unmarked comparison in the tumor growth data was not statistically significant.

Efficacy of checkpoint blockade in combination with CDN/H9-MSA therapy in the methylcholanthrene induced sarcoma model

Although the CDN/H9-MSA combination showed efficacy in treating primary MCA tumors, nearly all the mice eventually succumbed (Figure 4.11). Therefore, in collaboration with Cristina Blaj in the laboratory, we tested whether efficacy could be improved by adding checkpoint therapy to the combination. Addition of anti-PD-1 therapy did not result in an improvement in survival, nor did addition of anti-TIGIT therapy (Figure 5.22, Figure 5.23A). However, simultaneous blockade of PD-1 and TIGIT, in combination with CDN/H9-MSA, was significantly more effective than CDN/H9-MSA therapy alone (Figure 5.22, Figure 5.23A). When all four components were injected simultaneously, we observed instances of severe, rapid morbidity of unknown causes. However, we found that delaying the anti-TIGIT treatments by one day greatly ameliorated that toxicity. Therefore, we subsequently incorporated delayed anti-TIGIT treatment into our treatment regimen for analysis of additional animals.

Notably, in mice that received the four-component therapy regimen, 44% of the animals (8/18) survived tumor-free for >160 days. Interestingly, the chronic granulomatous histiocytic inflammation noted in some mice treated with CDN/H9-MSA in Chapter 4, was not observed in the mice receiving all four agents.

Mice that received anti-PD-1 or anti-TIGIT treatments alone or together did not show prolonged survival (Figure 5.23B). CDN therapy outcomes were also not improved by the addition of anti-PD-1 or anti-TIGIT separately to the CDN/H9-MSA therapy combination (Figure 5.23C). In conclusion, simultaneous blockade of PD-1 and TIGIT was necessary to unleash a fully effective antitumor immune response initiated by CDN/H9-MSA treatments.

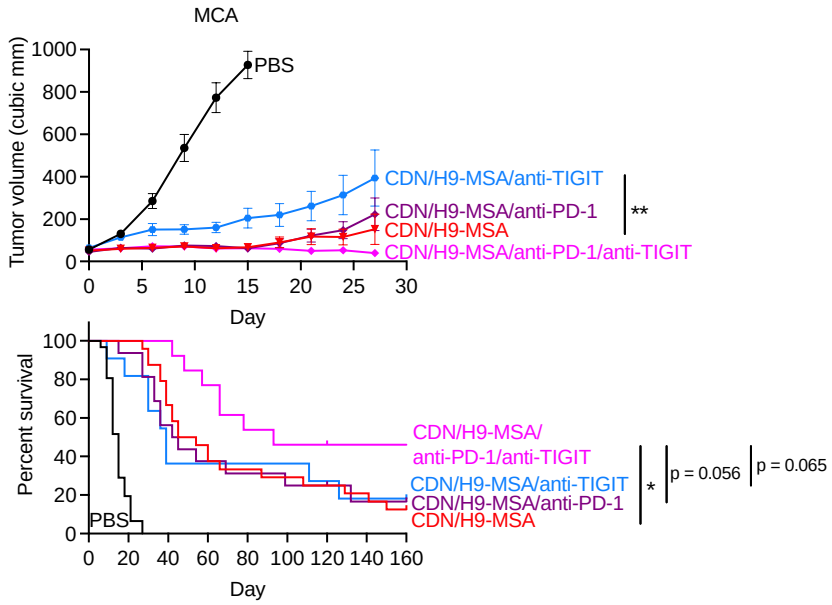

Figure 5.22. CDN/H9-MSA therapy induced potent antitumor effects with MHC I+ tumors, mediated by CD8 T cells. When MCA-induced tumors reached ~50 mm^3 in size

they were injected i.t. with PBS or 50 μg CDN on days 0, 3, and 6 and repeated every 6 six days, thereafter. Mice were also injected with 10 μg H9-MSA or PBS. The cytokine or PBS injections were repeated every three days. Addition of checkpoint inhibitors consisting of i.p. injections of anti-PD-1 (clone RMP1-14) and anti-TIGIT (clone MUR10A), increased tumor rejection and overall survival. Data in these panels are a combination of multiple experiments, such that some of the data (e.g. CDN/H9-MSA) are shared in different panels. n=11-24 mice per group. Data were analyzed by 2-way ANOVA. Error bars represent standard error of the mean (SEM). *P< 0.05, **P < 0.01, ***P < 0.001, ****P < 0.0001. Any unmarked comparison in the tumor growth data was not statistically significant.

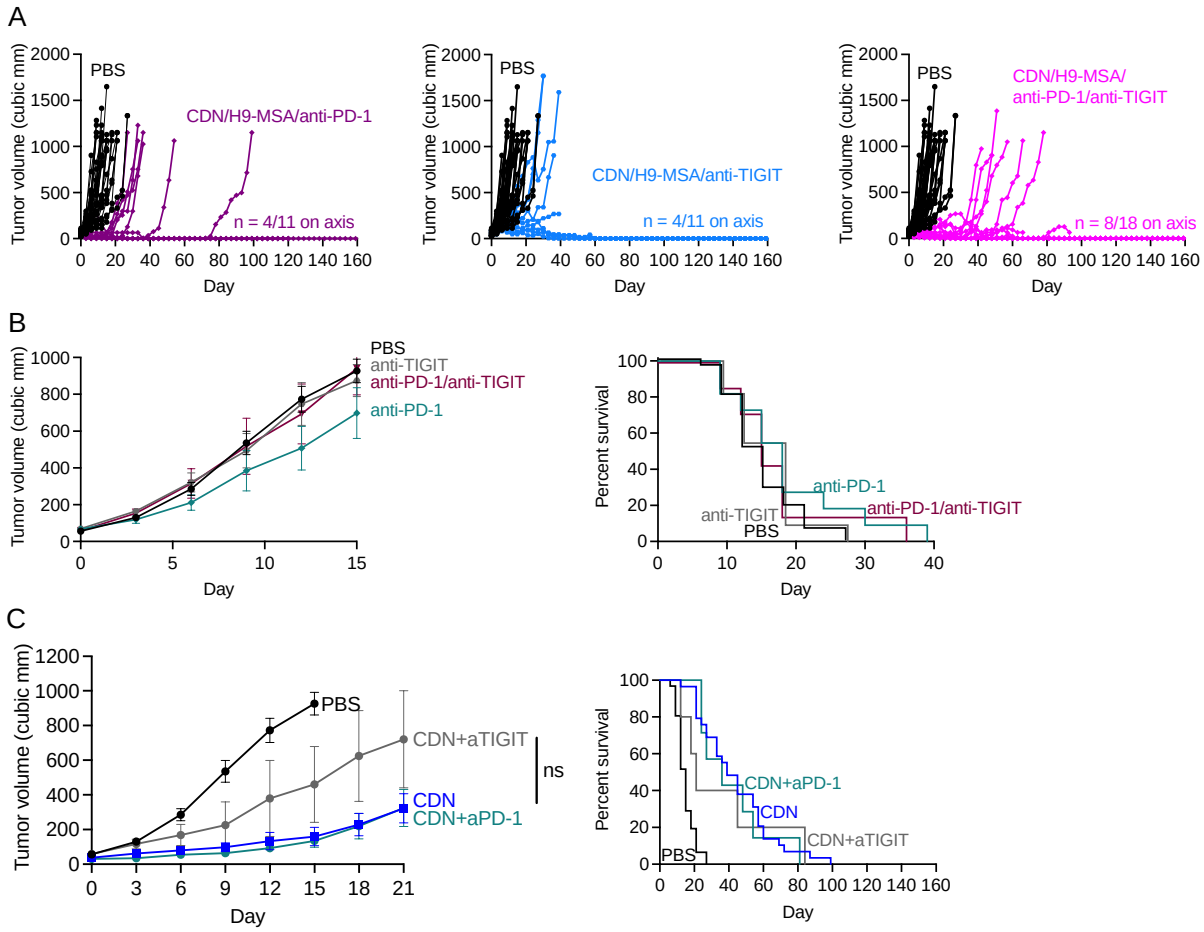

Figure 5.23. Combination immunotherapy for treating primary sarcomas induced by the carcinogen methylcholanthrene. (A) Spider plots for CDN/H9-MSA+checkpoint inhibitor combinations from Figure 5.22. **(B, C)** Tumor averages for single agent checkpoint inhibitors **(B)** or checkpoint inhibitors in combination with CDN **(C)**. The anti-TIGIT antibody employed in these panels was clone 1G9 (BioXCell). Tumor growth data were analyzed by 2-way ANOVA. Survival data were analyzed using log-rank (Mantel-Cox) test. n=7-11 mice per group. Error bars represent standard errors of the mean (SEM). *P< 0.05, **P < 0.01, ***P < 0.001, ****P < 0.0001. Any unmarked comparison in the tumor growth data was not statistically significant.

Discussion

The CDN/H9-MSA therapy combination synergistically induced profound antitumor responses in several solid tumor models, including MHC I-deficient and MHC I+ tumor transplant models. The combination was also effective for treating primary MCA-induced sarcomas, although in that model long-term survival was less frequent and depended on concomitant checkpoint therapy. The success of the combination in this autochthonous model is encouraging, however, because it is very difficult to cure and likely mimics human cancer better than s.c. tumors. We suspect that the therapy combination would be very effective for hematologic malignancies as well, considering that such tumor cells are frequently highly sensitive to NK-mediated killing.

Studies have demonstrated that exposure of NK cells to a cocktail of cytokines ─ IL-15, IL-12 and IL-18 ─ converted the cells into long-lived, activated NK cells called 'memory-like' NK cells (Cooper et al., 2009; Romee et al., 2012). These cells persist for weeks or months with augmented functional activity, suggesting their possible utility in cancer immunotherapy. In our syngeneic tumor transplant model, IL-12 and IL-18 in combination with CDN and/or H9-MSA modestly improved antitumor responses in the presence or absence of T cells. Further studies to examine the 'memory-like' nature of these NK cells are needed to understand how such cells play a role in tumor rejection.

The immunosuppressive environment of the TME causes many challenges in treating tumors. Many mediators, such as extracellular adenosine and prostaglandins, are produced by tumor cells or other cells in the TME and bind to and inhibit the activation of T cells and NK cells. However, blockade of these mediators in combination with CDN/H9-MSA did not boost tumor responses in our MHC I-deficient tumor models. These are only a few of the possible factors in the TME that could be targeted to improve tumor responses. One reason that blocking these mediators may not have improved antitumor effects in combination with CDN/H9-MSA combination therapy is that adenosine or prostaglandins were not produced in sufficiently high amounts by the tumors tested to have appreciable inhibitory effects on the immune cells infiltrating the tumors. Another possibility is that the CDN/H9-MSA therapy acts not only to activate immune cells, but also acts to counter the inhibitory effects of these mediators. Future efforts along these lines should focus on models where it is known that especially high amounts of these mediators are produced.

Along with such factors, many inhibitory receptors/ligands are upregulated in the TME and prevent immune responses. Using checkpoint blockade to reverse this negative interaction has proven to be effective in treating many tumors. These therapies are typically aimed towards amplifying T cell antitumor responses. However, these responses will have limited effects in tumors that lost MHC I or have a low mutational burden. Nevertheless, recent studies indicate that these checkpoint receptors can amplify NK cell responses as well in some tumor models. By examining NK cells in tumors after the treatment with CDN/H9-MSA, we identified several checkpoint receptors that were upregulated on NK cells and are therefore candidates to target in combination therapy regimens.

Unfortunately, in the MHC I-deficient tumor models studied, the addition of these checkpoint blockades did not significantly augment NK cell antitumor responses. One possible explanation is that CDN/H9-MSA therapy has already reversed the suppressive effects of checkpoint receptors leading to strong activation of NK cells without the need to block such interactions. Another possibility to consider is that after CDN/H9-MSA therapy, NK cells impart antitumor effects against MHC I-deficient tumors without a requirement for cell mediated contact and stimulation, such that checkpoint blockade is less relevant. A third possibility is that other checkpoint receptors, such as Tim3 or Lag3, play a bigger role in imparting suppressive effects upon NK cells and other immune cells infiltrating the TME. With better understanding of the TME emerging, new targets, including mediators and checkpoint receptors will likely emerge, and could show promise for efforts to amplify NK cell antitumor responses in combination with CDN/H9-MSA therapy.

CDNs and H9-MSA also synergized in the MCA sarcoma model, leading to highly delayed tumor growth and extended survival. Both NK cells and T cells contributed to the therapeutic effect (Chapter 4), providing a demonstration that this therapy combination can mobilize both types of responses in the same tumor model. The addition of checkpoint therapy to the CDN/H9-MSA therapy regimen resulted in tumor regressions and long-term tumor free survival in approximately 44% of the treated animals. These findings represent a dramatic example of long-term immunotherapy remissions in an autochthonous sarcoma model in mice, which is an especially substantive outcome considering that immunotherapy has given generally poor outcomes in treating human sarcomas (Birdi et al., 2021). Given that the schedule of treatments had an impact on toxicity of the therapy, any consideration of using such a regimen in human patients would require careful tests of different schedules of the individual therapeutics.

In conclusion, our results show that CDN therapy combined with the IL-2 superkine, H9-MSA, effectively enhanced the rejection of MHC I-deficient and MHC I+ tumors. The CDN/H9-MSA treatments proved to be remarkably effective against difficult-to-treat tumors, mobilizing various effector cells depending on tumor cell type. However, with larger transplanted tumors or in the case of primary MCA-induced sarcoma, the CDN/H9-MSA therapy failed to yield many longterm survivors. The addition of numerous additional test therapies to the CDN/H9-MSA combination did not significantly enhance tumor rejection compared to the CDN/H9-MSA combination by itself. The exception was the finding that the addition to the regiment of checkpoint blockade, consisting of anti-PD-1 and anti-TIGIT together, resulted in greatly improved tumor rejection and 44% longterm survivors. These results provide compelling support for testing combinations of innate immune system agonists, IL-2 family superkines and additional immunomodulatory agents as potential next-generation immunotherapies for tumors that are resistant to currently approved immunotherapy regimens.

References

Alexandrov, L.B., S. Nik-Zainal, D.C. Wedge, S.A. Aparicio, S. Behjati, A.V. Biankin, G.R. Bignell, N. Bolli, A. Borg, A.L. Borresen-Dale, S. Boyault, B. Burkhardt, A.P. Butler, C. Caldas, H.R. Davies, C. Desmedt, R. Eils, J.E. Eyfjord, J.A. Foekens, M. Greaves, F. Hosoda, B. Hutter, T. Ilicic, S. Imbeaud, M. Imielinski, N. Jager, D.T. Jones, D. Jones, S. Knappskog, M. Kool, S.R. Lakhani, C. Lopez-Otin, S. Martin, N.C. Munshi, H. Nakamura, P.A. Northcott, M. Pajic, E. Papaemmanuil, A. Paradiso, J.V. Pearson, X.S. Puente, K. Raine, M. Ramakrishna, A.L. Richardson, J. Richter, P. Rosenstiel, M. Schlesner, T.N. Schumacher, P.N. Span, J.W. Teague, Y. Totoki, A.N. Tutt, R. Valdes-Mas, M.M. van Buuren, L. van 't Veer, A. Vincent-Salomon, N. Waddell, L.R. Yates, I. Australian Pancreatic Cancer Genome, I.B.C. Consortium, I.M.-S. Consortium, I. PedBrain, J. Zucman-Rossi, P.A. Futreal, U. McDermott, P. Lichter, M. Meyerson, S.M. Grimmond, R. Siebert, E. Campo, T. Shibata, S.M. Pfister, P.J. Campbell, and M.R. Stratton. 2013. Signatures of mutational processes in human cancer. *Nature* 500:415-421.

Ardolino, M., C.S. Azimi, A. Iannello, T.N. Trevino, L. Horan, L. Zhang, W. Deng, A.M. Ring, S. Fischer, K.C. Garcia, and D.H. Raulet. 2014. Cytokine therapy reverses NK cell anergy in MHC-deficient tumors. *J Clin Invest* 124:4781-4794.

Ardolino, M., and D.H. Raulet. 2016. Cytokine therapy restores antitumor responses of NK cells rendered anergic in MHC I-deficient tumors. *Oncoimmunology* 5:e1002725.

Barrow, A.D., M.A. Edeling, V. Trifonov, J. Luo, P. Goyal, B. Bohl, J.K. Bando, A.H. Kim, J. Walker, M. Andahazy, M. Bugatti, L. Melocchi, W. Vermi, D.H. Fremont, S. Cox, M. Cella, C. Schmedt, and M. Colonna. 2017. Natural Killer Cells Control Tumor Growth by Sensing a Growth Factor. *Cell*

Barrow, A.D., C.J. Martin, and M. Colonna. 2019. The Natural Cytotoxicity Receptors in Health and Disease. *Frontiers in immunology* 10:909.

Barry, K.C., J. Hsu, M.L. Broz, F.J. Cueto, M. Binnewies, A.J. Combes, A.E. Nelson, K. Loo, R. Kumar, M.D. Rosenblum, M.D. Alvarado, D.M. Wolf, D. Bogunovic, N. Bhardwaj, A.I. Daud, P.K. Ha, W.R. Ryan, J.L. Pollack, B. Samad, S. Asthana, V. Chan, and M.F. Krummel. 2018. A natural killer-dendritic cell axis defines checkpoint therapy-responsive tumor microenvironments. *Nat Med* 24:1178-1191.

Bauer, S., V. Groh, J. Wu, A. Steinle, J.H. Phillips, L.L. Lanier, and T. Spies. 1999. Activation of NK cells and T cells by NKG2D, a receptor for stress-inducible MICA. *Science* 285:727-729.

Beldi-Ferchiou, A., M. Lambert, S. Dogniaux, F. Vely, E. Vivier, D. Olive, S. Dupuy, F. Levasseur, D. Zucman, C. Lebbe, D. Sene, C. Hivroz, and S. Caillat-Zucman. 2016. PD-1 mediates functional exhaustion of activated NK cells in patients with Kaposi sarcoma. *Oncotarget* 7:72961-72977.

Benson, D.M., Jr., C.E. Bakan, A. Mishra, C.C. Hofmeister, Y. Efebera, B. Becknell, R.A. Baiocchi, J. Zhang, J. Yu, M.K. Smith, C.N. Greenfield, P. Porcu, S.M. Devine, R. Rotem-Yehudar, G. Lozanski, J.C. Byrd, and M.A. Caligiuri. 2010. The PD-1/PD-L1 axis modulates the natural killer cell versus multiple myeloma effect: a therapeutic target for CT-011, a novel monoclonal anti-PD-1 antibody. *Blood* 116:2286-2294.

Bentebibel, S.E., M.E. Hurwitz, C. Bernatchez, C. Haymaker, C.W. Hudgens, H.M. Kluger, M.T. Tetzlaff, M.A. Tagliaferri, J. Zalevsky, U. Hoch, C. Fanton, S. Aung, P. Hwu, B.D. Curti, N.M. Tannir, M. Sznol, and A. Diab. 2019. A First-in-Human Study and Biomarker Analysis of NKTR-214, a Novel IL2Rbetagamma-Biased Cytokine, in Patients with Advanced or Metastatic Solid Tumors. *Cancer discovery* 9:711-721.

Beura, L.K., S.E. Hamilton, K. Bi, J.M. Schenkel, O.A. Odumade, K.A. Casey, E.A. Thompson, K.A. Fraser, P.C. Rosato, A. Filali-Mouhim, R.P. Sekaly, M.K. Jenkins, V. Vezys, W.N. Haining, S.C. Jameson, and D. Masopust. 2016. Normalizing the environment recapitulates adult human immune traits in laboratory mice. *Nature* 532:512-516.

Bhatnagar, N., F. Ahmad, H.S. Hong, J. Eberhard, I.N. Lu, M. Ballmaier, R.E. Schmidt, R. Jacobs, and D. Meyer-Olson. 2014. FcgammaRIII (CD16)-mediated ADCC by NK cells is regulated by monocytes and FcgammaRII (CD32). *Eur J Immunol* 44:3368-3379.

Bi, J., and Z. Tian. 2017. NK Cell Exhaustion. *Frontiers in immunology* 8:760.

Bi, J., X. Zheng, Y. Chen, H. Wei, R. Sun, and Z. Tian. 2014. TIGIT safeguards liver regeneration through regulating natural killer cell-hepatocyte crosstalk. *Hepatology* 60:1389-1398.

Binnewies, M., E.W. Roberts, K. Kersten, V. Chan, D.F. Fearon, M. Merad, L.M. Coussens, D.I. Gabrilovich, S. Ostrand-Rosenberg, C.C. Hedrick, R.H. Vonderheide, M.J. Pittet, R.K. Jain, W. Zou, T.K. Howcroft, E.C. Woodhouse, R.A. Weinberg, and M.F. Krummel. 2018. Understanding the tumor immune microenvironment (TIME) for effective therapy. *Nat Med* 24:541-550.

Birdi, H.K., A. Jirovec, S. Cortés-Kaplan, J. Werier, C. Nessim, J.-S. Diallo, and M. Ardolino. 2021. Immunotherapy for sarcomas: new frontiers and unveiled opportunities. *Journal for ImmunoTherapy of Cancer* 9:e001580.

BMS, and Nektar. 2022. Bristol Myers Squibb and Nektar Announce Update on Phase 3 PIVOT IO-001 Trial Evaluating Bempegaldesleukin (BEMPEG) in Combination with Opdivo (nivolumab) in Previously Untreated Unresectable or Metastatic Melanoma. *News release*

Boehm, U., T. Klamp, M. Groot, and J.C. Howard. 1997. Cellular responses to interferon-gamma. *Annu Rev Immunol* 15:749-795.

Bonavita, E., C.P. Bromley, G. Jonsson, V.S. Pelly, S. Sahoo, K. Walwyn-Brown, S. Mensurado, A. Moeini, E. Flanagan, C.R. Bell, S.C. Chiang, C.P. Chikkanna-Gowda, N. Rogers, B. Silva-Santos, S. Jaillon, A. Mantovani, C. Reis e Sousa, N. Guerra, D.M. Davis, and S. Zelenay. 2020. Antagonistic Inflammatory Phenotypes Dictate Tumor Fate and Response to Immune Checkpoint Blockade. *Immunity* 53:1215-1229 e1218.

Bottcher, J.P., E. Bonavita, P. Chakravarty, H. Blees, M. Cabeza-Cabrerizo, S. Sammicheli, N.C. Rogers, E. Sahai, S. Zelenay, and E.S.C. Reis. 2018. NK Cells Stimulate Recruitment of cDC1 into the Tumor Microenvironment Promoting Cancer Immune Control. *Cell* 172:1022-1037 e1014.

Bruno, A., L. Mortara, D. Baci, D.M. Noonan, and A. Albini. 2019. Myeloid Derived Suppressor Cells Interactions With Natural Killer Cells and Pro-angiogenic Activities: Roles in Tumor Progression. *Frontiers in immunology* 10:771.

Carlyle, J.R., A. Mesci, J.H. Fine, P. Chen, S. Belanger, L.H. Tai, and A.P. Makrigiannis. 2008. Evolution of the Ly49 and Nkrp1 recognition systems. *Semin Immunol* 20:321-330.

Carozza, J.A., V. Böhnert, K.C. Nguyen, G. Skariah, K.E. Shaw, J.A. Brown, M. Rafat, R. von Eyben, E.E. Graves, J.S. Glenn, M. Smith, and L. Li. 2020. Extracellular cGAMP is a cancer-cell-produced immunotransmitter involved in radiation-induced anticancer immunity. *Nature Cancer* 1:184-196.

Carson, W.E., J.E. Dierksheide, S. Jabbour, M. Anghelina, P. Bouchard, G. Ku, H. Yu, H. Baumann, M.H. Shah, M.A. Cooper, J. Durbin, and M.A. Caligiuri. 2000. Coadministration of interleukin-18 and interleukin-12 induces a fatal inflammatory

response in mice: critical role of natural killer cell interferon-gamma production and STAT-mediated signal transduction. *Blood* 96:1465-1473.

Castriconi, R., C. Cantoni, M. Della Chiesa, M. Vitale, E. Marcenaro, R. Conte, R. Biassoni, C. Bottino, L. Moretta, and A. Moretta. 2003. Transforming growth factor beta 1 inhibits expression of NKp30 and NKG2D receptors: consequences for the NK-mediated killing of dendritic cells. *Proc Natl Acad Sci U S A* 100:4120-4125.

Cerwenka, A., J.L. Baron, and L.L. Lanier. 2001. Ectopic expression of retinoic acid early inducible-1 gene (RAE-1) permits natural killer cell-mediated rejection of a MHC class I-bearing tumor in vivo. *Proc Natl Acad Sci U S A* 98:11521-11526.

Chambers, A.M., J. Wang, K.B. Lupo, H. Yu, N.M. Atallah Lanman, and S. Matosevic. 2018. Adenosinergic Signaling Alters Natural Killer Cell Functional Responses. *Frontiers in immunology* 9:

Chan, C.J., L. Martinet, S. Gilfillan, F. Souza-Fonseca-Guimaraes, M.T. Chow, L. Town, D.S. Ritchie, M. Colonna, D.M. Andrews, and M.J. Smyth. 2014. The receptors CD96 and CD226 oppose each other in the regulation of natural killer cell functions. *Nat Immunol* 15:431-438.

Charych, D.H., U. Hoch, J.L. Langowski, S.R. Lee, M.K. Addepalli, P.B. Kirk, D. Sheng, X. Liu, P.W. Sims, L.A. VanderVeen, C.F. Ali, T.K. Chang, M. Konakova, R.L. Pena, R.S. Kanhere, Y.M. Kirksey, C. Ji, Y. Wang, J. Huang, T.D. Sweeney, S.S. Kantak, and S.K. Doberstein. 2016. NKTR-214, an Engineered Cytokine with Biased IL2 Receptor Binding, Increased Tumor Exposure, and Marked Efficacy in Mouse Tumor Models. *Clinical cancer research : an official journal of the American Association for Cancer Research* 22:680-690.

Chin, E.N., C. Yu, V.F. Vartabedian, Y. Jia, M. Kumar, A.M. Gamo, W. Vernier, S.H. Ali, M. Kissai, D.C. Lazar, N. Nguyen, L.E. Pereira, B. Benish, A.K. Woods, S.B. Joseph, A. Chu, K.A. Johnson, P.N. Sander, F. Martinez-Pena, E.N. Hampton, T.S. Young, D.W. Wolan, A.K. Chatterjee, P.G. Schultz, H.M. Petrassi, J.R. Teijaro, and L.L. Lairson. 2020. Antitumor activity of a systemic STING-activating non-nucleotide cGAMP mimetic. *Science* 369:993-999.

Conant, E.F., K.R. Fox, and W.T. Miller. 1989. Pulmonary edema as a complication of interleukin-2 therapy. *AJR Am J Roentgenol* 152:749-752.

Concha-Benavente, F., B. Kansy, J. Moskovitz, J. Moy, U. Chandran, and R.L. Ferris. 2018. PD-L1 Mediates Dysfunction in Activated PD-1(+) NK Cells in Head and Neck Cancer Patients. *Cancer Immunol Res* 6:1548-1560.

Cooper, M.A., J.M. Elliott, P.A. Keyel, L. Yang, J.A. Carrero, and W.M. Yokoyama. 2009. Cytokine-induced memory-like natural killer cells. *Proc Natl Acad Sci U S A*

Cordova, A.F., C. Ritchie, V. Bohnert, and L. Li. 2021. Human SLC46A2 Is the Dominant cGAMP Importer in Extracellular cGAMP-Sensing Macrophages and Monocytes. *ACS Cent Sci* 7:1073-1088.

Corrales, L., L.H. Glickman, S.M. McWhirter, D.B. Kanne, K.E. Sivick, G.E. Katibah, S.R. Woo, E. Lemmens, T. Banda, J.J. Leong, K. Metchette, T.W. Dubensky, Jr., and T.F. Gajewski. 2015. Direct Activation of STING in the Tumor Microenvironment Leads to Potent and Systemic Tumor Regression and Immunity. *Cell Rep* 11:1018-1030.

Coudert, J.D., L. Scarpellino, F. Gros, E. Vivier, and W. Held. 2008. Sustained NKG2D engagement induces cross-tolerance of multiple distinct NK cell activation pathways. *Blood* 111:3571-3578.

Coughlin, C.M., K.E. Salhany, M. Wysocka, E. Aruga, H. Kurzawa, A.E. Chang, C.A. Hunter, J.C. Fox, G. Trinchieri, and W.M. Lee. 1998. Interleukin-12 and interleukin-18 synergistically induce murine tumor regression which involves inhibition of angiogenesis. *J Clin Invest* 101:1441-1452.

Cozar, B., M. Greppi, S. Carpentier, E. Narni-Mancinelli, L. Chiossone, and E. Vivier. 2021. Tumor-Infiltrating Natural Killer Cells. *Cancer discovery* 11:34-44.

Cursons, J., F. Souza-Fonseca-Guimaraes, M. Foroutan, A. Anderson, F. Hollande, S. Hediyeh-Zadeh, A. Behren, N.D. Huntington, and M.J. Davis. 2019. A Gene Signature Predicting Natural Killer Cell Infiltration and Improved Survival in Melanoma Patients. *Cancer Immunol Res* 7:1162-1174.

Deng, W., B.G. Gowen, L. Zhang, L. Wang, S. Lau, A. Iannello, J. Xu, T.L. Rovis, N. Xiong, and D.H. Raulet. 2015. Antitumor immunity. A shed NKG2D ligand that promotes natural killer cell activation and tumor rejection. *Science* 348:136-139.

Deuse, T., X. Hu, S. Agbor-Enoh, M.K. Jang, M. Alawi, C. Saygi, A. Gravina, G. Tediashvili, V.Q. Nguyen, Y. Liu, H. Valantine, L.L. Lanier, and S. Schrepfer. 2021. The SIRPalpha-CD47 immune checkpoint in NK cells. *J Exp Med* 218:

Devaiah, B.N., and D.S. Singer. 2013. CIITA and Its Dual Roles in MHC Gene Transcription. *Frontiers in immunology* 4:476.

Diefenbach, A., E.R. Jensen, A.M. Jamieson, and D.H. Raulet. 2001. Rae1 and H60 ligands of the NKG2D receptor stimulate tumour immunity. *Nature* 413:165-171.

Diner, E.J., D.L. Burdette, S.C. Wilson, K.M. Monroe, C.A. Kellenberger, M. Hyodo, Y. Hayakawa, M.C. Hammond, and R.E. Vance. 2013. The innate immune DNA sensor cGAS produces a noncanonical cyclic dinucleotide that activates human STING. *Cell Rep* 3:1355-1361.

Francica, B.J., A. Ghasemzadeh, A.L. Desbien, D. Theodros, K.E. Sivick, G.L. Reiner, L. Hix Glickman, A.E. Marciscano, A.B. Sharabi, M.L. Leong, S.M. McWhirter, T.W. Dubensky, Jr., D.M. Pardoll, and C.G. Drake. 2018. TNFalpha and Radioresistant Stromal Cells Are Essential for Therapeutic Efficacy of Cyclic Dinucleotide STING Agonists in Nonimmunogenic Tumors. *Cancer Immunol Res* 6:422-433.

Gao, D., J. Wu, Y.T. Wu, F. Du, C. Aroh, N. Yan, L. Sun, and Z.J. Chen. 2013. Cyclic GMP-AMP synthase is an innate immune sensor of HIV and other retroviruses. *Science* 341:903-906.

Gao, Y., F. Souza-Fonseca-Guimaraes, T. Bald, S.S. Ng, A. Young, S.F. Ngiow, J. Rautela, J. Straube, N. Waddell, S.J. Blake, J. Yan, L. Bartholin, J.S. Lee, E. Vivier, K. Takeda, M. Messaoudene, L. Zitvogel, M.W.L. Teng, G.T. Belz, C.R. Engwerda, N.D. Huntington, K. Nakamura, M. Holzel, and M.J. Smyth. 2017. Tumor immunoevasion by the conversion of effector NK cells into type 1 innate lymphoid cells. *Nat Immunol* 18:1004-1015.

Garrido, F., and I. Algarra. 2001. MHC antigens and tumor escape from immune surveillance. *Adv Cancer Res* 83:117-158.

Garrido, F., N. Aptsiauri, E.M. Doorduijn, A.M. Garcia Lora, and T. van Hall. 2016. The urgent need to recover MHC class I in cancers for effective immunotherapy. *Current opinion in immunology* 39:44-51.

Gasser, S., S. Orsulic, E.J. Brown, and D.H. Raulet. 2005. The DNA damage pathway regulates innate immune system ligands of the NKG2D receptor. *Nature* 436:1186-1190.

Ghiringhelli, F., C. Menard, F. Martin, and L. Zitvogel. 2006. The role of regulatory T cells in the control of natural killer cells: relevance during tumor progression. *Immunol Rev* 214:229-238.

Gopalakrishnan, V., C.N. Spencer, L. Nezi, A. Reuben, M.C. Andrews, T.V. Karpinets, P.A. Prieto, D. Vicente, K. Hoffman, S.C. Wei, A.P. Cogdill, L. Zhao, C.W. Hudgens, D.S. Hutchinson, T. Manzo, M. Petaccia de Macedo, T. Cotechini, T. Kumar, W.S. Chen, S.M. Reddy, R. Szczepaniak Sloane, J. Galloway-Pena, H. Jiang, P.L. Chen, E.J. Shpall, K. Rezvani, A.M. Alousi, R.F. Chemaly, S. Shelburne, L.M. Vence, P.C. Okhuysen, V.B. Jensen, A.G. Swennes, F. McAllister, E. Marcelo Riquelme Sanchez, Y. Zhang, E. Le Chatelier, L. Zitvogel, N. Pons, J.L. Austin-Breneman, L.E. Haydu, E.M. Burton, J.M. Gardner, E. Sirmans, J. Hu, A.J. Lazar, T. Tsujikawa, A. Diab, H. Tawbi, I.C. Glitza, W.J. Hwu, S.P. Patel, S.E. Woodman, R.N. Amaria, M.A. Davies, J.E. Gershenwald, P. Hwu, J.E. Lee, J. Zhang, L.M. Coussens, Z.A. Cooper, P.A. Futreal, C.R. Daniel, N.J. Ajami, J.F. Petrosino, M.T. Tetzlaff, P. Sharma, J.P. Allison, R.R. Jenq, and J.A. Wargo. 2018. Gut microbiome modulates response to anti-PD-1 immunotherapy in melanoma patients. *Science* 359:97-103.

Gowen, B.G., B. Chim, C.D. Marceau, T.T. Greene, P. Burr, J.R. Gonzalez, C.R. Hesser, P.A. Dietzen, T. Russell, A. Iannello, L. Coscoy, C.L. Sentman, J.E. Carette, S.A. Muljo, and D.H. Raulet. 2015. A forward genetic screen reveals novel independent regulators of ULBP1, an activating ligand for natural killer cells. *Elife* 4:e08474.

Guerra, N., Y.X. Tan, N.T. Joncker, A. Choy, F. Gallardo, N. Xiong, S. Knoblaugh, D. Cado, N.R. Greenberg, and D.H. Raulet. 2008. NKG2D-deficient mice are defective in tumor surveillance in models of spontaneous malignancy. *Immunity* 28:571-580.

Haabeth, O.A., A.A. Tveita, M. Fauskanger, F. Schjesvold, K.B. Lorvik, P.O. Hofgaard, H. Omholt, L.A. Munthe, Z. Dembic, A. Corthay, and B. Bogen. 2014. How Do CD4(+) T Cells Detect and Eliminate Tumor Cells That Either Lack or Express MHC Class II Molecules? *Frontiers in immunology* 5:174.

Hanahan, D., and R.A. Weinberg. 2000. The hallmarks of cancer. *Cell* 100:57-70.

Hanahan, D., and R.A. Weinberg. 2011. Hallmarks of cancer: the next generation. *Cell* 144:646-674.

Harding, S.M., J.L. Benci, J. Irianto, D.E. Discher, A.J. Minn, and R.A. Greenberg. 2017. Mitotic progression following DNA damage enables pattern recognition within micronuclei. *Nature* 548:466-470.

Harrington, K.J., J. Brody, M. Ingham, J. Strauss, S. Cemerski, M. Wang, A. Tse, A. Khilnani, A. Marabelle, and T. Golan. 2018. Preliminary results of the first-in-human (FIH) study of MK-1454, an agonist of stimulator of interferon genes (STING), as monotherapy or in combination with pembrolizumab (pembro) in patients with advanced solid tumors or lymphomas. *Ann. Oncol.* VIII712:

Hellmann, M.D., L. Paz-Ares, R. Bernabe Caro, B. Zurawski, S.-W. Kim, E. Carcereny Costa, K. Park, A. Alexandru, L. Lupinacci, E. de la Mora Jimenez, H. Sakai, I. Albert, A. Vergnenegre, S. Peters, K. Syrigos, F. Barlesi, M. Reck, H. Borghaei, J.R. Brahmer, K.J. O'Byrne, W.J. Geese, P. Bhagavatheeswaran, S.K. Rabindran, R.S. Kasinathan, F.E. Nathan, and S.S. Ramalingam. 2019. Nivolumab plus Ipilimumab in Advanced Non–Small-Cell Lung Cancer. *New England Journal of Medicine* 381:2020-2031.

Ho, S.S., W.Y. Zhang, N.Y. Tan, M. Khatoo, M.A. Suter, S. Tripathi, F.S. Cheung, W.K. Lim, P.H. Tan, J. Ngeow, and S. Gasser. 2016. The DNA Structure-Specific Endonuclease

MUS81 Mediates DNA Sensor STING-Dependent Host Rejection of Prostate Cancer Cells. *Immunity* 44:1177-1189.

Hosomi, S., J. Grootjans, M. Tschurtschenthaler, N. Krupka, J.D. Matute, M.B. Flak, E. Martinez-Naves, M. Gomez Del Moral, J.N. Glickman, M. Ohira, L.L. Lanier, A. Kaser, and R. Blumberg. 2017. Intestinal epithelial cell endoplasmic reticulum stress promotes MULT1 up-regulation and NKG2D-mediated inflammation. *J Exp Med*

Hsu, J., J.J. Hodgins, M. Marathe, C.J. Nicolai, M.C. Bourgeois-Daigneault, T.N. Trevino, C.S. Azimi, A.K. Scheer, H.E. Randolph, T.W. Thompson, L. Zhang, A. Iannello, N. Mathur, K.E. Jardine, G.A. Kirn, J.C. Bell, M.W. McBurney, D.H. Raulet, and M. Ardolino. 2018. Contribution of NK cells to immunotherapy mediated by PD-1/PD-L1 blockade. *J Clin Invest* 128:4654-4668.

Ishikawa, H., and G.N. Barber. 2008. STING is an endoplasmic reticulum adaptor that facilitates innate immune signalling. *Nature* 455:674-678.

Jamieson, A.M., A. Diefenbach, C.W. McMahon, N. Xiong, J.R. Carlyle, and D.H. Raulet. 2002. The role of the NKG2D immunoreceptor in immune cell activation and natural killing. *Immunity* 17:19-29.

Johansson, S., M. Johansson, E. Rosmaraki, G. Vahlne, R. Mehr, M. Salmon-Divon, F. Lemonnier, K. Karre, and P. Hoglund. 2005. Natural killer cell education in mice with single or multiple major histocompatibility complex class I molecules. *J Exp Med* 201:1145-1155.

Johnston, R.J., L. Comps-Agrar, J. Hackney, X. Yu, M. Huseni, Y. Yang, S. Park, V. Javinal, H. Chiu, B. Irving, D.L. Eaton, and J.L. Grogan. 2014. The immunoreceptor TIGIT regulates antitumor and antiviral CD8(+) T cell effector function. *Cancer Cell* 26:923-937.

Jung, H., B. Hsiung, K. Pestal, E. Procyk, and D.H. Raulet. 2012. RAE-1 ligands for the NKG2D receptor are regulated by E2F transcription factors, which control cell cycle entry. *J Exp Med* 209:2409-2422.

Kalbasi, A., and A. Ribas. 2020. Tumour-intrinsic resistance to immune checkpoint blockade. *Nat Rev Immunol* 20:25-39.

Karlhofer, F.M., R.K. Ribaudo, and W.M. Yokoyama. 1992. MHC class I alloantigen specificity of Ly-49+ IL-2-activated natural killer cells. *Nature* 358:66-70.

Karre, K., H.G. Ljunggren, G. Piontek, and R. Kiessling. 1986. Selective rejection of H-2-deficient lymphoma variants suggests alternative immune defence strategy. *Nature* 319:675-678.

Kearney, C.J., S.J. Vervoort, S.J. Hogg, K.M. Ramsbottom, A.J. Freeman, N. Lalaoui, L. Pijpers, J. Michie, K.K. Brown, D.A. Knight, V. Sutton, P.A. Beavis, I. Voskoboinik, P.K. Darcy, J. Silke, J.A. Trapani, R.W. Johnstone, and J. Oliaro. 2018. Tumor immune evasion arises through loss of TNF sensitivity. *Science immunology* 3:

Kerdiles, Y., S. Ugolini, and E. Vivier. 2013. T cell regulation of natural killer cells. *J Exp Med* 210:1065-1068.

Kim, R., M. Emi, and K. Tanabe. 2007. Cancer immunoediting from immune surveillance to immune escape. *Immunology* 121:1-14.

Konno, H., S. Yamauchi, A. Berglund, R.M. Putney, J.J. Mule, and G.N. Barber. 2018. Suppression of STING signaling through epigenetic silencing and missense mutation impedes DNA damage mediated cytokine production. *Oncogene* 37:2037-2051.

Labani-Motlagh, A., M. Ashja-Mahdavi, and A. Loskog. 2020. The Tumor Microenvironment: A Milieu Hindering and Obstructing Antitumor Immune Responses. *Frontiers in immunology* 11:

Lahey, L.J., R.E. Mardjuki, X. Wen, G.T. Hess, C. Ritchie, J.A. Carozza, V. Bohnert, M. Maduke, M.C. Bassik, and L. Li. 2020. LRRC8A:C/E Heteromeric Channels Are Ubiquitous Transporters of cGAMP. *Mol Cell* 80:578-591 e575.

Lam, A.R., N. Le Bert, S.S. Ho, Y.J. Shen, M.L. Tang, G.M. Xiong, J.L. Croxford, C.X. Koo, K.J. Ishii, S. Akira, D.H. Raulet, and S. Gasser. 2014. RAE1 ligands for the NKG2D receptor are regulated by STING-dependent DNA sensor pathways in lymphoma. *Cancer Res* 74:2193-2203.

Lanier, L.L. 2005. NK cell recognition. *Annu Rev Immunol* 23:225-274.

Leach, D.R., M.F. Krummel, and J.P. Allison. 1996. Enhancement of antitumor immunity by CTLA-4 blockade. *Science* 271:1734-1736.

Lechner, M.G., S.S. Karimi, K. Barry-Holson, T.E. Angell, K.A. Murphy, C.H. Church, J.R. Ohlfest, P. Hu, and A.L. Epstein. 2013. Immunogenicity of murine solid tumor models as a defining feature of in vivo behavior and response to immunotherapy. *J Immunother* 36:477-489.

Levin, A.M., D.L. Bates, A.M. Ring, C. Krieg, J.T. Lin, L. Su, I. Moraga, M.E. Raeber, G.R. Bowman, P. Novick, V.S. Pande, C.G. Fathman, O. Boyman, and K.C. Garcia. 2012. Exploiting a natural conformational switch to engineer an interleukin-2 'superkine'. *Nature* 484:529-533.

Li, J., M.A. Duran, N. Dhanota, W.K. Chatila, S.E. Bettigole, J. Kwon, R.K. Sriram, M.P. Humphries, M. Salto-Tellez, J.A. James, M.G. Hanna, J.C. Melms, S. Vallabhaneni, K. Litchfield, I. Usaite, D. Biswas, R. Bareja, H.W. Li, M.L. Martin, P. Dorsaint, J.A. Cavallo, P. Li, C. Pauli, L. Gottesdiener, B.J. DiPardo, T.J. Hollmann, T. Merghoub, H.Y. Wen, J.S. Reis-Filho, N. Riaz, S.M. Su, A. Kalbasi, N. Vasan, S.N. Powell, J.D. Wolchok, O. Elemento, C. Swanton, A.N. Shoushtari, E.E. Parkes, B. Izar, and S.F. Bakhoum. 2021. Metastasis and Immune Evasion from Extracellular cGAMP Hydrolysis. *Cancer discovery* 11:1212-1227.

Liao, N., M. Bix, M. Zijlstra, R. Jaenisch, and D. Raulet. 1991. MHC class I deficiency: susceptibility to natural killer (NK) cells and impaired NK activity. *Science* 253:199-202.

Liu, Y., Y. Cheng, Y. Xu, Z. Wang, X. Du, C. Li, J. Peng, L. Gao, X. Liang, and C. Ma. 2017. Increased expression of programmed cell death protein 1 on NK cells inhibits NK-cell-mediated anti-tumor function and indicates poor prognosis in digestive cancers. *Oncogene* 36:6143-6153.

Ljunggren, H.G., and K. Karre. 1990. In search of the 'missing self': MHC molecules and NK cell recognition. *Immunol. Today* 11:237-244.

Londei, M., J.R. Lamb, G.F. Bottazzo, and M. Feldmann. 1984. Epithelial cells expressing aberrant MHC class II determinants can present antigen to cloned human T cells. *Nature* 312:639-641.

Lucas, M., W. Schachterle, K. Oberle, P. Aichele, and A. Diefenbach. 2007. Dendritic cells prime natural killer cells by trans-presenting interleukin 15. *Immunity* 26:503-517.

Luteijn, R.D., S.A. Zaver, B.G. Gowen, S.K. Wyman, N.E. Garelis, L. Onia, S.M. McWhirter, G.E. Katibah, J.E. Corn, J.J. Woodward, and D.H. Raulet. 2019. SLC19A1 transports immunoreactive cyclic dinucleotides. *Nature* 573:434-438.

Madera, S., M. Rapp, M.A. Firth, J.N. Beilke, L.L. Lanier, and J.C. Sun. 2016. Type I IFN promotes NK cell expansion during viral infection by protecting NK cells against fratricide. *J Exp Med* 213:225-233.

Maleno, I., N. Aptsiauri, T. Cabrera, A. Gallego, A. Paschen, M.A. Lopez-Nevot, and F. Garrido. 2011. Frequent loss of heterozygosity in the beta2-microglobulin region of chromosome 15 in primary human tumors. *Immunogenetics* 63:65-71.

Marcus, A., B.G. Gowen, T.W. Thompson, A. Iannello, M. Ardolino, W. Deng, L. Wang, N. Shifrin, and D.H. Raulet. 2014. Recognition of tumors by the innate immune system and natural killer cells. *Adv Immunol* 122:91-128.

Marcus, A., A.J. Mao, M. Lensink-Vasan, L. Wang, R.E. Vance, and D.H. Raulet. 2018. Tumor-Derived cGAMP Triggers a STING-Mediated Interferon Response in Non-tumor Cells to Activate the NK Cell Response. *Immunity* 49:754-763 e754.

Martinez, J., X. Huang, and Y. Yang. 2008. Direct action of type I IFN on NK cells is required for their activation in response to vaccinia viral infection in vivo. *J Immunol* 180:1592-1597.

Mattei, F., G. Schiavoni, F. Belardelli, and D.F. Tough. 2001. IL-15 is expressed by dendritic cells in response to type I IFN, double-stranded RNA, or lipopolysaccharide and promotes dendritic cell activation. *J Immunol* 167:1179-1187.

McGranahan, N., R. Rosenthal, C.T. Hiley, A.J. Rowan, T.B.K. Watkins, G.A. Wilson, N.J. Birkbak, S. Veeriah, P. Van Loo, J. Herrero, C. Swanton, and T.R. Consortium. 2017. Allele-Specific HLA Loss and Immune Escape in Lung Cancer Evolution. *Cell* 171:1259-1271 e1211.

McWhirter, S.M., R. Barbalat, K.M. Monroe, M.F. Fontana, M. Hyodo, N.T. Joncker, K.J. Ishii, S. Akira, M. Colonna, Z.J. Chen, K.A. Fitzgerald, Y. Hayakawa, and R.E. Vance. 2009. A host type I interferon response is induced by cytosolic sensing of the bacterial second messenger cyclic-di-GMP. *J Exp Med*

McWhirter, S.M., and C.A. Jefferies. 2020. Nucleic Acid Sensors as Therapeutic Targets for Human Disease. *Immunity* 53:78-97.

Melaiu, O., V. Lucarini, L. Cifaldi, and D. Fruci. 2019. Influence of the Tumor Microenvironment on NK Cell Function in Solid Tumors. *Frontiers in immunology* 10:3038.

Meric-Bernstam, F., S.K. Sandhu, O. Hamid, A. Spreafico, S. Kasper, R. Dummer, T. Shimizu, N. Steeghs, N. Lewis, C.C. Talluto, S. Dolan, A. Bean, R. Brown, D. Trujillo, N. Nair, and J.J. Luke. 2019. Phase Ib study of MIW815 (ADU-S100) in combination with spartalizumab (PDR001) in patients (pts) with advanced/metastatic solid tumors or lymphomas. *Journal of Clinical Oncology* 37:2507.

Michelet, X., L. Dyck, A. Hogan, R.M. Loftus, D. Duquette, K. Wei, S. Beyaz, A. Tavakkoli, C. Foley, R. Donnelly, C. O'Farrelly, M. Raverdeau, A. Vernon, W. Pettee, D. O'Shea, B.S. Nikolajczyk, K.H.G. Mills, M.B. Brenner, D. Finlay, and L. Lynch. 2018. Metabolic reprogramming of natural killer cells in obesity limits antitumor responses. *Nat Immunol* 19:1330-1340.

Moretta, A., and L. Moretta. 1997. HLA class I specific inhibitory receptors. *Current opinion in immunology* 9:694-701.

Motzer, R.J., A. Rakhit, L.H. Schwartz, T. Olencki, T.M. Malone, K. Sandstrom, R. Nadeau, H. Parmar, and R. Bukowski. 1998. Phase I trial of subcutaneous recombinant human

interleukin-12 in patients with advanced renal cell carcinoma. *Clinical cancer research : an official journal of the American Association for Cancer Research* 4:1183-1191.
Moynihan, K.D., C.F. Opel, G.L. Szeto, A. Tzeng, E.F. Zhu, J.M. Engreitz, R.T. Williams, K. Rakhra, M.H. Zhang, A.M. Rothschilds, S. Kumari, R.L. Kelly, B.H. Kwan, W. Abraham, K. Hu, N.K. Mehta, M.J. Kauke, H. Suh, J.R. Cochran, D.A. Lauffenburger, K.D. Wittrup, and D.J. Irvine. 2016. Eradication of large established tumors in mice by combination immunotherapy that engages innate and adaptive immune responses. *Nat Med* 22:1402-1410.
Mullard, A. 2021. Restoring IL-2 to its cancer immunotherapy glory. *Nat Rev Drug Discov* 20:163-165.
Narni-Mancinelli, E., L. Gauthier, M. Baratin, S. Guia, A. Fenis, A.E. Deghmane, B. Rossi, P. Fourquet, B. Escaliere, Y.M. Kerdiles, S. Ugolini, M.K. Taha, and E. Vivier. 2017. Complement factor P is a ligand for the natural killer cell-activating receptor NKp46. *Science immunology* 2:
National Research Council Committee for the Update of the Guide for the, C., and A. Use of Laboratory. 2011. The National Academies Collection: Reports funded by National Institutes of Health. In Guide for the Care and Use of Laboratory Animals. National Academies Press (US)
Nguyen, K.G., M.R. Vrabel, S.M. Mantooth, J.J. Hopkins, E.S. Wagner, T.A. Gabaldon, and D.A. Zaharoff. 2020. Localized Interleukin-12 for Cancer Immunotherapy. *Frontiers in immunology* 11:575597.
Ni, J., M. Miller, A. Stojanovic, N. Garbi, and A. Cerwenka. 2012. Sustained effector function of IL-12/15/18-preactivated NK cells against established tumors. *J Exp Med* 209:2351-2365.
Nice, T.J., L. Coscoy, and D.H. Raulet. 2009. Posttranslational regulation of the NKG2D ligand Mult1 in response to cell stress. *J Exp Med* 206:287-298.
Nicolai, C.J., and D.H. Raulet. 2020. Killer cells add fire to fuel immunotherapy. *Science* 368:943-944.
Nicolai, C.J., N. Wolf, I.C. Chang, G. Kirn, A. Marcus, C.O. Ndubaku, S.M. McWhirter, and D.H. Raulet. 2020. NK cells mediate clearance of CD8(+) T cell-resistant tumors in response to STING agonists. *Science immunology* 5:eaaz2738.
Niehrs, A., W.F. Garcia-Beltran, P.J. Norman, G.M. Watson, A. Holzemer, A. Chapel, L. Richert, A. Pommerening-Roser, C. Korner, M. Ozawa, G. Martrus, J. Rossjohn, J.H. Lee, R. Berry, M. Carrington, and M. Altfeld. 2019. A subset of HLA-DP molecules serve as ligands for the natural cytotoxicity receptor NKp44. *Nat Immunol* 20:1129-1137.
O'Shea, D., and A.E. Hogan. 2019. Dysregulation of Natural Killer Cells in Obesity. *Cancers (Basel)* 11:
Obiedat, A., Y. Charpak-Amikam, J. Tai-Schmiedel, E. Seidel, M. Mahameed, T. Avril, N. Stern-Ginossar, L. Springuel, J. Bolsee, D.E. Gilham, P. Dipta, M. Shmuel, E. Chevet, O. Mandelboim, and B. Tirosh. 2020. The integrated stress response promotes B7H6 expression. *Journal of molecular medicine* 98:135-148.
Ohlen, C., G. Kling, P. Höglund, M. Hansson, G. Scangos, C. Bieberich, G. Jay, and K. Karre. 1989. Prevention of allogeneic bone marrow graft rejection by H-2 transgene in donor mice. *Science* 246:666-668.

Osaki, T., J.M. Peron, Q. Cai, H. Okamura, P.D. Robbins, M. Kurimoto, M.T. Lotze, and H. Tahara. 1998. IFN-gamma-inducing factor/IL-18 administration mediates IFN-gamma- and IL-12-independent antitumor effects. *J Immunol* 160:1742-1749.

Pan, B.S., S.A. Perera, J.A. Piesvaux, J.P. Presland, G.K. Schroeder, J.N. Cumming, B.W. Trotter, M.D. Altman, A.V. Buevich, B. Cash, S. Cemerski, W. Chang, Y. Chen, P.J. Dandliker, G. Feng, A. Haidle, T. Henderson, J. Jewell, I. Kariv, I. Knemeyer, J. Kopinja, B.M. Lacey, J. Laskey, C.A. Lesburg, R. Liang, B.J. Long, M. Lu, Y. Ma, E.C. Minnihan, G. O'Donnell, R. Otte, L. Price, L. Rakhilina, B. Sauvagnat, S. Sharma, S. Tyagarajan, H. Woo, D.F. Wyss, S. Xu, D.J. Bennett, and G.H. Addona. 2020. An orally available non-nucleotide STING agonist with antitumor activity. *Science* 369:

Pardoll, D.M., and S.L. Topalian. 1998. The role of CD4+ T cell responses in antitumor immunity. *Current opinion in immunology* 10:588-594.

Park, C.G., C.A. Hartl, D. Schmid, E.M. Carmona, H.J. Kim, and M.S. Goldberg. 2018. Extended release of perioperative immunotherapy prevents tumor recurrence and eliminates metastases. *Science translational medicine* 10:

Paust, S., C.A. Blish, and R.K. Reeves. 2017. Redefining Memory: Building the Case for Adaptive NK Cells. *J Virol* 91:

Pende, D., M. Falco, M. Vitale, C. Cantoni, C. Vitale, E. Munari, A. Bertaina, F. Moretta, G. Del Zotto, G. Pietra, M.C. Mingari, F. Locatelli, and L. Moretta. 2019. Killer Ig-Like Receptors (KIRs): Their Role in NK Cell Modulation and Developments Leading to Their Clinical Exploitation. *Frontiers in immunology* 10:1179.

Poznanski, S.M., K. Singh, T.M. Ritchie, J.A. Aguiar, I.Y. Fan, A.L. Portillo, E.A. Rojas, F. Vahedi, A. El-Sayes, S. Xing, M. Butcher, Y. Lu, A.C. Doxey, J.D. Schertzer, H.W. Hirte, and A.A. Ashkar. 2021. Metabolic flexibility determines human NK cell functional fate in the tumor microenvironment. *Cell metabolism* 33:1205-1220 e1205.

Quezada, S.A., T.R. Simpson, K.S. Peggs, T. Merghoub, J. Vider, X. Fan, R. Blasberg, H. Yagita, P. Muranski, P.A. Antony, N.P. Restifo, and J.P. Allison. 2010. Tumor-reactive CD4+ T cells develop cytotoxic activity and eradicate large established melanoma after transfer into lymphopenic hosts. *J Exp Med*

Raskov, H., A. Orhan, J.P. Christensen, and I. Gögenur. 2021. Cytotoxic CD8+ T cells in cancer and cancer immunotherapy. *British journal of cancer* 124:359-367.

Raulet, D.H. 2004. Interplay of natural killer cells and their receptors with the adaptive immune response. *Nat Immunol* 5:996-1002.

Raulet, D.H., S. Gasser, B.G. Gowen, W. Deng, and H. Jung. 2013. Regulation of ligands for the NKG2D activating receptor. *Annu Rev Immunol* 31:413-441.

Raulet, D.H., and N. Guerra. 2009. Oncogenic stress sensed by the immune system: role of natural killer cell receptors. *Nat Rev Immunol* 9:568-580.

Raulet, D.H., R.E. Vance, and C.W. McMahon. 2001. Regulation of the natural killer cell receptor repertoire. *Annu Rev Immunol* 19:291-330.

Ribas, A., and J.D. Wolchok. 2018. Cancer immunotherapy using checkpoint blockade. *Science* 359:1350-1355.

Ritchie, C., A.F. Cordova, G.T. Hess, M.C. Bassik, and L. Li. 2019. SLC19A1 Is an Importer of the Immunotransmitter cGAMP. *Mol Cell* 75:372-381 e375.

Robinson, D., K. Shibuya, A. Mui, F. Zonin, E. Murphy, T. Sana, S.B. Hartley, S. Menon, R. Kastelein, F. Bazan, and A. O'Garra. 1997. IGIF does not drive Th1 development but

synergizes with IL-12 for interferon-gamma production and activates IRAK and NFkappaB. *Immunity* 7:571-581.

Roemer, M.G., R.H. Advani, R.A. Redd, G.S. Pinkus, Y. Natkunam, A.H. Ligon, C.F. Connelly, C.J. Pak, C.D. Carey, S.E. Daadi, B. Chapuy, D. de Jong, R.T. Hoppe, D.S. Neuberg, M.A. Shipp, and S.J. Rodig. 2016. Classical Hodgkin Lymphoma with Reduced beta2M/MHC Class I Expression Is Associated with Inferior Outcome Independent of 9p24.1 Status. *Cancer Immunol Res* 4:910-916.

Romee, R., S.E. Schneider, J.W. Leong, J.M. Chase, C.R. Keppel, R.P. Sullivan, M.A. Cooper, and T.A. Fehniger. 2012. Cytokine activation induces human memory-like NK cells. *Blood* 120:4751-4760.

Rosenberg, S.A., M.T. Lotze, L.M. Muul, A.E. Chang, F.P. Avis, S. Leitman, W.M. Linehan, C.N. Robertson, R.E. Lee, J.T. Rubin, and et al. 1987. A progress report on the treatment of 157 patients with advanced cancer using lymphokine-activated killer cells and interleukin-2 or high-dose interleukin-2 alone. *N Engl J Med* 316:889-897.

Rosenberg, S.A., J.J. Mule, P.J. Spiess, C.M. Reichert, and S.L. Schwarz. 1985. Regression of established pulmonary metastases and subcutaneous tumor mediated by the systemic administration of high-dose recombinant interleukin 2. *J Exp Med* 161:1169-1188.

Sade-Feldman, M., Y.J. Jiao, J.H. Chen, M.S. Rooney, M. Barzily-Rokni, J.P. Eliane, S.L. Bjorgaard, M.R. Hammond, H. Vitzthum, S.M. Blackmon, D.T. Frederick, M. Hazar-Rethinam, B.A. Nadres, E.E. Van Seventer, S.A. Shukla, K. Yizhak, J.P. Ray, D. Rosebrock, D. Livitz, V. Adalsteinsson, G. Getz, L.M. Duncan, B. Li, R.B. Corcoran, D.P. Lawrence, A. Stemmer-Rachamimov, G.M. Boland, D.A. Landau, K.T. Flaherty, R.J. Sullivan, and N. Hacohen. 2017. Resistance to checkpoint blockade therapy through inactivation of antigen presentation. *Nat Commun* 8:1136.

Schadt, L., C. Sparano, N.A. Schweiger, K. Silina, V. Cecconi, G. Lucchiari, H. Yagita, E. Guggisberg, S. Saba, Z. Nascakova, W. Barchet, and M. van den Broek. 2019. Cancer-Cell-Intrinsic cGAS Expression Mediates Tumor Immunogenicity. *Cell Rep* 29:1236-1248 e1237.

Scharton, T.M., and P. Scott. 1993. Natural killer cells are a source of interferon gamma that drives differentiation of CD4+ T cell subsets and induces early resistance to Leishmania major in mice. *Journal of Experimental Medicine* 178:567-577.

Schumacher, T.N., and R.D. Schreiber. 2015. Neoantigens in cancer immunotherapy. *Science* 348:69-74.

Seaman, W.E., M. Sleisenger, E. Eriksson, and G.C. Koo. 1987. Depletion of natural killer cells in mice by monoclonal antibody to NK-1.1. Reduction in host defense against malignancy without loss of cellular or humoral immunity. *J Immunol* 138:4539-4544.

Seitz, L., L. Jin, M. Leleti, D. Ashok, J. Jeffrey, A. Rieger, R.G. Tiessen, G. Arold, J.B.L. Tan, J.P. Powers, M.J. Walters, and J. Karakunnel. 2019. Safety, tolerability, and pharmacology of AB928, a novel dual adenosine receptor antagonist, in a randomized, phase 1 study in healthy volunteers. *Invest New Drugs* 37:711-721.

Sharbi-Yunger, A., M. Grees, G. Cafri, D. Bassan, S.B. Eichmüller, E. Tzehoval, J. Utikal, V. Umansky, and L. Eisenbach. 2019. A universal anti-cancer vaccine: Chimeric invariant chain potentiates the inhibition of melanoma progression and the improvement of survival. *International journal of cancer. Journal international du cancer* 144:909-921.

Sharma, P., and J.P. Allison. 2015. Immune checkpoint targeting in cancer therapy: toward combination strategies with curative potential. *Cell* 161:205-214.

Sharma, P., B.A. Siddiqui, S. Anandhan, S.S. Yadav, S.K. Subudhi, J. Gao, S. Goswami, and J.P. Allison. 2021. The Next Decade of Immune Checkpoint Therapy. *Cancer discovery* 11:838-857.

Shifrin, N., D.H. Raulet, and M. Ardolino. 2014. NK cell self tolerance, responsiveness and missing self recognition. *Semin Immunol* 26:138-144.

Silva, D.A., S. Yu, U.Y. Ulge, J.B. Spangler, K.M. Jude, C. Labao-Almeida, L.R. Ali, A. Quijano-Rubio, M. Ruterbusch, I. Leung, T. Biary, S.J. Crowley, E. Marcos, C.D. Walkey, B.D. Weitzner, F. Pardo-Avila, J. Castellanos, L. Carter, L. Stewart, S.R. Riddell, M. Pepper, G.J.L. Bernardes, M. Dougan, K.C. Garcia, and D. Baker. 2019. De novo design of potent and selective mimics of IL-2 and IL-15. *Nature* 565:186-191.

Sivick, K.E., A.L. Desbien, L.H. Glickman, G.L. Reiner, L. Corrales, N.H. Surh, T.E. Hudson, U.T. Vu, B.J. Francica, T. Banda, G.E. Katibah, D.B. Kanne, J.J. Leong, K. Metchette, J.R. Bruml, C.O. Ndubaku, J.M. McKenna, Y. Feng, L. Zheng, S.L. Bender, C.Y. Cho, M.L. Leong, A. van Elsas, T.W. Dubensky, Jr., and S.M. McWhirter. 2018. Magnitude of Therapeutic STING Activation Determines CD8(+) T Cell-Mediated Anti-tumor Immunity. *Cell Rep* 25:3074-3085 e3075.

Smyth, M.J., N.Y. Crowe, and D.I. Godfrey. 2001. NK cells and NKT cells collaborate in host protection from methylcholanthrene-induced fibrosarcoma. *International immunology* 13:459-463.

Smyth, M.J., M. Taniguchi, and S.E.A. Street. 2000. The anti-tumor activity of IL-12: Mechanisms of innate immunity that are model and dose dependent. *J Immunol* 165:2665-2670.

Srivastava, S., N. Salim, and M.J. Robertson. 2010. Interleukin-18: biology and role in the immunotherapy of cancer. *Curr Med Chem* 17:3353-3357.

Stanietsky, N., H. Simic, J. Arapovic, A. Toporik, O. Levy, A. Novik, Z. Levine, M. Beiman, L. Dassa, H. Achdout, N. Stern-Ginossar, P. Tsukerman, S. Jonjic, and O. Mandelboim. 2009. The interaction of TIGIT with PVR and PVRL2 inhibits human NK cell cytotoxicity. *Proc Natl Acad Sci U S A* 106:17858-17863.

Street, S.E., Y. Hayakawa, Y. Zhan, A.M. Lew, D. MacGregor, A.M. Jamieson, A. Diefenbach, H. Yagita, D.I. Godfrey, and M.J. Smyth. 2004. Innate immune surveillance of spontaneous B cell lymphomas by natural killer cells and gammadelta T cells. *J Exp Med* 199:879-884.

Sun, L., J. Wu, F. Du, X. Chen, and Z.J. Chen. 2013. Cyclic GMP-AMP synthase is a cytosolic DNA sensor that activates the type I interferon pathway. *Science* 339:786-791.

Tay, R.E., E.K. Richardson, and H.C. Toh. 2021. Revisiting the role of CD4+ T cells in cancer immunotherapy—new insights into old paradigms. *Cancer Gene Therapy* 28:5-17.

Terren, I., A. Orrantia, J. Vitalle, G. Astarloa-Pando, O. Zenarruzabeitia, and F. Borrego. 2020. Modulating NK cell metabolism for cancer immunotherapy. *Semin Hematol* 57:213-224.

Terren, I., A. Orrantia, J. Vitalle, O. Zenarruzabeitia, and F. Borrego. 2019. NK Cell Metabolism and Tumor Microenvironment. *Frontiers in immunology* 10:2278.

Textor, S., N. Fiegler, A. Arnold, A. Porgador, T.G. Hofmann, and A. Cerwenka. 2011. Human NK Cells Are Alerted to Induction of p53 in Cancer Cells by Upregulation of the NKG2D Ligands ULBP1 and ULBP2. *Cancer Res* 71:5998-6009.

Thompson, T.W., B.T. Jackson, P.J. Li, J. Wang, A.B. Kim, K.T.H. Huang, L. Zhang, and D.H. Raulet. 2018. Tumor-derived CSF-1 induces the NKG2D ligand RAE-1delta on tumor-infiltrating macrophages. *Elife* 7:e32919.

Thompson, T.W., A.B. Kim, P.J. Li, J. Wang, B.T. Jackson, K.T.H. Huang, L. Zhang, and D.H. Raulet. 2017. Endothelial cells express NKG2D ligands and desensitize anti-tumor NK responses. *Elife* 6:e30881.

Tomura, M., X.Y. Zhou, S. Maruo, H.J. Ahn, T. Hamaoka, H. Okamura, K. Nakanishi, T. Tanimoto, M. Kurimoto, and H. Fujiwara. 1998. A critical role for IL-18 in the proliferation and activation of NK1.1+ CD3- cells. *J Immunol* 160:4738-4746.

Vari, F., D. Arpon, C. Keane, M.S. Hertzberg, D. Talaulikar, S. Jain, Q. Cui, E. Han, J. Tobin, R. Bird, D. Cross, A. Hernandez, C. Gould, S. Birch, and M.K. Gandhi. 2018. Immune evasion via PD-1/PD-L1 on NK cells and monocyte/macrophages is more prominent in Hodgkin lymphoma than DLBCL. *Blood* 131:1809-1819.

Varn, F.S., Y. Wang, D.W. Mullins, S. Fiering, and C. Cheng. 2017. Systematic Pan-Cancer Analysis Reveals Immune Cell Interactions in the Tumor Microenvironment. *Cancer Res* 77:1271-1282.

Vigano, S., D. Alatzoglou, M. Irving, C. Ménétrier-Caux, C. Caux, P. Romero, and G. Coukos. 2019. Targeting Adenosine in Cancer Immunotherapy to Enhance T-Cell Function. *Frontiers in immunology* 10:

Vivier, E., D.H. Raulet, A. Moretta, M.A. Caligiuri, L. Zitvogel, L.L. Lanier, W.M. Yokoyama, and S. Ugolini. 2011. Innate or adaptive immunity? The example of natural killer cells. *Science* 331:44-49.

Voskoboinik, I., J.C. Whisstock, and J.A. Trapani. 2015. Perforin and granzymes: function, dysfunction and human pathology. *Nat Rev Immunol* 15:388-400.

Wagner, J.A., M. Rosario, R. Romee, M.M. Berrien-Elliott, S.E. Schneider, J.W. Leong, R.P. Sullivan, B.A. Jewell, M. Becker-Hapak, T. Schappe, S. Abdel-Latif, A.R. Ireland, D. Jaishankar, J.A. King, R. Vij, D. Clement, J. Goodridge, K.J. Malmberg, H.C. Wong, and T.A. Fehniger. 2017. CD56bright NK cells exhibit potent antitumor responses following IL-15 priming. *J Clin Invest* 127:4042-4058.

Waldmann, T.A. 2006. The biology of interleukin-2 and interleukin-15: implications for cancer therapy and vaccine design. *Nat Rev Immunol* 6:595-601.

Wang, D., and R.N. Dubois. 2010. Eicosanoids and cancer. *Nat Rev Cancer* 10:181-193.

Wang, J., and S. Matosevic. 2018. Adenosinergic signaling as a target for natural killer cell immunotherapy. *Journal of molecular medicine* 96:903-913.

Wang, R., J.J. Jaw, N.C. Stutzman, Z. Zou, and P.D. Sun. 2012. Natural killer cell-produced IFN-gamma and TNF-alpha induce target cell cytolysis through up-regulation of ICAM-1. *J Leukoc Biol* 91:299-309.

Weiss, G.R., M.A. O'Donnell, K. Loughlin, K. Zonno, R.J. Laliberte, and M.L. Sherman. 2003. Phase 1 study of the intravesical administration of recombinant human interleukin-12 in patients with recurrent superficial transitional cell carcinoma of the bladder. *J Immunother* 26:343-348.

Wiedemann, G.M., E.K. Santosa, S. Grassmann, S. Sheppard, J.B. Le Luduec, N.M. Adams, C. Dang, K.C. Hsu, J.C. Sun, and C.M. Lau. 2021. Deconvoluting global cytokine signaling networks in natural killer cells. *Nat Immunol* 22:627-638.

Wolf, N.K., C. Blaj, L. Picton, G. Snyder, L. Zhang, C.J. Nicolai, C.O. Ndubaku, S.M. McWhirter, K.C. Garcia, and D.H. Raulet. 2022a. Synergistic effects of a STING agonist and an IL-2 superkine in cancer immunotherapy against MHC I-deficient and MHC I+ tumors. *Proc Natl Acad Sci U S A* In press.

Wolf, N.K., D.U. Kissiov, and D.H. Raulet. 2022b. Roles of natural killer cells in immunity to cancer, and applications to immunotherapy. . *Nature Reviews Immunology* In press.
Woo, S.R., M.B. Fuertes, L. Corrales, S. Spranger, M.J. Furdyna, M.Y. Leung, R. Duggan, Y. Wang, G.N. Barber, K.A. Fitzgerald, M.L. Alegre, and T.F. Gajewski. 2014. STING-dependent cytosolic DNA sensing mediates innate immune recognition of immunogenic tumors. *Immunity* 41:830-842.
Wu, J., L. Sun, X. Chen, F. Du, H. Shi, C. Chen, and Z.J. Chen. 2013. Cyclic GMP-AMP is an endogenous second messenger in innate immune signaling by cytosolic DNA. *Science* 339:826-830.
Xia, T., H. Konno, J. Ahn, and G.N. Barber. 2016a. Deregulation of STING Signaling in Colorectal Carcinoma Constrains DNA Damage Responses and Correlates With Tumorigenesis. *Cell Rep* 14:282-297.
Xia, T., H. Konno, and G.N. Barber. 2016b. Recurrent Loss of STING Signaling in Melanoma Correlates with Susceptibility to Viral Oncolysis. *Cancer Res* 76:6747-6759.
Xie, Y., A. Akpinarli, C. Maris, E.L. Hipkiss, M. Lane, E.K. Kwon, P. Muranski, N.P. Restifo, and P.A. Antony. 2010. Naive tumor-specific CD4(+) T cells differentiated in vivo eradicate established melanoma. *J Exp Med* 207:651-667.
Yang, K.M., Y. Jung, J.M. Lee, W. Kim, J.K. Cho, J. Jeong, and S.J. Kim. 2013a. Loss of TBK1 induces epithelial-mesenchymal transition in the breast cancer cells by ERalpha downregulation. *Cancer Res* 73:6679-6689.
Yang, L., X. Wu, M. Wan, Y. Yu, Y. Yu, and L. Wang. 2013b. CpG oligodeoxynucleotides with double stem-loops show strong immunostimulatory activity. *Int Immunopharmacol* 15:89-96.
Yarchoan, M., A. Hopkins, and E.M. Jaffee. 2017. Tumor Mutational Burden and Response Rate to PD-1 Inhibition. *N Engl J Med* 377:2500-2501.
Yokoyama, W.M., and W.E. Seaman. 1993. The Ly-49 and NKR-P1 gene families encoding lectin-like receptors on natural killer cells: the NK gene complex. *Annu. Rev. Immunol.* 11:613-635.
Young, A., S.F. Ngiow, Y. Gao, A.M. Patch, D.S. Barkauskas, M. Messaoudene, G. Lin, J.D. Coudert, K.A. Stannard, L. Zitvogel, M.A. Degli-Esposti, E. Vivier, N. Waddell, J. Linden, N.D. Huntington, F. Souza-Fonseca-Guimaraes, and M.J. Smyth. 2018. A2AR Adenosine Signaling Suppresses Natural Killer Cell Maturation in the Tumor Microenvironment. *Cancer Res* 78:1003-1016.
Zamai, L., M. Ahmad, I.M. Bennett, L. Azzoni, E.S. Alnemri, and B. Perussia. 1998. Natural killer (NK) cell-mediated cytotoxicity: differential use of TRAIL and Fas ligand by immature and mature primary human NK cells. *J Exp Med* 188:2375-2380.
Zaretsky, J.M., A. Garcia-Diaz, D.S. Shin, H. Escuin-Ordinas, W. Hugo, S. Hu-Lieskovan, D.Y. Torrejon, G. Abril-Rodriguez, S. Sandoval, L. Barthly, J. Saco, B. Homet Moreno, R. Mezzadra, B. Chmielowski, K. Ruchalski, I.P. Shintaku, P.J. Sanchez, C. Puig-Saus, G. Cherry, E. Seja, X. Kong, J. Pang, B. Berent-Maoz, B. Comin-Anduix, T.G. Graeber, P.C. Tumeh, T.N. Schumacher, R.S. Lo, and A. Ribas. 2016. Mutations Associated with Acquired Resistance to PD-1 Blockade in Melanoma. *N Engl J Med* 375:819-829.
Zelenay, S., A.G. van der Veen, J.P. Bottcher, K.J. Snelgrove, N. Rogers, S.E. Acton, P. Chakravarty, M.R. Girotti, R. Marais, S.A. Quezada, E. Sahai, and C. Reis e Sousa. 2015. Cyclooxygenase-Dependent Tumor Growth through Evasion of Immunity. *Cell* 162:1257-1270.

Zhang, M., B. Wen, O.M. Anton, Z. Yao, S. Dubois, W. Ju, N. Sato, D.J. DiLillo, R.N. Bamford, J.V. Ravetch, and T.A. Waldmann. 2018a. IL-15 enhanced antibody-dependent cellular cytotoxicity mediated by NK cells and macrophages. *Proc Natl Acad Sci U S A* 115:E10915-E10924.

Zhang, Q., J. Bi, X. Zheng, Y. Chen, H. Wang, W. Wu, Z. Wang, Q. Wu, H. Peng, H. Wei, R. Sun, and Z. Tian. 2018b. Blockade of the checkpoint receptor TIGIT prevents NK cell exhaustion and elicits potent anti-tumor immunity. *Nat Immunol* 19:723-732.

Zhang, Z., Y. Zhang, S. Xia, Q. Kong, S. Li, X. Liu, C. Junqueira, K.F. Meza-Sosa, T.M.Y. Mok, J. Ansara, S. Sengupta, Y. Yao, H. Wu, and J. Lieberman. 2020. Gasdermin E suppresses tumour growth by activating anti-tumour immunity. *Nature* 579:415-420.

Zhou, C., X. Chen, R. Planells-Cases, J. Chu, L. Wang, L. Cao, Z. Li, K.I. Lopez-Cayuqueo, Y. Xie, S. Ye, X. Wang, F. Ullrich, S. Ma, Y. Fang, X. Zhang, Z. Qian, X. Liang, S.Q. Cai, Z. Jiang, D. Zhou, Q. Leng, T.S. Xiao, K. Lan, J. Yang, H. Li, C. Peng, Z. Qiu, T.J. Jentsch, and H. Xiao. 2020a. Transfer of cGAMP into Bystander Cells via LRRC8 Volume-Regulated Anion Channels Augments STING-Mediated Interferon Responses and Anti-viral Immunity. *Immunity* 52:767-781 e766.

Zhou, Z., H. He, K. Wang, X. Shi, Y. Wang, Y. Su, Y. Wang, D. Li, W. Liu, Y. Zhang, L. Shen, W. Han, L. Shen, J. Ding, and F. Shao. 2020b. Granzyme A from cytotoxic lymphocytes cleaves GSDMB to trigger pyroptosis in target cells. *Science* 368:

Zhu, E.F., S.A. Gai, C.F. Opel, B.H. Kwan, R. Surana, M.C. Mihm, M.J. Kauke, K.D. Moynihan, A. Angelini, R.T. Williams, M.T. Stephan, J.S. Kim, M.B. Yaffe, D.J. Irvine, L.M. Weiner, G. Dranoff, and K.D. Wittrup. 2015. Synergistic innate and adaptive immune response to combination immunotherapy with anti-tumor antigen antibodies and extended serum half-life IL-2. *Cancer Cell* 27:489-501.